Title
NEUTRON PAIRING STATES IN DOUBLY EVEN NUCLEI

Author
Sorensen, Bent.

Publication Date
1969-04-01

Submitted to Nuclear Physics

UCRL-18834
Preprint

NEUTRON PAIRING STATES IN DOUBLY EVEN NUCLEI

Bent Sørensen

April 1969

AEC Contract No. W-7405-eng-48

LAWRENCE RADIATION LABORATORY
UNIVERSITY of CALIFORNIA BERKELEY

UCRL-18834

DISCLAIMER

UCRL-18834

NEUTRON PAIRING STATES IN DOUBLY EVEN NUCLEI[†]

Bent Sørensen[††]

Lawrence Radiation Laboratory
University of California
Berkeley, California 94720

April 1969

Abstract: Neutron J=0 states in even-N nuclei are calculated with a pairing force, using the boson expansion method. All regions of isotopes which are close to a fairly good shell-closure are covered, and a comparison is made between calculated and experimental two-nucleon transfer cross-sections. In general we find a remarkably good agreement, even for the ground state mass systematics, suggesting that for the isotopes under consideration the simple pairing interaction is the dominant producer of ground state correlations. A lack of agreement with experiments in certain regions is proposed to be connected with couplings to definite other degrees of freedom under the influence of predominantly particle-hole interactions.

[†]Work performed under the auspices of the U.S. Atomic Energy Commission.

[††]On leave from Niels Bohr Institute, University of Copenhagen, Denmark.

1. Introduction

The picture we are going to present develops around a closed neutron shell N_0. The basic ingredients in the description are the pairing type (seniority zero) levels in the neighbouring even nuclei N_0-2 and N_0+2. We here assume that in each of these nuclei there is one branch of levels which carry the main part of pairing correlations, and that these branches can be built out of two definite operators, one of which describes a correlated set of J=0 hole-pairs (with respect to the closed shell N_0) and the other a correlated set of J=0 particle-pairs. These two branches are characterized by two boson operators, c_2^+ and c_1^+, which apart from Pauli principle corrections are collective two-hole and two-particle operators. In a similar manner we describe the remaining set of two-hole and two-particle states, which we denote non-collective branches. We now describe pairing states in any nucleus N_0-2q or N_0+2p by superimposing appropriate numbers of the collective and non-collective boson operators. In this process we distinguish between collective and non-collective bosons by performing an additional diagonalization of the residual parts of the pairing force which acts among the collective bosons and on the other hand neglecting such anharmonicties for the non-collective bosons. Details of the formalism will be given in sect. 2. In fig. 1 we have schematically shown some of the states obtained in this way. Heavy lines indicate states formed entirely out of collective boson quanta, thin lines states formed directly by acting with the calculated non-collective quanta on the closed shell, while dashed lines indicate states built of both collective and non-collective quanta. The excited, collective states are usually called pair (or pairing) vibrations,

and in the absence of anharmonic correlations the two-nucleon transfer cross-sections among them would obey the selection rules discussed by Bès and Broglia (Be 66). It should be mentioned, that the cross-sections leading to non-collective states often are of the same order of magnitude as those involving collective states, so that a detailed calculation often will be necessary in order to distinguish the collective states in a given experiment.

We will now anticipate some of the possible shortcomings of the description given above. First of all the truncation of the boson expansions may cause inaccurate description of superfluid nuclei or transitional regions. For superfluid sequences of isotopes the ground state energies will lie on a parabola, which means that there are large deviations from the harmonic energies (linear raise of the ground state energies to both sides of N_0). Definite examples in sect. 4 will show that the fourth order boson description is able to describe superfluid systems, but that the energies become gradually poorer as one goes away from N_0.

From evidence in lighter nuclei it has been suggested that one should use an isoscalar pairing interaction acting among $J=0$, $T=1$ pairs (Bo 68), which would on the other hand not affect the heavier nuclei, where the strong alignment of isospin imply decoupling of proton and neutron pairing states plus the absence of proton-neutron pairing correlations. An isovector component of the pairing average field would explain the difference in the proton and neutron pairing strengths usually assumed. One can then view the parabolic energy behaviour of ground state energies of superfluid nuclei as arising from the rotation in isospace of a pairing distorted system which is directed in isospace.

The spectra of lighter nuclei show definite deviations from isospin-independence, both in ground state and excitation energies. In a phenomenological description of these effects one might consider interactions among the boson quanta, which contain both isoscalar and isovector $(t_1 \cdot t_2)$ parts. This leads to anharmonic spectra and to splitting of isospin multiplets of the form $\Delta E_T = (a_1 + a_2\, T(T+1))$. Experimental evidence for the T-splitting of pair vibrational levels does roughly support the $T(T+1)$ rule, although it is not followed very accurately (Sø 69).

In sect. 3 we will discuss the type of interaction which may give the observed isospin structure. It is pointed out that the splitting of the pair vibration implied by an isoscalar pairing interaction is small and not of the form $T(T+1)$. The simplest interaction which can give the $T(T+1)$ splittings is a monopole force acting on $T=1$ particle-hole pairs in partially filled shells (which are already formed by pair excitations). From the assumption of such an interaction it also becomes clear, why the isospin structure gets destroyed for heavy nuclei, where proton-holes and neutron-particles (or vice versa) no longer occupy the same orbits, thereby restricting the $T=1$, $J=0$ interaction to connect only pairs separated by two major shells.

The interplay between pairing and particle-hole forces has another aspect, which is also revealed by experimental evidence on $J=0$ states. One has in a number of cases observed low-lying 0^+ states which get fair to very strong two-nucleon transfer strengths. These states are lower in excitation energy than possible for pairing states (this conclusion is only definite in closed neutron shells where such states can not be confused with

non-collective pairing states), and in many cases the excitation energy is close to twice that of the lowest collective multipole state (often 3- at doubly closed major shells, otherwise 2+). There are two ways in which such a "two-phonon" state can get two-nucleon transfer cross-section. One is through inelastic effects, which are appreciable when collective multipole transitions are involved (As 68), the other is through admixtures of the ground state (with its pairing structure) or the excited pairing states with large cross-sections. The presence of admixtures are necessary in some cases, where the cross-sections to the "non-pairing" states are extremely large. The classification of these states as "two-phonon" states is in a few cases impossible, possibly pointing to the co-existence of different shapes or structures. It may here be either the ground state or the excited state, which has a large parentage to the N-2 and N+2 ground states. Experimental evidence of this is contained in the survey in sect. 4. Fig. 2 shows schematically some of the deviations from the pure pairing picture, which has been discussed above.

2. The Boson Method

The formalism employed in our calculation is identical to the one described in sect. 7 of Sø 67, except that we have often defined the collective bosons by means of TDA rather than RPA, which is necessary since we are considering some neutron shells which are so "bad" closed shells that the system is superfluid, in which case RPA fails to describe the collective boson. Since we are also going further away from the closed shells than the single step described in Sø 67, a brief outline of the theory is repeated here together with the additional formulae.

The neutron Hamiltonian consists of a single particle part and a pairing interaction

$$H_n = \sum_j \hat{j}\, \varepsilon_j\, B_j - \frac{G}{4} \sum_{jj'} \hat{j}\hat{j}'\, A_j^+\, A_{j'} \tag{2.1}$$

where

$$B_j = (a_j^+ \bar{a}_j)_0,\ A_j^+ = (a_j^+ a_j^+)_0,\ \bar{a}_{jm} = (-)^{j+m}\, a_{j-m} \tag{2.2}$$

and

$$\hat{j} = (2j+1)^{1/2}\ .$$

We now choose a neutron closed shell $|\,CS\,\rangle$ as a reference vacuum and define particle and hole operators with respect to this vacuum by

$$\mathcal{A}_j\, |\,CS\,\rangle = 0,$$

$$\mathcal{A}_j^+ = \begin{cases} -A_j & \text{for} \quad j \leqslant CS \\ A_j^+ & \text{for} \quad j > CS \end{cases} \tag{2.3}$$

$$\mathcal{B}_j = \begin{cases} -B_j & \text{for} \quad j \leqslant CS \\ B_j & \text{for} \quad j > CS\ . \end{cases}$$

Since the monopole, seniority zero states of even systems can be described entirely by combining $J=0$ boson operators $b_j^+ = b_{J=0}^+(jj)$ satisfying $[b_j, b_{j'}^+] = \delta_{jj'}$. We shall include only such operators in the boson expansions of the two

fermion operators of eq. (2.3), obtaining in fact independent expansions for each j-value (Br 68)

$$\mathcal{A}_j^+ = x^{10}\, b_j^+ + x_j^{31}\, b_j^+ b_j^+ b_j + \ldots . \,,$$
$$\mathcal{B}_j^+ = y_j^{21}\, b_j^+ b_j \,, \tag{2.4}$$

where the coefficients (see Sø 68, which also explains why the expansion parameter y^0 should be zero for seniority zero) are

$$x^{10} = \sqrt{2},\ x_j^{31} = -\sqrt{2}\,(1 - (1 - 2/\hat{j}^2)^{1/2}),\ y_j^{21} = 2/\hat{j} \,. \tag{2.5}$$

The Hamiltonian eq. (2.1) now becomes

$$H_n = H_0 + H_1 + H_2 \tag{2.6}$$

with

$$H_0 = 2\left(\sum_{j>} \varepsilon_j\, b_j^+ b_j - \sum_{j\leqslant} \varepsilon_j\, b_j^+ b_j \right) - \frac{G}{2} \sum_{\substack{j,j'> \\ \text{or } j,j'\leqslant}} \hat{j}\hat{j}'\, b_j^+ b_{j'} \,, \tag{2.7}$$

$$H_1 = \frac{G}{2} \sum_{\substack{j> \\ j'\leqslant}} \hat{j}\hat{j}'\, b_j^+ b_{j'}^+ + \text{h.c.} \,, \tag{2.8}$$

$$H_2 = \frac{G}{2} \sum_{\substack{j,j'> \\ \text{or } j,j'\leqslant}} \frac{\hat{j}'}{\hat{j}}\, b_j^+ b_j^+ b_j\, b_{j'} - \frac{G}{2} \sum_{\substack{j> \\ j'\leqslant}} \left(\frac{\hat{j}}{\hat{j}'}\, b_{j'}^+ b_j^+ b_j^+ b_j\, b_{j'} + \frac{\hat{j}'}{\hat{j}}\, b_j^+ b_j^+ b_{j'}^+ b_j \right) + \text{h.c.} \tag{2.9}$$

where sixth order and higher terms have been neglected and the coefficients x_j^{31} approximated correspondingly for consistency.

The normal mode bosons are now defined by canonical transformations

$$c_n^+ = \sum_{j>} r_n(j)\, b_j^+ - \sum_{j\leqslant} s_n(j)\, b_j \quad , \tag{2.10}$$

$$c_m^+ = \sum_{j\leqslant} r_m(j)\, b_j^+ - \sum_{j>} s_m(j)\, b_j \quad , \tag{2.11}$$

where

$$\begin{aligned} &\sum_{j>} r_n(j)\, r_{n'}(j) - \sum_{j\leqslant} s_n(j)\, s_{n'}(j) = \delta_{nn'} \quad , \\ &\sum_{j\leqslant} r_m(j)\, r_{m'}(j) - \sum_{j>} s_m(j)\, s_{m'}(j) = \delta_{mm'} \quad , \\ &\sum_{j>} r_n(j)\, s_m(j) - \sum_{j\leqslant} r_m(j)\, s_n(j) = 0 \quad . \end{aligned} \tag{2.12}$$

The transformation may be defined by the requirement that H_0+H_1 be diagonalized (RPA)

$$H_0 + H_1 = \sum_n \omega_n\, c_n^+ c_n + \sum_m \omega_m\, c_m^+ c_m \tag{2.13}$$

or by the requirement that H_0 be diagonalized (TDA) which implies $s_n(j) = s_m(j) = 0$

$$H_0 = \sum_n \omega_n c_n^+ c_n + \sum_m \omega_m c_m^+ c_m \quad . \tag{2.14}$$

As discussed in Sø 69a RPA is a bad starting point for the boson expansions whenever the system is close to being superfluid. When the system is well non-superfluid one should obtain approximately the same results starting from RPA or TDA. An example of this is given together with the discussion of Si-isotopes (see sect. 4). One might question whether in the case of transitional or superfluid nuclei the collective branch of excitations defined by the TDA bosons is a fair approximation to the correct one (comprising mainly ground states). Surprisingly enough this is so to a large extent, according to the comparison with an exact solution made for the two-level model (Br 68) and a comparison with BCS wave functions discussed in sect. 4 for Sn-isotopes. For these reasons we have employed the TDA representation, eq. (2.14), in most cases.

The bosons characterizing the collective branch of excitations (ground states and pair vibrations) are the two-particle boson c_n^+ and the two-hole boson c_m^+ with lowest energies ω_n and ω_m. We shall in the following denote these bosons c_1^+ and c_2^+ (with energies ω_1 and ω_2) and the non-collective ones by primes $c_{1'}^+$, $c_{1''}^+$, ... ($\Delta N=2$) and $c_{2'}^+$, $c_{2''}^+$, ... ($\Delta N=-2$) after ordering them according to increasing energies $\omega_{1'}$, $\omega_{1''}$, ... and $\omega_{2'}$, $\omega_{2''}$, ...

It is assumed that the non-collective states (in the even neighbour isotopes to the closed shell) are well enough given by the normal mode bosons, whereas non-harmonic correlations must be included for the collective

branches. We thus introduce the normal mode bosons in the residual interaction (H_1+H_2 for TDA or just H_2 for RPA) and keep only the collective bosons

$$H_{res} = B_1 c_1^+ c_1 + B_2 c_2^+ c_2 + A_1 c_1^+ c_2^+ + A_2 c_1^+ c_1^+ c_2^+ c_2^+$$
$$+ A_3 c_1^+ c_1^+ c_2^+ c_1 + A_4 c_2^+ c_2^+ c_1^+ c_2 + A_5 c_1^+ c_1^+ c_1 c_1 + A_6 c_2^+ c_2^+ c_2 c_2$$
$$+ A_7 c_1^+ c_2^+ c_1 c_2 + h.c. \quad . \tag{2.15}$$

The coefficients B_1, B_2, A_1, ... , A_7 are for the RPA case given by Sø 67. The same expressions hold in TDA when the proper transformation (2.10) to (2.12) is used, except that

$$A_1 = A_1^{RPA} + \frac{G}{2} \sum_{j>} \hat{j}\, r_1(j) \sum_{j'\leqslant} \hat{j}'\, r_2(j') \tag{2.16}$$

because of the presence of H_1 in H_{res}.

The collective eigenstates of the nucleus with neutron number $N=N_0$ + 2p-2q, where N_0 is the closed shell, are given in the form

$$|N,\alpha\rangle = \sum_n \phi_n(N,\alpha) \frac{(c_1^+)^{n+p}\,(c_2^+)^{n+q}}{\sqrt{(n+p)!}\,\sqrt{(n+q)!}}\,|0\rangle \quad , \tag{2.17}$$

where $|0\rangle$ is the common vacuum of c_1 and c_2 and n is extended to the maximum number consistent with the number of configurations included. If the total degeneracies of all included levels above and below the closed shell are D_1 and D_2, we thus extend n from zero to $D_1/2$ or $D_2/2$, whichever is smallest, for the eigenstates of the closed shell nucleus $N=N_0$. Using the basis states

$$|n\rangle = \frac{(c_1^+)^{n+p}}{\sqrt{(n+p)!}} \frac{(c_2^+)^{n+q}}{\sqrt{(n+q)!}} |0\rangle \quad , \tag{2.18}$$

where for a given N either p or q is zero, we can evaluate the matrix elements of each term in eq. (2.15), which are needed for the diagonalization,

$$\begin{aligned}
\langle n|c_1^+ c_1|n\rangle &= n+p \quad , \\
\langle n|c_2^+ c_2|n\rangle &= n+q \quad , \\
\langle n+1|c_1^+ c_2^+|n\rangle &= (n+1)^{1/2}\,(n+1+p+q)^{1/2} \quad , \\
\langle n+2|c_1^+ c_1^+ c_2^+ c_2^+|n\rangle &= (n+1)^{1/2}(n+2)^{1/2}(n+1+p+q)^{1/2}(n+2+p+q)^{1/2} \quad , \\
\langle n+1|c_1^+ c_1^+ c_2^+ c_1|n\rangle &= (n+p)(n+1)^{1/2}(n+1+p+q)^{1/2} \quad , \\
\langle n+1|c_2^+ c_2^+ c_1^+ c_2|n\rangle &= (n+q)(n+1)^{1/2}(n+1+p+q)^{1/2} \quad , \\
\langle n|c_1^+ c_1^+ c_1 c_1|n\rangle &= (n+p)(n-1+p) \quad , \\
\langle n|c_2^+ c_2^+ c_2 c_2|n\rangle &= (n+q)(n-1+q) \quad , \\
\langle n|c_1^+ c_2^+ c_1 c_2|n\rangle &= n(n+p+q) \quad .
\end{aligned} \tag{2.19}$$

The collective correlations are supposed to underlie the non-collective excitations, which then are given by $c_1^+,|N_0,0\rangle$ and $c_2^+,|N_0,0\rangle$ rather than by $c_1^+,|0\rangle$ and $c_2^+,|0\rangle$.

We now turn to the two-neutron transfer operator

$$T_j = -\frac{1}{\sqrt{2}} A_j^+ = -\frac{1}{\sqrt{2}} \mathcal{A}_j^+ \delta_{j>} - \frac{1}{\sqrt{2}} \mathcal{A}_j \delta_{j\leqslant} \tag{2.20}$$

which is transformed to the boson picture under the same approximations as for the Hamiltonian

$$T_j = \sum_{n\neq 1} C_n\, c_n^+ + \sum_{m\neq 2} C_m\, c_m + C_1\, c_1^+ + C_2\, c_2$$

$$+ D_1\, c_1^+ c_1^+ c_1 + D_2\, c_2^+ c_2\, c_2 + D_3\, c_1^+ c_2^+ c_2 + D_4\, c_1^+ c_1^+ c_2^+ \quad (2.21)$$

$$+ D_5\, c_1^+ c_1\, c_2 + D_6\, c_2\, c_2\, c_1$$

where the coefficients involving collective bosons are given in Sø 67 [†])
and the non-collective ones are

$$C_n = r_n(j)\, \delta_{j>} - s_n(j)\, \delta_{j\leqslant}\,, \quad C_m = s_m(j)\, \delta_{j>} - r_m(j)\, \delta_{j\leqslant}\,. \quad (2.22)$$

We are describing the L=0 transfer reactions between the pairing states in terms of the structure factors G_S (Gl 65) arising from the expansion of the radial part of the reaction amplitude on a basis characterized by harmonic oscillator quantum numbers. Assuming zero relative angular momentum for the transferred neutron pair (in a (t,p) or (p,t) reaction) we have

$$G_S(i,f) = \sum_{\substack{n\ell j \\ N=2n+\ell-S}} \langle f|T_j|i\rangle\, (-)^{\ell}\, \Omega_N\, \frac{\hat{j}}{\hat{\ell}\,\sqrt{2}}\, \langle N0,S0,0|n\ell,n\ell,0\rangle\,, \quad (2.23)$$

[†]) Note that $D_3 = D_4 = D_5 = D_6 = 0$ for TDA normal mode bosons.

where N is the radial quantum number of the relative motion of the two neutrons to be transferred, S that of the center-of-mass motion, $\langle\ ,\ ,\ |\ ,\ ,\ \rangle$ a Moshinsky bracket and Ω_N the overlap between the relative motion in the triton and in the nucleus. Assuming a Gaussian wave function in the triton and oscillator wave functions in the nucleus one may estimate (Gl 65)

$$\Omega_N = \frac{\sqrt{(2N+2)!}}{2^N(N+1)!}\left(1 - \frac{2\nu}{6\eta^2+\nu}\right)^N \left(\frac{\nu}{6}\right)^3 \left(\frac{2\eta}{\eta^2+\nu/6}\right)^{3/2} \tag{2.24}$$

where $\nu \approx A^{-1/3}\ \text{fm}^{-2}$ and $\eta \approx 0.242\ \text{fm}^{-1}$.

The structure coefficients G_S may be entered in a DWBA calculation in order to obtain the differential cross section

$$\sigma_{i\to f}(\theta) = \left| \sum_S G_S(i,f)\ \rho_S^{\text{DWBA}}(\theta) \right|^2 , \tag{2.25}$$

but since we will consider several cases where either no experiments have been performed or several experiments have been done at different projectile energies, we will in general not go through the DWBA calculation but simply quote

$$\overline{\sigma}_{i\to f} \propto \sum_S G_S(i,f)^2 , \tag{2.26}$$

which represents the probability of the reaction taking place at any spatial separation. One could alternatively choose the probability for the reaction taking place at a definite radius R, assuming the amplitude $\rho_S(R,\theta)$ to be independent of S except for the alternating phase,

$$\bar{\bar{\sigma}}_{i\to f} \propto \left| \sum_S (-)^S G_S(i,f) \right|^2 . \qquad (2.27)$$

We have tried both estimates and compared them with integrated DWBA cross sections for a few cases, and we find that $\bar{\sigma}$ of eq. (2.26) is the best estimate, although both fail in cases of peculiar kinematics and generally should not be considered as more than order-of-magnitude estimates.

In order to evaluate the nuclear matrix element $\langle f|T_j|i\rangle$ in eq. (2.23), we evaluate the matrix elements of each term of eq. (2.21) for the collective basis states in eq. (2.18). For neutron numbers $N \leq N_0-2$ we get

$$\begin{aligned}
\langle q-1,n'+1|c_1^+|q,n\rangle &= (n+1)^{1/2} , \\
\langle q-1,n'|c_2|q,n\rangle &= (n+q)^{1/2} , \\
\langle q-1,n'+1|c_1^+ c_1^+ c_1|q,n\rangle &= n(n+1)^{1/2} , \\
\langle q-1,n'|c_2^+ c_2 c_2|q,n\rangle &= (n+q-1)(n+q)^{1/2} , \qquad (2.28) \\
\langle q-1,n'+1|c_1^+ c_2^+ c_2|q,n\rangle &= (n+q)(n+1)^{1/2} , \\
\langle q-1,n'+2|c_1^+ c_1^+ c_2^+|q,n\rangle &= (n+q+1)^{1/2}(n+1)^{1/2}(n+2)^{1/2} , \\
\langle q-1,n'|c_1^+ c_1 c_2|q,n\rangle &= n(n+q)^{1/2} , \\
\langle q-1,n'-1|c_2 c_2 c_1|q,n\rangle &= n^{1/2}(n+q)^{1/2}(n+q-1)^{1/2} ,
\end{aligned}$$

and for $N \geqslant N_0$ we get

$$\langle p+1,n'|c_1^+|p,n\rangle = (n+p+1)^{1/2} \quad ,$$

$$\langle p+1,n'-1|c_2|p,n\rangle = n^{1/2}$$

$$\langle p+1,n'|c_1^+ c_1^+ c_1|p,n\rangle = (n+p)(n+p+1)^{1/2} \quad ,$$

$$\langle p+1,n'-1|c_2^+ c_2 c_2|p,n\rangle = (n-1)n^{1/2} \quad , \qquad (2.29)$$

$$\langle p+1,n'|c_1^+ c_2^+ c_2|p,n\rangle = n(n+p+1)^{1/2} \quad ,$$

$$\langle p+1,n'+1|c_1^+ c_1^+ c_2^+|p,n\rangle = (n+1)^{1/2}(n+p+1)^{1/2}(n+p+2)^{1/2} \quad ,$$

$$\langle p+1,n'-1|c_1^+ c_1 c_2|p,n\rangle = n^{1/2}(n+p) \quad ,$$

$$\langle p+1,n'-2|c_2 c_2 c_1|p,n\rangle = n^{1/2}(n-1)^{1/2}(n+p)^{1/2} \quad .$$

In the cases where we have performed a DWBA calculation, the harmonic oscillator wave functions entering into the expansion given in eq. (2.25) have been matched with Hankel functions of correct asymptotical behaviour, using a computer code written by N. K. Glendenning.

3. Influence of Residual Interaction

The neutron pairing force with constant matrix element within a certain subspace is certainly a crude approximation to the full interaction and presumably also to the part of the full interaction which is effective in correlating the neutron pairing states of even-N nuclei. By comparing the fairly reliable boson calculation based on only the pairing force to experimental evidence we hope to learn about the mechanism of producing neutron J=0 states, not only by pointing out the regions of agreement, but also by considering in detail the possible causes for lack of agreement. This will be done during the separate discussion of each region of isotopes in sect. 4, but we shall in this section formulate briefly the mechanisms of additional correlation invoked in various cases.

Considering the importance of the isospin quantum number for lighter elements, one should here use an isospin invariant formalism, which for the pairing force would imply a Hamiltonian

$$H = \sum_j \varepsilon_j \hat{j} \sqrt{\frac{3}{4}}\, B_j(00) - \frac{G}{4} \sum_{jj'} \hat{j}\hat{j}' \sqrt{3}\, (A_j^+(1)\, \tilde{A}_{j'}(1))_{00}^{00} \qquad (3.1)$$

where

$$A_j^+(1M_T) = (a_j^+(t=\tfrac{1}{2})\, a_j^+(t=\tfrac{1}{2}))_{J=0,0}^{T=1,M_T},$$

$$B_j(00) = (a_j^+(\tfrac{1}{2})\, \tilde{a}_j(\tfrac{1}{2}))_{00}^{00} \qquad (3.2)$$

and

$$\tilde{\mathcal{O}}_{JM}(TM_T) = (-)^{J+M+J+M_T} \mathcal{O}_{J-M}(T-M_T) \quad . \tag{3.3}$$

In analogy to the procedure in sect. 2 we can apply the boson expansions in the combined angular momentum and isospin space, obtaining a Hamiltonian similar to eqs. (2.13) - (2.15) except for couplings of isospin. For like quanta this leads to an isospin dependence of the form

$$\sum_{TT'} \hat{T}'^2 \, W(\tfrac{1}{2}\tfrac{1}{2} T'1;1\tfrac{1}{2})^2 W(1111;T'T) \, \hat{T} \, [(c_1^+ c_1^+)_0^T (\tilde{c}_1 \tilde{c}_1)_0^T]_0^0$$

$$= \frac{1}{36} \sum_T (-2+T(T+1)) \, \hat{T} \, [c_1^+ c_1^+)_0^T (\tilde{c}_1 \tilde{c}_1)_0^T]_0^0 \tag{3.4}$$

and similar for c_2^+ bosons. This may account for the observed splittings of T=0 and T=2 states in the nuclei $A_0 \pm 4$ (where the A_0 ground state has T=0), the T=0, 2, 4 splittings in $A_0 \pm 8$ etc. For A_0=56 we get around 5 MeV splitting of the pairs of like bosons coupled to T=0 and T=2 (using the same G as in the neutron calculation), which is a considerable fraction of the experimentally observed splitting, so that it may be expected that the pairing force is to a large extent responsible for this effect. For the unlike quanta the only type of coupling implied by the pairing interaction is of the form

$$\sum_T (-2+T(T+1)) \, \hat{T} \, [(c_1^+ c_1^+)_0^T (\tilde{c}_1 c_2^+)_0^T]_0^0 \quad , \tag{3.5}$$

or the analogous with c_1 and c_2 interchanged, both of which only through higher order admixtures in the wave functions split the T-members of the pair vibrational states, and not very likely produce splittings proportional to T(T+1) (as the observed ones roughly are).

We thus have to look for a non-pairing interaction as the source of the isospin structure of levels involving coupled, unlike boson quanta c_1^+ and c_2^+. The simplest interaction which will give the desired T-splitting is a particle-hole monopole interaction, i.e. a force which is not important for a closed shell nucleus before another interaction begins to excite particles and thereby produce unfilled j-shells. In order that this interaction can split the T-members of the pair vibration, the particle-hole pairs must be T=1

$$H_M = \frac{\sqrt{3}}{4} \sum_{jj'} V_{jj'} \, (B_j^+(1) \, \tilde{B}_{j'}(1))_{00}^{00} \quad . \tag{3.6}$$

In the collective boson representation we get a term proportional to

$$((c_1^+ \, \tilde{c}_1)_0^1 \, (c_2^+ \, \tilde{c}_2)_0^1)_0^0 = \sum_T W(1111;1T) \, \hat{T} \, ((c_1^+ \, c_2^+)_0^T \, (\tilde{c}_1 \, \tilde{c}_2)_0^T)^0 \quad , \tag{3.7}$$

which gives the pair vibrations a splitting proportional to $(4-T(T+1))$. At the same time the like bosons get an additional splitting of the same form, which judging from the splittings of the pair vibrations compared to those of equal quanta generally are of the same order of magnitude, although definite variations can be observed from case to case. Around $A=56$ one would need 4-5 MeV splitting of the $T=0$ and 2 states in $A_0 \pm 4$ from the monopole interaction.

For a particle-hole force of the type corresponding to eq. (3.6) the isospin of the particle-hole pair tells whether proton-neutron interaction is present or not. If the $B_j^+(TM)$ operators have $T=0$ only proton p-h pairs or

neutron p-h pairs are correlated, whereas for T=1 also proton-particle and neutron-hole pairs (or vice versa) get correlated. In heavy nuclei with large isospin alignment only the M=0 part of the interaction in eq. (3.6) can be effective, so that it no longer produces any isospin structure.

A detailed investigation of the simultaneous action of the pairing and monopole T=1 forces is planned for a forthcoming communication, and we will in the discussion of the experimental spectra in sect. 4 only qualitatively estimate whether the picture given above is relevant or not.

We shall now try to estimate the role played by the surface multipole vibrations $|\lambda\pi\rangle = 2+, 3-, \ldots$ which usually appears as the lowest excited states in even nuclei. Although the vibrational bands are known usually to possess large anharmonicities (Sø 69a), we can get a qualitative idea of the influence of the 0+ members of these bands on the pairing states by assuming the harmonic wave functions

$$|0+\rangle = |(\lambda,\pi=(-)^{\lambda})^{2}_{J=0}\rangle \approx \left[\sum_{ph}\{\psi_{ph}(a^{+}_{p}\bar{a}_{h})_{\lambda} + \phi_{ph}(a^{+}_{h}\bar{a}_{p})_{\lambda}\}\right]^{2}|\hat{0}\rangle \quad . \tag{3.8}$$

The particle-hole basis employed here (or its equivalent in the boson space, cf. Sø 67) has a certain overlap with the J=0 basis for the pairing states. If the particle-hole vacuum $|\hat{0}\rangle$ corresponds to a closed neutron shell $\langle 0+|c^{+}_{1}\,c^{+}_{2}|N_{0},0\rangle$ is different from zero, and otherwise we have $\langle 0+|c^{+}_{2},|N_{0}+2,0\rangle \neq 0$ or $\langle 0+|c^{+}_{1},|N_{0}-2,0\rangle \neq 0$. In fig. 3 we illustrate the influence of these overlaps on the two-nucleon L=0 transfer reactions. The total transfer strength which in the pairing picture went to the excited pairing state (collective or non-collective according to whether the nucleus is a neutron closed shell or not) is now

shared with the two-phonon multipole state. If further the multipole force has produced ground state correlations, as it has if the ϕ_{ph}'s of eq. (3.8) are non-zero (RPA), then the ground state has the form

$$|\hat{0}\rangle = \exp\left\{-\frac{\hat{\lambda}}{2}\sum_{php'h'}\psi_{ph}(\phi^{-1})_{ph}[(a_p^+ \bar{a}_h)_\lambda(a_p^+ \bar{a}_h)_\lambda]_0\right\}|0\rangle \quad , \qquad (3.9)$$

which means that part of the paired structure of the ground state is destroyed so that the ground-to-ground state transfer cross sections is reduced. The figure illustrates this in two steps, assuming first that the multipole states do not produce ground state correlations (TDA, $\phi_{ph}=0$ in eq. (3.8)). The transfer strength to the multipole 0+ state is thus proportional to $\sum \psi_{ph}\,\psi_{p'h'}$ and a recoupling coefficient, and this strength is taken from the pairing type configuration $c_1^+ c_2^+ |N_0,0\rangle$ (at a closed shell), or from the simplest non-collective states $c_{2'}^+ |N+2,0\rangle$ (below the closed shell) or $c_{1'}^+ |N+2,0\rangle$ (above the closed shell). In the figure the closed shell pairing state is assumed to have the structure $c_1^+ c_2^+ |0\rangle$, otherwise the strength is taken from several pairing states containing this component. We can now add the multipole ground state correlations to the picture, which eq. (3.9) shows to first order implies an admixture of the uncorrelated ground state and the TDA 0+ two-phonon state. For this reason the strength missing in the ground state has in fig. 3(c) been added to the two-phonon 0+ state. It should also be mentioned that two-phonon multipole states of collective nature can be reached by a two-step process combining the transfer process with an inelastic scattering (As 68), and that the two-phonon states in this way can get of the order of 10% of the ground state cross section.

The admixture of the ground state and the two-phonon TDA-state is also of this order of magnitude, whereas the overlap of the two-phonon state with the pairing states except for extraordinary situations only can be expected to be a few percent.

All together the picture outlined above seems to be able to explain small transfer cross sections to the non-pairing 0+ states (at most around 20% of the ground state). Such are observed in many isotopes, but in addition there are a number of cases where excited states whose main source does not seem to be the pairing interaction have been observed, and which nevertheless gets cross-sections comparable to or larger than the ground state. We feel that these transitions have to be explained in terms of rather sudden changes in the structure of neighbouring isotopes. It could thus be that the description given above truly represents the nucleus A, but that the ground state of A-2 has a larger parentage with some other 0+ state than with the pairing ground state, in which case the (t,p) cross sections would change drastically. The structure differences between neighbouring isotopes may e.g. be due to differences in the quadrupole type ground state correlations, which are likely to occur a) when going from a major closed shell to the $A \pm 2$ isotopes and b) when permanent deformation occurs. A kind of coexistence has to be assumed in order to provide the parentage relation necessary for large transfer cross-sections. A similar change in pairing distortion and coexistence of superfluid and normal phases is possible. That, however, can not be sufficiently well described by the boson expansions truncated at fourth order, as further discussed in appendix 2.

A weak coupling between pairing and quadrupole quanta has interesting implications for certain $J=2$ or 4 levels with pair vibrational structure (Bo 68), and although the study of these excitations are outside the scope of the present investigation, it should be mentioned that the boson method (including two-particle and two-hole $J=2$ operators) provides a natural basis for analysing such states.

4. Comparison Between Fourth Order Boson Calculation and Experiments

The calculations of neutron pairing states has been performed around major as well as some minor shell closings N_0 and in some cases also for various proton numbers, reflecting the interactions with protons only through the neutron average potential. Before comparing the experimental levels and transfer cross sections with the calculated ones, we have subtracted the Coulomb energy, which of course is not included in the calculation. In doing so we have assumed a Coulomb energy (Be 36)

$$E_c = \frac{3Z^2e^2}{5R_c}\left(1 - 5\left(\frac{3}{16\pi Z}\right)^{2/3}\right) \simeq 0.7\,\frac{Z^2}{A^{1/3}}\left(1 - 0.76\,Z^{-2/3}\right)\ \text{MeV}\ . \tag{4.1}$$

In the Ca-region there is evidence against the N-dependence of E_c (Oo 66), but the ground state energies predicted by the pairing calculations are not reliable enough to provide conclusive distinction between eq. (4.1) and the assumption of zero Coulomb energy difference between ^{40}Ca and ^{48}Ca, although the trend would be slightly better given if R_c were constant or decreased slightly through the increasing-N Ca-isotopes.

In order to ease the reading of the figures, a term proportional to $N-N_0$ has been subtracted from the energies of each isotope, so that the ground state energies of the isotopes $N_0 \pm 2$ become equal, in the experimental as well as in the theoretical spectra. For each isotope we give the experimental spectrum to the right, and at each level the (p,t) and (t,p) intensities are given for the reactions leading to this level from the

ground state of N+2 or N-2 (arrow pointing left or right), similarly for the calculated levels (left) using eq. (2.26). Transitions to excited states are quoted relative to the ground state transition and below the ground states relative ground state transitions are given when possible. The experimental absolute values are normally very inaccurate for a number of reasons including in some cases unobservable $\theta=0°$ maxima or otherwise incomplete angular distributions. The dependence on kinematics is not included in the estimate eq. (2.26). This can be an important factor as several cases where experiments have been performed at different incident energies will show. The results of every experiment are labelled at each level. In a few cases where we wanted to emphasise a particular point in the discussion, a DWBA calculation of the cross-sections and angular distributions were performed.

The parameters of the boson calculation are the neutron pairing strength G and the neutron single particle energies. The pairing strength is assumed to be of the form (Bo 69)

$$G = \frac{G_0}{A}\left(1 - G_1 \frac{N-Z}{A}\right) \quad , \tag{4.2}$$

in consistency with the occurence of a symmetry energy term in the empirical mass formula and the similar parametrization of the optical model potential depth. G_1 was fixed at 0.75 and G_0 was taken as 23 MeV except for slight variations related to the number of single particle levels included.

The single particle levels were at first extracted from single-stripping experiments by means of the sum rule method (Fr 61), whenever data was available, but in most cases these energies were later varied, since they did not reproduce the energies of known non-collective pairing states which we

felt was a necessary requirement for the present type of calculation. Formally, we are also not interested in the "bare" single-particle levels, but rather in the energies associated with a self-consistent average field produced by all non-pairing parts of the two-nucleon interaction.† In a few cases we have employed such potentials obtained by a Hartree-Fock calculation (see e.g. Ca-isotopes), but the status of the present generation of HF calculations is such, that the extremely model-dependent single particle energies obtained from this source should probably only be taken as a rough guidance. In regions where the single particle strength is distributed over a number of complex states, we have relied on variational searches with the aim of fitting odd mass spectra, again adding corrections dictated by the available evidence of pairing states in the even isotopes, and in these cases by readjusting the critical energy difference between filled and unfilled levels, to which the odd-even mass difference is critical.

The final single-particle energies employed are listed in table 2 of appendix 1, where also the pairing strengths G (table 1) and the collective boson Hamiltonians (table 3) are given.

It follows now a separate discussion of each region of isotopes. When no other source is mentioned, the experimental ground state energies are taken from Ma 65 and information on excited 0+ states from Aj 68,

---

†For non-superfluid systems the pairing force does not contribute to the average field, and for superfluid systems only in higher orders.

En 67 or Le 67 when not from quoted two-nucleon stripping experiments. The boson states are shown with heavy lines if they are built entirely of collective quanta, thin full lines if they are formed by one non-collective boson operator operating on the closed shell and dashed lines if they correspond to one of the other possibilities sketched in fig. 1. In some cases the non-pairing structure discussed in sect. 3 are indicated in a special column in the middle between the calculated and experimental spectrum. Unless otherwise stated the TDA normal mode representation has been used in the calculations.

He-ISOTOPES

In fig. 4, ^{4}He has been used as closed shell. The ^{4}He(p,t) experiment has been performed at E_p = 49.5 MeV (Gr 68). The calculated ^{2}He system consists of two protons without any correlation, since only neutron interaction is included. The T=0 resonance in ^{4}He, which has been reached by (p,^{3}He) (Ce 65), may be interpreted as the T=0 member of the pair vibration triplet. The T-splitting increases the discrepancy for the ^{8}He ground state which presumably is lowered by strong multipole forces ("deformation").

C-ISOTOPES

In fig. 5, ^{12}C has been used as closed shell. The (p,t) reaction on ^{12}C has been performed at an incident energy of 155 MeV (Ba 65), an energy at which there is very little structure in the angular cross sections to the excited states (yet a state at 5.6 MeV is assigned 0+), at 50 MeV (Gr 66) where a level seen at 7.2 MeV is the only one not known to be J≠0 and at 43 and 52 MeV (Be 67), which seems to rule out the 0+ assignment for a 5.3 MeV level believed to be identical to the 5.6 MeV level mentioned above. The suggestion of a 5.03 - 5.29 - 5.60 triplet

suggested from (^{3}He,t) (Ma 66) appears to be ruled out (Br 68a). Further experiments at 50 MeV (Ne 67), 54.9 MeV (Ta 67) and 20 - 54 MeV (Co 67) see no 0+ states except the ground state. The ^{14}C(p,t) reaction has been done at 18.5 MeV (Le 63) and 47.5 (Ga 69, Ce 68), in which experiment the T=2, 0+ level is observed and a level at 17.77 MeV may be associated with the T=1 0+. Both states are weakly excited. The reaction ^{12}C(t,p) has been performed at E_t = 5.5 MeV (Ja 60), assigning the 6.58 MeV level 1- and suggesting a 0+ at 7.01 MeV, at 0.4 - 1.2 MeV (Ku 62) and at 11 MeV (Mi 64), supporting the 6.58 MeV, 1- assignment but disfavouring the 7.01, 0+ assignment. Newer evidence from other sources (Aj 69) firmly suggests 0+ for the 6.58 MeV level but leaves the 7.01 MeV level unassigned. The ^{16}C ground state has been observed in (t,p) experiments at E_t = 6 MeV (Hi 61) and E_t = 12 MeV (Mi 64). The ^{12}C ground state is believed to be quadrupole deformed, and the 7.65 MeV 0+ state a possible β-vibration or coexisting spherical state (Ba 69).

The calculated ground state energies appear to be in good agreement with the experimental ones, and so is the first non-collective state in ^{14}C. In order to settle the 0+ assignment of the 6.58 MeV state we performed a DWBA analysis with the G_S-coefficients of the pairing calculation. The results which are shown in fig. 6, strongly disagree with the earlier plane wave calculation which led to the 1- assignment, and there seems to be no doubt of the correctness of the 0+ assignment.

The strength of the pair vibration in ^{12}C should be seen in (p,t), so we conclude that its strength is shared by several states and tentatively suggests an isospin splitting which incorporates the observed T=2 and

(presumably) T=1 0+ states together with the highest lying of the T=0 states. The lowest excited 0+ state is close to twice the 2+ energy and it may not be worthwhile to discuss the lowlying spectrum in terms of deformed and spherical multipole surfaces in view of the few particles involved. If the extremely large T-splitting suggested above is correct, one would also expect a considerable shift of the T=2 ground state of ^{16}C. That this is not observed may well be connected to the fact that the ^{16}C ground state has particles in the s-d shell, thus presumably being far from made up of two identical quanta. For this reason the boson energy of ^{16}C cannot be completely trusted. However, since the collective boson has only an amplitude 0.85 for the particles being in the $0p_{1/2}$ orbit, it may yet provide a fair description of the nuclei with four or more particles outside the closed $0p_{3/2}$ shell. It is a general fact that the structure of the collective boson branch may be expected to change each time one passes a considerable gap in the single particle spectrum. Formally this will appear as strong couplings between collective and non-collective branches, which has not been taken into account in the present calculation.

O-ISOTOPES

In fig. 7, ^{16}O has been used as closed shell. The ^{14}O ground state is seen in (p,t) at E_p = 43.7 MeV (Ce 64) and E_p = 50 MeV (Ne 67), the ^{16}O ground state at E_p = 17.6 MeV (Le 63). The excited levels are seen in (p,t) at E_p = 43.7 MeV (Ce 64a). As expected the deformed 0+ level at 6.06 MeV does not carry any (p,t) strength. A number of T=1 states are observed between 14 and 18 MeV, and one 0+ assignment has been made

(Ch 67). The spin assignment of the excited 0+ state in ^{14}O (Aj 69) is made from another member of the isospin multiplet (Re 69). The reaction ^{16}O (t,p) was studied at E_t = 5.5 (Ja 60), and at 10 MeV (Pu 62), the ground state transition further at 0.7 - 1.1 MeV (Kü 63) and 1.2 - 1.6 MeV (Ko 67). Reactions (t,p) on both ^{16}O and ^{18}O (first performed by (Ja 59)) has been performed at E_t = 2.0 - 2.6 MeV (Ja 60a), at 6 MeV (Hi 62), at 10 MeV (Mi 64) and at 5.5 MeV (Mo 65). The relative ground state cross sections quoted are presumably rather inaccurate.

The pairing calculation give good agreement for ground states and non-collective pairing excitations. The weak transition to the first excited 0+ state in ^{18}O is easily explained by assuming it to be a two-phonon quadrupole state (cf. sect. 3). A line is inserted in the middle column at twice the 2+ energy. In ^{16}O we have tentatively proposed the non-pairing type of isospin splitting. If the trend of the observed ground-to-ground transitions is correct, we will have to assume that the ^{20}O ground state has correlations other than pairing, which might also compensate the increase in energy caused by the isospin dependent pairing or monopole force. In an earlier study of the oxygen transfer reactions (Dö 67) the structure coefficients were calculated from shell-model wave functions including deformed configurations. Unusual optical parameters were needed to explain the angular distributions. Presumably the wave functions contain too little pairing type correlation, since the ratios of cross sections to excited states and to ground states are too large. The pairing calculation do somewhat better, and after the kinematics are introduced in DWBA the relative ground state transition ratio $^{18}O(t,p)/^{16}O(t,p)$ reduces to 1.1.

Ne-ISOTOPES

The ^{18}Ne closed shell has been used in fig. 8, the ^{24}Ne closed shell in fig. 9. The ^{20}Ne(p,t) experiment has been performed at E_p = 50 MeV (Ec 68), the ^{22}Ne(p,t) experiment at E = 43.7 MeV (Ce 64a). The ^{20}Ne ground state is deformed and one of the excited 0+ states around 7 MeV is probably a β-vibration. Since a pairing-type two particle state is present in this region, one might expect that the β-vibration is the state which does not receive (p,t) strength. However, this could also be a coexisting spherical state and in that case most likely the pairing state. The ground state energies calculated from the almost superfluid N=14 subshell suggest that the structure of ^{18}Ne is different from the other three, presumably of small deformation. This is further supported by the observation of a weak 0+ state in (p,t) at approximately twice the 2+ energy. The N=14 calculation appears superior to that based on N=8 in predicting the ground-to-ground transitions to be strong in the middle of the shell as compared to both closed shell ends, as one would expect.

Mg-ISOTOPES

The closed shell used for the presentation in fig. 10 is ^{26}Mg which is superfluid and presumably also deformed. The (p,t) pick-up reaction leading to ^{22}Mg has been performed at E_p = 50 MeV (Ga 68), the one leading to ^{24}Mg at E_p = 28 MeV together with the (α,^{6}He) reaction at E_α = 40 MeV (Ri 64), further (p,t) at E_p = 38.7 MeV (Ga 64), at E_p = 20 - 54 MeV (Co 67), at E_p = 50 MeV (Gr 67), at E_p = 42.1 MeV (Mc 67) and at E_p = 45.0 MeV (Ce 69). The (t,p) reaction leading to ^{26}Mg has been reported at E_t = 5.95 MeV

(Hi 61a, no angular distributions) and E_t = 11 MeV (Hi 65), the one leading to ^{28}Mg at E_t = 10 MeV (Mi 64a) and at E_t = 3.5 MeV (Mo 67, only ground state).

The situation is here different from that of C or O in that the closed shell nucleus has isospin T=1. The ground states of ^{24}Mg and ^{22}Mg are thus only the lowest isospin possibilities, so that an isospin splitting interaction can account for the deviations of ground state energies which are calculated with only neutron pairing. The T=2 state in ^{24}Mg which is rather strongly excited in (p,t) must relate its structure either to the ground state of that nucleus or to the non-collective, but strongly (p,t) favoured excited state. Several of the weak or in transfer non-observed ^{24}Mg levels can then be interpreted as the T-components of the pair vibration, especially since the lowest excited 0+ state has no E2 transition to the 2+. The three excited levels observed in ^{26}Mg are all T=1 and those in ^{28}Mg all T=2. One possibility is to associate the T=1 member of the ^{26}Mg pair vibration with the highest experimental state and accounting for the large strength to the lowest excited state by assuming large quadrupole admixtures between this and the ground state. The same sharing of strength is again found in ^{28}Mg, except that the combined mixing in target and final nucleus makes the (t,p) strength even more distributed. In each of the two nuclei there is still a 0+ level unaccounted for. The ^{28}Mg pair vibration is not supposed to play an important role, but the coupling of $(d_{3/2})^2_{J=0}$ configurations (the so-called non-collective ^{28}Mg excitation) the the ^{26}Mg β-vibration (denoted $|Q\rangle$ in fig. 10) and to the ^{24}Mg ground state can provide two states in the right energy region. In this picture the ^{26}Mg(t,p) ^{28}Mg ground state transition would be reduced with respect to the value in the pure pairing picture.

definite discrepancies, the most conspicuous being the absence of the strong non-collective state from the ^{38}Ar(p,t) data and the large shift of the ^{34}Ar ground state. The latter might be explained by introducing the isospin splitting of $\Delta N = -2$ bosons, but it then appears strange, that no similar splitting is observed for the $\Delta N = 2$ bosons.

Ca-ISOTOPES

Both the N=20 and the N=28 closed shells have been used for calculations. Fig. 15 uses ^{40}Ca as closed shell. In contrast to other regions of the periodic table the Coulomb energy in the Ca-isotopes seem not to follow the trend given by eq. (4.1), but rather to be the same for all the isotopes (Oo 66 and later Stanford data quoted by Sc 69). In fig. 15 a constant Coulomb energy has been assumed, but the comparison with ground state energies corrected for a Coulomb energy of the form (4.1) is given in fig. 16.

The reaction ^{40}Ca(p,t) has been investigated at E_p = 39.8 MeV (Ha 66), reporting an excited 0+ state at E_x = 4.36 MeV. The same reaction has been studied at 50 MeV (Da 67), where no excited 0+ state is seen, but a 2+ is assigned at roughly the same energy. The (p,t) reactions on ^{42}Ca to ^{48}Ca have been performed at 40 MeV (Ba 64), the ^{42,44}Ca(p,t) at 25.6 MeV (Sm 69) and at E_p = 18 MeV that on ^{48}Ca (Pe 68), ^{44}Ca and ^{42}Ca (Pe 67), the ^{42}Ca(p,t) reaction further at 42 MeV (Garvey and Cerny as quoted by Ce 68). The isotope ^{50}Ca has been seen in (t,p) studies at E_t = 3.2 MeV (Sh 64), 12.0 MeV (Hi 66), 7.5 MeV (Wi 66) and together with ^{42}Ca to ^{48}Ca at E_t = 10.1 - 12.08 MeV (Bj 67). The ^{40}Ca(t,p) reaction was already studied at E_t = 7.2 MeV (Mi 64a) and together with ^{44}Ca(t,p) at E_t = 7.5 MeV (Wi 67), disagreeing with Bj 67 only

in the 0+ assignment of the 6.7 MeV level. The 0+ assignments of excited levels in ^{50}Ca made by Hi 66 is not confirmed by Bj 67. Some of the data have been DWBA analysed by Ba 68 and Br 68b.

The lowest non-collective state calculated in ^{38}Ca should be extremely strong in (p,t) so we conclude that the weak observed state (if the spin assignment is correct) is a two-phonon quadrupole state, which agrees perfectly with its position. The lowest excited state in ^{40}Ca is supposedly deformed (Ge 67), and the third excited 0+ state agrees in energy with a two-phonon octupole state. The two remaining excited 0+ states could be the T=0 and T=2 members of a split pair vibration. No candidate for the T=1 member is present in the rather detailed (p,t) data available, but although the state close to twice the octupole vibrational energy has a reasonable position, its strength is much too small for being interpreted as the T=1 part of the pair vibration. Probably the interplay with quadrupole deformed states destroys the simple pairing picture. The fact that the deformed state gets a third of the ground state cross section implies a considerable deformed component in the ^{42}Ca ground state, accounting for the weakness of the (p,t) cross section to the pair vibration. An alternative interpretation of the 5.20 MeV 0+ state as an 8p - 8h configuration (Ge 69) required 7% of a similar parent component in ^{42}Ca. If the first excited 0+ state in ^{42}Ca is deformed its (t,p) intensity requires around 10% of the parent configuration in ^{40}Ca, i.e. less ground state correlations than in ^{42}Ca but still an appreciable amount. The corresponding configuration is not present in the ^{44}Ca ground state, judging from the weak (p,t) transition to the excited ^{42}Ca state. As one goes away from ^{40}Ca the pair vibration rapidly increases its energy, but

an extremely strong non-collective state in ^{42}Ca can be identified in this nucleus and its analogue in ^{44}Ca. This is of course the state which transforms into the pair vibration in ^{46}Ca and ^{48}Ca (based on the ^{48}Ca core). Some fractionation of its strength may be present in ^{42}Ca and ^{46}Ca. In ^{42}Ca there is one other non-collective pairing state present, and the two remaining states seen (possibly only one) must be other states (β-vibrations etc.) which mix with the pairing states. All together it is evident that the presence of complex core excited states in the closed shell nucleus on which we build our pairing calculation causes major disturbances in the pairing scheme. This is also beared out by the sequence of ground state energies.

We have tried to vary the single particle energies, an example of which is given in figs. 16 and 17. A set of single particle energies is here introduced, which is taken directly from a (spherical) Hartree-Fock calculation (Pa 68) except for the closed shell gap, which is still from the odd-even mass differences. As seen in fig. 16 the fit to ground state energies is slightly improved, but on the other hand the position of the lowest non-collective states in ^{38}Ca and ^{42}Ca (fig. 17) disagree with experiment. In order to avoid the influence of the deformed admixtures in the ^{40}Ca and ^{42}Ca ground states on the comparison for the remaining isotopes, we have also in fig. 16 given the calculated ground state energies referred to ^{44}Ca and ^{46}Ca, both for the calculation based on the HF single particle energies and that based on s-p energies adjusted from one-particle stripping experiments to reproduce non-collective two-particle and two hole 0+ states. However, with this gauge we still get fine agreement for the ^{42}Ca ground state energy, while the ^{48}Ca and especially the ^{38}Ca ground state would be implied to have additional correlation.

One additional piece of evidence comes from the ratios of ground state intensities and their absolute cross sections which are all known[†]). None of the calculated sequences of relative cross sections reproduce the experimental trend, and if we adjust the stripping interaction to give the absolute value of the $^{46}Ca(t,p)$ cross-section correctly for the calculation shown in fig. 15, it is 50% too large when the HF basis is used. On the other hand the $^{40}Ca(t,p)$ cross section then becomes 50% and 30% too small, respectively, in the two calculations mentioned.

The strong and rather continuously varying ground-to-ground cross sections supports the claim of correlations in the ground states, but on the other hand excludes any abrupt change in the structure of the ground states. As an exception the measured $^{40}Ca(p,t)^{38}Ca$ ground state cross section is only 21% of the $^{42}Ca(p,t)^{38}Ca$ cross section (fig. 15), which indicates a major difference between the ^{40}Ca and ^{38}Ca ground state wave functions. The experimental value is rather uncertain, since the two experiments are performed under different conditions, but the qualitative indication is that the ^{38}Ca ground state may be in fair agreement with the pairing wave function, contrary to the ^{40}Ca ground state. The ground state admixtures in the pairing wave functions are nearly the same in all the isotopes, namely around 0.25 - 0.30 (in amplitude)of the n=1 (see eq. (2.18)) or 2p2h configurations and 5% of the n=2 or 4p4h configurations.

[†]Our discussion is based on the absolute cross-sections coming from the relative data of Bj 67 in conjunction with the elastic triton scattering of some targets under the same conditions reported by Gl 67.

In fig. 18 we use ^{48}Ca as a closed shell. Here the c_1^+ boson contains 0.94 (amplitude) of $p_{3/2}^2$, the c_2^+ boson 0.91 of $f_{7/2}^{-2}$, leading to a total amount of ground state correlation which is 0.40 (still amplitude) in ^{48}Ca and about 0.55 in ^{46}Ca and ^{50}Ca. The amount of ground state correlation in ^{46}Ca is in agreement with experiment (Be 66a), that of ^{50}Ca in agreement with the predicted one from Br 68b although our ground state energy is 300 keV closer to experiment. The ground state correlation predicted for ^{48}Ca is in agreement with Pe 68, which quote a total amplitude 0.5 of admixtures, and as far as the $f_{7/2}^{-2}\ p_{3/2}^2$ component concerns, we predict 0.32 as compared to 0.3 to 0.42 (Pe 68), both in contradiction to an earlier given value of 0.17 (Co 66). The calculated ground state energies (fig. 18) are in reasonable agreement with the experimental ones in the region ^{40}Ca to ^{50}Ca. There are small deviations for ^{40}Ca and for the difference between ^{48}Ca and its two neighbours. Correcting for the latter difference by adding a little amount of correlation in the ^{48}Ca ground state we would get an increasing shift when approaching ^{40}Ca, as might be expected in view of the anticipated admixtures of deformed components. The pair vibration in ^{48}Ca is too high, and a lower-lying 0+ state is unaccounted for. This might be a deformed state, in which case the extra ground state correlation is explained. On the other hand there is no particular reason to expect a deformed state in ^{48}Ca. The similar lowlying state in ^{46}Ca has the exact energy and small transfer cross section which would be expected for a two-phonon quadrupole state mixing slightly with the pairing degree of freedom and so has the lowest (possible) 0+ excited state in ^{50}Ca. The claim that the ^{46}Ca state should be deformed (Mc 68) is thus not quite convincing. Further a deformed ^{48}Ca state which mixes

with ground state or pair vibrational state to get the observed (t,p) strength would push these states apart, contrary to the fact that both excited 0+ states are below the sum of the ^{46}Ca and the ^{50}Ca energies. It should be mentioned that the fourth order boson method with pure pairing force inevitably predicts the pair vibration to be above the sum of the neighbouring ground state energies. A speculative suggestion explaining the two excited ^{48}Ca levels is to assume in this nucleus a coexistence of normal and superfluid phases, such that the lowest excited 0+ state has the main superfluid component and the higher 0+ state has small average pairing distortion. A support for this idea comes from the potential energy surface (shown in appendix 2), which is very flat in the region $\Delta = 0$ to $\Delta = 3$, thus making important the higher order terms that are needed in order to produce a second equilibrium with $\Delta \neq 0$. Such terms are not considered in the present calculation and they may arise from other sources than the model pairing interaction. The presence of a second minimum will automatically lower the 0+ excitation energies, and the sharing of strength will remove strength from the ground state. In order to explain the large ratio of the ^{48}Ca(t,p) to ^{46}Ca(t,p) cross sections one will further have to assume that the coexistence of normal and superfluid phases are present both in ^{46}Ca and ^{48}Ca but not in ^{50}Ca. A phenomenological search for simple shell model wave functions which can explain the sharing of strength between the three ^{48}Ca states (Ko 69), finds no solutions which agree with the experimental limits for ^{46,48}Ca ground state correlations.

The ground state energies seem not to leave any room for isospin interaction between the boson quanta, and all states excited by the (t,p) reaction above ^{40}Ca must of course have the same isospin as the corresponding ground state.

As with the ^{40}Ca core, we have also here tried a calculation with single particle energies derived from a Hartree-Fock calculation (Pa 68), shown in fig. 19. The amount of ground state correlation is now increased. The ground state energies are much poorer, the ^{48}Ca pair vibration a little better and the overall variation of ground-to-ground cross section closer to the experimental one. This may, however, not be significant, since the values calculated with the first set of single particle energies (fig. 18) just leaves room for the inclusion of deformed components in ^{40}Ca and ^{42}Ca, thereby decreasing the cross sections involving these isotopes, and allowing for similar reductions due to residual correlations around ^{48}Ca.

None of the calculations have completely accounted for the sharing of strength between several levels at excitation energies around 5 MeV in ^{42}Ca and in ^{46}Ca. The dashed ^{42}Ca states indicated in fig. 18, of which some correspond to non-collective states and the pair vibration in fig. 15, at least show qualitatively that a large number of 0+ states can be expected. Also in ^{46}Ca several states are predicted, although not quite as many as are seen experimentally. Additional possibilities are numerous, such as e.g. coupling the lowest ^{44}Ca 2+ to the quantum creating the lowest ^{50}Ca 2+ state from the ^{48}Ca core. Some amount of admixture seems to be required if the fairly large (t,p) cross sections, which several of these states receive, shall be explained. A particular problem arises for the third and fourth excited state in ^{46}Ca, which are so close to each other, that they could not have been separated if much mixing were present. It is most likely that one of these states is the pair vibration lowered similar to the one in ^{48}Ca and the other one non-collective, in which case only higher order mixing can take place (one state is 2h, the other at least 2p4h).

In order to compare the pairing wave functions with the ^{50}Ca wave functions of Br 68b, which are calculated using the Hamada-Johnson G-matrix as effective interaction, we have calculated absolute cross sections for the $^{46,48}Ca(t,p)$ ground state reactions at E_t = 11.97 MeV (Bj 67), using the same optical model parameters as Br 68b and adjusting the stripping interaction (zero range limit of $V_0 \exp(-\beta R^2)$) to give the correct $^{46}Ca(t,p)$ cross section (implying V_0 = - 50 MeV and β = 0.2 fm^{-2}, the oscillator parameter was $A^{-1/3}$ fm^{-2}). In units of this integrated cross section the $^{48}Ca(t,p)$ cross section becomes 1.621 for the pairing boson wave functions and 0.738 for the H-J wave function (assuming here similar to Br 68b that no ground state correlations are present in ^{48}Ca, otherwise the number would be still smaller). The experimental number is 2.54 ± 0.06. It seems very unlikely that the prediction of the H-J wave function for the $^{48}Ca(t,p)$ cross section can be correct, since that would require a considerable change in the stripping interaction quoted above, which already uses parameters which approximately fits the two-nucleon transfer cross-sections in other medium heavy nuclei (e.g. the Zr transitions considered in fig. 28). One may conclude that the H-J type ^{50}Ca wave function lacks pairing type correlation but that the amount of pair correlation in our ^{50}Ca (or in the ^{48}Ca or both) ground state is too large. It is interesting that the pairing and H-J ^{50}Ca wave functions considered here have the same amount of $p_{3/2}^2$ configuration.

Ti-ISOTOPES

In fig. 20 the isotope ^{50}Ti has been used as a closed shell. The ^{44}Ti to ^{48}Ti ground states have been observed in (p,t) experiments at E_p = 40 MeV (Ba 64 and Ba 64a), those of ^{46}Ti and ^{48}Ti further at E_p = 28 MeV (Ri 64a). The T=2 state in ^{44}Ti was seen with E_p = 38.7 MeV (Ga 64). The ^{50}Ti(t,p) reaction has been studied at E_t = 7.5 MeV (Wi 66) and the ^{46}Ti, ^{48}Ti(t,p) reactions at 9.64 and 11.14 MeV (Hi 67).

As expected the picture is very similar to that of the Ca-isotopes. In particular a very strong 0+ state is seen in ^{50}Ti, apparently below the pair vibrations. The position of this lowest excited 0+ state is well above what would be expected for a two-phonon quadrupole state (in fact there are weak states present in the (t,p) data which may be candidates for that), and a deformed state can not get the huge amount of transfer strength unless the structure of the ^{48}Ti ground state is similar, which appears to be ruled out by the nearly harmonic quadrupole vibrational spectrum in ^{48}Ti. So it is tempting also here to suggest that the excited ^{50}Ti state is a superfluid state similar in structure to the ^{48}Ti ground state. Like in Ca the ground state energies seem to indicate a change in structure as the N=20 closed shell is approached, so a detailed study of the (p,t) reactions in this region would be very desirable. The T=2 state in ^{44}Ti is likely to be a pair vibration built on the ^{42}Ti core (similar in structure to the lowest non-collective state in ^{48}Ti). The third excited 0+ state in ^{48}Ti may be the pair vibration, lowered in energy by the same mechanism which describes the coexistence in ^{50}Ti. The pairing type of coexistence is only expected to occur at shell closures, since the inverted coexistence - superfluid ground state and normal excited state - is not possible with a pairing force,

which implies $\partial V_{pot}/\partial\Delta < 0$ for every system with superfluid ground state. On the other hand, no matter what the structure of the potential energy is at low excitation energies, it is possible (and for the truncated boson expansion a fact) that highly excited states all have $\Delta \approx 0$.

A total of four excited states have been observed in ^{50}Ti (in contrast to two in ^{48}Ca). Having described the two lowest as superfluid and pair vibrational, it is possible to associate the remaining, weaker states with quadrupole degrees of freedom. The energy of the 2+ state in ^{52}Ti is 1.05 MeV (Wi 66), and that of the ^{48}Ti 2+ state 1.56 MeV, combining to a 0+ state in ^{50}Ti at around 6.6 MeV. This state is excited via a two-step process and therefore rather weak. Slightly higher will come the states combining the two-phonon quadrupole state of ^{52}Ti with the ground state of ^{48}Ti and vice versa. The former of these will be strongest in the (t,p) reaction. All of these states will be affected by anharmonic quadrupole coupling effects. Similar structures can be formed in ^{48}Ti, but are probably higher in energy than the range covered by the quoted experiment. Isospin splitting may affect particularly the pair vibrational states by lowering them and shifting strength to the higher T-members, which can not be observed in the (t,p)-experiments.

It should be mentioned that Hartree-Fock calculations of ^{44}Ti to ^{50}Ti (Pa 68) predict systematic prolate quadrupole deformations. However, these authors suggest that the HF minima may not be very stable towards pair correlations, a remark which should apply to most shallow HF minima. Unfortunately, the quoted argument (Pa 68) is based on non-superfluid ^{44}Ti wave functions, but it is almost certain that similar conclusions will

emerge from the appropriate Hartree-Bogliubov calculations, thus reconciling the remarkable success of the mass predictions of the present pairing calculation with the picture offered by ordinary HF method.

Cr-ISOTOPES

Fig. 21 uses ^{52}Cr as closed shell. The ^{52}Cr(p,t) experiment has been performed at E_p = 40 MeV (Ba 64a) and together with ^{54}Cr(p,t) at 17.5 MeV (Wh 67). The ^{50,52,54}Cr(t,p) reaction has been studied at E_t = 12 MeV (Ch 68). The intensities quoted in the figure from the latter experiment are ratios at 5°, whereas the (p,t) data lacks forward angles and hence are quoted at the "second maximum". This may make a difference, e.g. the (t,p) cross section to the first excited 0+ state in ^{52}Cr is only 0.5 of the ground state transition if quoted at the second maximum as compared to 1.17 at forward angles. Further the (t,p) angular distributions are rather state dependent. The low value quoted for the ^{52}Cr(p,t) cross section (E_p = 17.5) may thus be partly due to kinematics, as also suggested from the fact that the (rather uncertain) cross section from the E_p = 40 MeV experiment is about 5 times larger (in absolute value).

That a significant change in cross section occurs when passing from mainly p-shell configurations to mainly f-shell configurations is beared out by the calculation, predicting a reduction by a factor of two. The excitation spectra are similar to the corresponding Ca and Ti cases, except for the fact that the first excited 0+ state in ^{52}Cr lies in the region of the two-phonon quadrupole vibration. It is thus conceivable that the latter state gets its strength from the pair vibration rather than from the ground state, due to

the common $f_{7/2}^{-2}\ p_{3/2}^{2}$ component. Otherwise the large (t,p) and small (p,t) strength of the pair vibration would be unaccounted for. As the figure indicates, both non-collective pairing states and states with quadrupole type correlations may be candidates for the two highest observed states. Isospin splitting would be another mechanism for removing (t,p) strength from the pairing states, but in order to investigate the effect of that the (p,t)-experiments above N=28 will have to be carried to higher excitation energies.

The remarks on ground state deformations made under Ti also apply here.

Fe-ISOTOPES

In Fig. 22 ^{54}Fe has been used as closed shell. The reactions ^{54,56,58}Fe(p,t) have been studied at E_p = 40 MeV (Ba 64a), the two latter ones further at 28 MeV (Ri 64a) and ^{58}Fe(p,t) at 22 MeV (Ba 63). The T=2 state in ^{52}Fe has been looked at with E_p = 38.7 MeV (Ga 64) and 40 MeV (quoted by Ce 68 and Ce 69). The (t,p) experiments are performed at E_t = 12 MeV (on ^{54}Fe, Co 66a, on ^{56}Fe, Co 67a). The ground state (p,t) data of Ba 64a does not include the forward angles, which gives rise to the big ratio ^{58}Fe/^{56}Fe of Ri 64a. If the ratios were considered at the second maximum, the two experiments agree. It thus appears as if the ratio obtained from the (t,p) experiments are more trustworthy. The performance of the (p,t) experiment leading to the closed shell nucleus suggests itself.

The calculation does not reproduce the ground state energies very well, and it appears as if some of the isotopes may be deformed (e.g.

^{56}Fe and not ^{58}Fe). The T=2 state in ^{52}Fe is naturally explained as the T=2 component of the lowest non-collective state (a T=1 2-hole pair coupled to the T=1 ^{54}Fe ground state). The impressive amount of 0+ levels in ^{56}Fe and ^{58}Fe includes multipole vibrational states etc.

Ni-ISOTOPES

Calculations based on both the ^{56}Ni and the ^{68}Ni closed shells have been performed, the results being compared with experiment in figs. 23 and 24. The ^{58}Ni(p,t) experiments have been performed at E_p = 28 MeV (Ho 65), at 50 MeV (Da 68) and at 45 MeV (Garvey and Cerny, Ga 69a). Further this reaction was studied together with ^{60,62}Ni(p,t) at E_p = 28 MeV (Ri 64a and Ko 64) and together with ^{60,62,64}Ni(p,t) at E_p = 40 MeV (Ba 64a) and at 28 MeV (Da 68a). The ^{58,60,64}Ni(t,p) reactions are investigated at E_t = 12.12 MeV (Da 69).

There are several indications that ^{56}Ni is not a "good" closed shell. The form of the pairing interaction in eq. (4.2) makes it comparatively stronger in T=0 nuclei, in fact making ^{56}Ni superfluid with the chosen parameters. Hartree-Fock calculations using Yale-Shakin potentials (Pa 68) predicts either strong prolate deformation or almost zero (slightly oblate) deformation. A calculation using Hamada-Johnson G-matrix elements as effective interaction (Wo 68) predicts 46% of 2p2h and 38% of 4p4h components. One of their excited states in the 5 MeV region has 81% 4p4h, which would fit with the lowest 0+ excited state, if the ^{60}Ni ground state remains spherical. A DWBA analysis of some of the (p,t) data using pairing interaction has been presented by Ba 68. The T=0,1,2 triplet at 6.7 to 10 MeV excitation

energy gave rise to the proposal of isospin structure of the pair vibration by Bo 68.

The calculation based on ^{56}Ni is shown in fig. 23. The single particle energies are adjusted from experimental ones, but very similar results are obtained with a set of Hartree-Fock energies which simulate the deformed solution mentioned (this set is denoted "quasi-deformed" by Pa 68). However, the ground state energies do not follow the experimental ones, and in order to find the region of discrepancy we have in the middle columns (dashed lines) added a term linear in N_1 so that ^{60}Ni and ^{62}Ni are exactly reproduced rather than ^{56}Ni and ^{58}Ni. Thereby we actually obtain reasonable agreement except for a 1-2 MeV discrepancy at N=28 and 30. We thus conclude that these two isotopes contain non-pairing type correlations, which explains why basing the energy scaling on forcing the pairing states to reproduce these two isotopes leads to completely wrong ground state sequences. Actually the pairing wave function of the ^{56}Ni ground state contain 0.84 (in amplitude) of the closed shell configuration, in contrast to the effective interaction calculation mentioned above. Assuming the weak excited 0+ state to be mainly 4p4h, the pairing spectrum appears quite reasonable, exhibiting the isospin splitting of the pair vibration and sharing of its total (p,t)-strength, which is only about a quarter of the ground state cross section due to the superfluidity of the ground state. If this splitting is of the nature discussed in sect. 3, it will also increase the energy of the N=32 (and higher) isotope by a couple of MeV. Introducing further the isospin independent pairing force Bo 69, see eq. (3.1), this will raise the T=2 ground state of ^{60}Ni by an estimated 2.5 MeV, altogether bringing it close to the experimental value. Until decisive evidence on the structure

of ^{56}Ni becomes available, the two interpretations presented appear equally attractive, either to consider ^{60}Ni to ^{66}Ni as mainly governed by a neutron pairing force and 2p2h components entering into the ^{58}Ni and ^{56}Ni ground state wave functions or, alternatively, to view the nuclei around ^{56}Ni as governed by an isospin independent pairing force plus some T-splitting interaction, which presumably will have to decrease in magnitude when adding particles to the closed shell, since the isospin shifts do not increase as rapidly as T(T+1).

The lowest 0+ excited states in the isotopes above N=28 are apparently identical to the two-phonon quadrupole vibrations, and the combinations of non-collective pairing states give enough candidates for the remaining states. The predictions for the ground state intensities are rather good, thus supporting the pairing picture as far as ground state correlations are concerned, and at the same time disfavouring the HJ-effective force ^{56}Ni wave function, which can hardly be expected to connect with a conventional ^{60}Ni ground state wave function without abrupt lowering of at least one of the two-neutron transfer cross sections. The claim that the ^{60}Ni wave function must have a large component of the pairing wave function is based on its pretty harmonic multipole spectra and the presumption that large ground state admixtures would imply large anharmonicities[†]).

It should be pointed out that the boson calculation reproduces the rise of the ground-to-ground cross sections when going from a major shell

---

[†])Evidence in the opposite direction may be offered by the observation of large static quadrupole moments in quadrupole vibrational states exhibiting almost harmonic spectra, but in these cases the cross-over E2 transitions are extremely weak, suggesting that the ground states do not receive much admixtures.

closing towards the middle of the shell and the subsequent decrease when approaching the next gap in the single particle spectrum (in this case at N=40). The harmonic treatment of the pair quanta of course cannot reproduce this systematic trend.

In fig. 24 the calculation is based on the (unknown) ^{68}Ni isotope, thereby providing a more reliable set of non-collective pairing excitations for the upper end of the series of known isotopes. However, approaching N=32 the calculated transfer cross sections become extremely small, due to a complete change in the boson wave functions. This change is caused by the emptying of two single-particle levels and the corresponding action of the exclusion principle through the boson expansions, which happens in the truncation employed to cause a failure to describe nuclei with more than six holes in the N=40 core. Such a failure may be expected to occur accidentally when several shells of low degeneracies are bordering the closed shell nucleus, but far from always as e.g. the calculation based on ^{56}Ni shows.

Zn-ISOTOPES

In fig. 25 ^{70}Zn has been used as closed shell. The (p,t) reaction on ^{64}Zn to ^{70}Zn have been studied at E_p = 40 MeV (Ba 64a) and 17.5 MeV (Mc 66), ^{68}Zn(p,t) further at E_p = 55.17 MeV (Ya 67), the ^{64,66}Zn(t,p) reactions at E_t = 12 MeV (Gl 69 and Hu 68). Since ^{70}Zn is superfluid, N=40 is not a good closed shell in this Z-region, and it is interesting to see whether the fourth order boson calculation is able to describe this series of superfluid isotopes. In fact, the similarities of the wave functions of corresponding states in different isotopes and the approximate constancy of the transfer

cross-sections are features of the calculation, although the quadratic increase in ground state energies when going away from the "closed shell" is not quite reached. Of course, the "pair vibrations" become weak and must interact with the non-collective states, since the definitions of collective and non-collective would partly interchange if another "closed shell" was employed.

Sr-ISOTOPES

In fig. 26, ^{88}Sr has been used as closed shell. The ^{86,88}Sr(p,t) reaction has been studied at E_p = 49.5 MeV (Da 68a). The only excited 0+ states observed can be associated with the two-phonon quadrupole vibrations. The quoted ground state transition ratio is preliminary since the thickness of the ^{86}Sr target used has not yet been accurately measured.

Zr-ISOTOPES

In fig. 27 we use ^{90}Zr as closed shell. The ^{92}Zr(p,t) has been studied at E_p = 22 MeV (Ba 63), ^{92,94,96}Zr(p,t) at the same energy (Go 63) and $^{90-96}$Zr(p,t) at 40 MeV (Ba 64). A more exotic two-neutron transfer reaction,(^{15}N,^{17}N), has been applied to the isotopes ^{90,92,94}Zr at ^{15}N energies ranging from 70 to 120 MeV (Po 63). No excited 0+ states were identified in any of these experiments. The ^{90}Zr(p,t) reaction has been studied at E_p = 55 MeV (Ta 69), at 31 MeV (Ba 69a) and together with $^{92-96}$Zr(p,t) at 38 MeV (Ba 69b). The ^{96}Zr(t,p) has been studied at E_t = 20 MeV (Bl 69) together with $^{90-94}$Zr(t,p) (Be 68 and Fl 69).

The calculated ground state energies are generally good, probably indicating that N=50 is a very good closed shell. The lowest excited 0+ state observed in most isotopes is likely to be a proton excitation mixing slightly with the ground state. In ^{88}Zr there is further evidence for the two-phonon quadrupole state. The large jump in the 2+ energy occurring in ^{96}Zr seems to indicate a change in structure, supported by the sudden shift of (t,p) strength from the ground state to the first excited 0+ state, which may be the lowest non-collective pairing state, which decreases in energy as moving away from the closed shell. At the same time we expect the assumption of independence of the collective and non-collective branches to become less valid so that these will mix and share (t,p) strength (^{96}Zr), eventually producing only one pairing state with (t,p) strength in ^{98}Zr where no excited 0+ state has been identified below 4 MeV. It should be beared in mind, that there is a 1.3 MeV energy gap between the $1d_{5/2}$ shell closed at ^{96}Zr and the $2s_{1/2}$ and then again 1.3 MeV to the next shell, which might imply that

the ^{96}Zr and ^{98}Zr ground states are closer to being pure shell model states than to the pairing wave functions.

Three 0+ states are seen in $^{92}Zr(p,t)$ at ^{90}Zr excitation energies between 4 MeV and 5.5 MeV. The two-phonon octupole state in ^{90}Zr is expected at approximately the same energy as the pair vibration, but of course with less transfer strength unless they mix. Further the two-phonon quadrupole and 2^5-pole vibrations are expected in this region, and if our single-particle energies are correct no non-collective pairing states can occur below 8 MeV. The DWBA calculation shown in fig. 28 shows that the expected (p,t) strength of the pair vibration is 45% of the ground state (rather than the 73% from the simple estimate (2.26)). One is thus tempted to suggest that the strength of the pair vibration is fractionated among three states, indicating a strong mixing between the pairing degree of freedom and the other two, which most likely are the quadrupole and octupole fields.

In an attempt to understand the difference between the relative ground state transitions derived from the (t,p) and (p,t) experiments, we have performed a DWBA calculation of both using the pairing wave functions, the results of which is shown in fig. 28. One should note the large difference in the $^{90}Zr(p,t)$ angular distributions obtained with incident energies 31 MeV and 38 MeV. This explains why one cannot expect the (p,t) experiments at 38 MeV to give results approximately related by time-reversal to the 20 MeV (t,p) experiments. In most other regions of nuclei a similar difference in energies would not make any drastic difference. The calculated ratios of total ground state (t,p) cross sections for final nuclei 92:94:96:98 are 1.00:1.27:1.28:1.11 as compared with the experimental 1.00:1.40:1.55:1.50. The calculated ratios of total ground state (p,t) cross sections for final nuclei 88:90:92:94 are 1.04:1.00:1.19:1.11 as compared with the experimental

intensity ratios 0.6:1.0:1.3:1.0. In contrast to the simple estimates given on fig. 27 the DWBA values reproduce the earlier decrease of the (p,t) than the (t,p) cross sections. The calculated cross sections shown in fig. 28 agree quite well with the experimental ones with the exception of the ^{96}Zr(t,p) which is slightly underestimated and ^{90}Zr(p,t), which is much too large. The over-estimation of this transition is likely to lead to a similar error in the (p,t) cross section to the pair vibrations. For that reason the actual strength of this state in ^{90}Zr may already be exhausted by the observed 5.45 MeV level. The DWBA value for the (p,t) cross section to the ^{92}Zr pair vibration is 23% of the ground state. If this number is to be further reduced by the ratio between calculated and experimental ^{90}Zr(p,t) cross sections, it may explain why the ^{92}Zr pair vibration has not yet been recognized.

Cd-ISOTOPES

In fig. 29 we use ^{114}Cd as a closed shell. The $^{110-116}$Cd(p,t) experiments have been carried out at E_p = 40 MeV (Ba 65a and Ba 64), ^{110}Cd(t,p) at E_t = 10 MeV (Mi 64a) and $^{110-116}$Cd(t,p) at 11.14 MeV (Hi 67a). The single particle energies used in the pairing calculation are predominantly from a least square fit to the odd-A spectrum (Be 68a).

Again we see the fair ability of the fourth order boson calculation in a number conserving basis to describe a series of superfluid nuclei, including the concentration of transfer strength in the ground state transitions. Only if the p-n correlation energy stays constant one can neglect the protons in calculating the ground state energies. High-lying non-collective states

are predicted which involves excitation of pairs from the next lower (or higher) major shell, to which the superfluidity does not reach, so that larger cross sections may again be expected. The structure of the "pair vibration" is not qualitatively different from that of low lying non-collective states. In the same region two-phonon quadrupole vibrations are present, which again get transfer strength either by the mechanisms described in sect. 3 or by two-step processes involving inelastic excitation to (or from) the 2+ state.

Sn-ISOTOPES

Both ^{116}Sn (fig. 30) and ^{120}Sn (fig. 31) have been used as closed shell. There have been reported (p,t) experiments at E_p = 40 covering ^{112}Sn to ^{124}Sn (Ba 65a, $^{116-120}$Sn(p,t) also reported in Ba 64), ^{120}Sn(p,t) at 20 MeV (Ho 67), ^{118}Sn(p,t) at 55.15 MeV (Ya 68) and all Sn isotopes at E_p = 30 MeV (Ca 67). The ^{116,118}Sn(t,p) has been investigated at E_t = 12 - 13 MeV (Bj 68a) and the ^{122,124}Sn(t,p) at 20 MeV (Be 68).

The reason for the changes in single particle energies from ^{114}Cd to ^{116}Sn (cf. table 2) is the difference in proton correlations, which in the pairing calculation should be reflected in the average field.

The ground state energies above the ^{116}Sn shell closure are very well reproduced, somewhat better than the ones below. At ^{108}Sn a jump occurs indicating a complete change in structure. The ground state transitions are reasonable, considering an estimated ± 15% inaccuracy in the experimental values, but for the large-N isotopes the calculated values drop unphysically. The predicted excited 0+ energies are in agreement with the experimental ones in the region around the assumed closed shell, so are the (t,p) strengths, but some

of the (p,t) strengths appear to be too large. In this region of isotopes we have also indicated the strong non-collective states involving the next lower or higher major shell.

The calculation starting from ^{120}Sn (fig. 31) shows similar agreement for the ground state energies, best at the higher isotopes, and the calculated transfer cross sections are fairly constant in all cases as expected for a set of superfluid isotopes, although the detailed fluctuations in the experimental values are not reproduced. However, at least from ^{114}Sn to ^{126}Sn, it is within experimental errors to consider the cross sections as constant. The calculated transitions to excited states are in better agreement with the available data than those of the ^{116}Sn calculation. The position of the $1f_{7/2}$ and $2p_{3/2}$ levels have been adjusted in such a way that the non-collective states involving mainly these configurations have the energies in ^{124}Sn and ^{126}Sn corresponding to the two strong states observed in the (t,p) reactions.

In order to exhibit the ability of the fourth order boson method to deal with with superfluid systems, we have calculated the occupation numbers of the various single particle levels in the ^{120}Sn ground state

$$N_j = \langle 2b_j^+ b_j \rangle = 2 \langle c^+ c \rangle \left(r_1^2(j)\, \delta_{j>} + r_2^2(j)\, \delta_{j\leqslant}\right) \qquad (4.3)$$

where for the N_0 nucleus

$$\langle c^+ c \rangle = \langle c_1^+ c_1 \rangle = \langle c_2^+ c_2 \rangle = \sum_n n\, \phi_n^2 \qquad (4.4)$$

in the notation of sect. 2. These we compare in fig. 32 with the corresponding numbers v_j^2 of the BCS ground state wave function.

A discussion of the ^{116,118}Sn(t,p) reactions in terms of the BCS model plus harmonic correlations are given in Br 68c.

Te-ISOTOPES

In fig. 33, ^{134}Te has been used as a closed shell. Although this isotope has been produced (Fe 62), no mass determination is available. We include Te in our survey because (p,t) experiments are planned at the Oak Ridge National Laboratory. Despite the N=82 shell closure, the calculation predicts ^{134}Te to be superfluid. Similar (t,p) experiments on Ba-isotopes are in progress at Los Alamos Scientific Laboratory. The known excited 0+ states are two-phonon quadrupole states.

Ce-ISOTOPES

In fig. 34, ^{140}Ce has been used as a closed shell. This N=82 nucleus seems to provide an excellent opportunity to look for pair vibrational degrees of freedom, but no two-nucleon transfer experiments have yet been performed. Both (p,t) and (t,p) experiments are planned at Los Alamos Scientific Laboratory. The excited state observed in ^{140}Ce (Ch 65) is mainly a two-proton quasi-particle configuration.

Nd-ISOTOPES

In fig. 35, ^{142}Nd has been used as closed shell. The ^{148,150}Nd(p,t) reaction has been studied at E_p = 40 MeV (Ma 66a).

The calculated ground state energies are in remarkably good agreement with the experimental ones, yet ^{148}Nd and ^{150}Nd are deformed nuclei. This is probably due to the cancellations of two contributions to the ground state energy, one coming directly from the deformation and one from a simultaneous discontinuous change in superfluidity, both of which would be incorporated in a Hartree-Boguliubov calculation. Comparing the experimental ground state cross sections with the calculated ones, it appears that the strength going to the first excited 0+ state in ^{148}Nd is entirely taken from the pairing ground state. The excited state in ^{142}Nd is a two-proton quasi-particle state. It is not clear at present what becomes of the pair vibration in deformed nuclei, but if no significant gap exists in the relevant Hartree-Fock spectrum, one would expect it to be absent. In quadrupole transitional regions the spherical pair vibration may exist as a coexisting level.

Sm-ISOTOPES

In fig. 36, ^{144}Sm has been used as closed shell. The ^{150,152}Sm(p,t) experiments were first performed at E_p = 40 MeV (Ma 66a), more recently together with ^{154}Sm(p,t) at 55 MeV (Is 67) and together with ^{144,148,154}Sm(p,t) at E_p = 50 MeV (Ga 67). The ^{150}Sm(t,p) reaction was studied at E_t = 12 MeV (Hi 65a) and together with ^{144,148,152,154}Sm(t,p) at the same energy (Bj 66).

Because of lack of experimental evidence the predictions of the pairing model for the closed shell nucleus cannot be discussed. The onset of quadrupole deformation for increasing neutron number naturally destroys the pairing picture. Judging from the ground state energies, the admixture of deformed components starts already in ^{148}Sm. This is in agreement with the experimental quadrupole moment of the 2+ state and with a

calculation of the potential energy for this nucleus as function of quadrupole deformation (Sø 69a) which, however, disagrees with a calculation based on the adiabatic assumption (Ku 68)). Despite the change in ground state energies, the ^{148}Sm and ^{150}Sm wave functions appear to be mainly given by the pairing ground states, as the correctly predicted ^{148}Sm(t,p) to ^{150}Sm ground state cross section suggests. On the other hand, increasing (p,t) cross section to lowlying excited 0+ states suggests that these nuclei are very soft and presumably transitional. The highest 0+ state in ^{148}Sm is a candidate for the spherical pair vibration. A similar strong state is observed in ^{150}Sm and ^{152}Sm, but in these cases the large parentage to the N+2 ground states suggests that these excited states are more quadrupole deformed than the respective ground states. Other lowlying excited states are strongly excited by the (t,p) as well as (p,t) reactions, including the β-vibrations. This is to be expected since these states are two-quasi-particle states in the deformed representations, which means that they may be reached by two-nucleon transfer processes in the same way the quadrupole one-phonon vibration is reached in spherical nuclei. Viewed from the spherical representation both the deformed ground states and the two-quasi-particle collective states have large components of the spherical pairing ground states, which enables us to understand that the sum of the cross sections to these lowlying deformed states add up to approximately the cross section predicted for the corresponding spherical pairing ground state.

The clearest indication of the transitional character of ^{150}Sm are the two first excited 0+ states, which are strong in (p,t) but of which one is not seen at all in (t,p). Adding the similarity between the ^{148}Sm

and ^{150}Sm ground states it appears that ^{150}Sm is an example of coexistence of the type discussed in fig. 2c.

Pb-ISOTOPES

In fig. 37 ^{208}Pb is used as closed shell. At E_p = 40 (p,t) reactions on ^{208}Pb (Sm 67) and ^{204,206,208}Pb (Re 67) have been studied, the ^{208}Pb(p,t) reaction further at 22 MeV (Fl 67, Ho 67a and Br 67, Ig 68) and at 20 MeV (Ho 67a and Br 67), the ^{210}Pb(p,t) reaction at 20.5 MeV (Ig 68). The ^{204}Pb(t,p) reaction has been studied at E_t = 11.95 MeV (Bj 67a) and 20 MeV (Fl 67), the ^{206}Pb(t,p) reaction at 12 MeV (Bj 66a) and at 20 MeV (Ig 68). Finally the ^{208}Pb(t,p) reaction at E_t = 13 MeV (Bj 68) and 20 MeV (Ig 68).

The ground state energies below N=124 are not well reproduced by the boson calculation, reflecting the change in structure occuring between ^{206}Pb and the isotopes below because of the low degeneracy of the $2p_{1/2}$ level. This change of structure will in the boson picture be caused by interaction between the chosen collective c_2^+ boson (containing a substantial $2p_{1/2}^{-2}$ component) and the non-collective ($\Delta N = -2$) bosons, an interaction which has been neglected in the present calculation. As, however, the single particle levels below N=126 are rather close together and the collective branch therefore contains considerable components other than $2p_{1/2}$, the exclusion principle acts through the boson expansion of the interaction and we still expect the structure of at least the isotopes fairly close to N=126 to be reasonably well described, which we think is indicated by the agreement between calculated and experimental (p,t) ground state transitions.

Two non-collective states in ^{206}Pb and the pair vibration in ^{208}Pb are found in both (t,p) and (p,t) experiments. The assumption in our model, that the non-collective pairing states do not mix with the corresponding ground states is very strongly supported in ^{206}Pb by an inelastic proton scattering experiment (Va 67), which do not see the 1.16 MeV or 2.32 MeV states, implying for both states a maximum differential cross section of 5 μb/st. In ^{208}Pb further a 0+ state is seen above the pair vibration. This state has an energy of a harmonic two octupole phonon vibration but then has to mix with ground state or pair vibration. A non-collective state is expected at approximately the same energy, so both interpretations seem possible. Half an MeV higher in excitation energy the 2+ states have been observed (Ig 68), which may be interpreted as combinations of the ^{210}Pb ground state with the ^{206}Pb quadrupole vibration ($2_- \; 0_+$) and the ^{204}Pb ground state with the ^{210}Pb quadrupole vibration ($0_- \; 2_+$) (cf. Bo 68), so we expect around 6.6 MeV to see a 0+ state formed out of the two quadrupole vibrations ($2_- \; 2_+$). Candidates for this state are present in the partially analysed Los Alamos data (Ig 68).

The ^{208}Pb pair vibration was the first to be recognized as such (Br 67a). Other calculations of 0+ states have studied the reactions ^{204}Pb(t,p) (Br 67b), ^{206}Pb(t,p) (Sø 67), ^{208}Pb(t,p)(Ri 68 and Gl 68) and ^{208}Pb(p,t) (Gl 67a and Gl 68).

U-ISOTOPES

The calculation shown in fig. 38 uses ^{228}U as closed shell. The ^{236,238}U(t,p) reactions have been studied at E_t = 12.05 MeV (Mi 63). These isotopes are the most superfluid which have been included in the present survey and the boson calculation must be considered as rather inaccurate,

exemplified by a 3.66 MeV shift of the ^{228}U ground state from its TDA energy due to anharmonicities. Evidence for rotational spectra are present in $^{230-240}U$.

5. Conclusions

We believe in the calculations presented in the preceeding survey to have demonstrated the importance of pairing type correlations in the structure of even-N nuclei, both in explaining the ground state energy systematics and in describing excited 0+ states, of which the collective pair vibrations have attracted special attention ever since their existence was first anticipated (Bo 64). It is further clear that the consideration of anharmonic effects is necessary if a comparison is to be made with experimental energies and two-nucleon transfer cross sections.

We have found evidence for a number of deviations from the picture provided by the neutron pairing calculation, most of which are mentioned in sect. 3. The isospin structure is mainly found for $Z \leqslant 20$, but the magnitude of splittings, both between like and unlike quanta, are of little regularity and suggests that the residual interaction responsible for these effects, i.e. mainly the p-n interaction, cannot be described by a constant J=0 matrix element similar to the n-n pairing interaction.

Couplings between collective and non-collective pairing branches are found to be important in some regions, which just means that one has to use a more exact diagonalization of the pairing force than the one used in the present calculation.

Various kinds of coexistence have been proposed. The coexistence of a superfluid ground state and normal excited states is trivially present in most of the cases being discussed, namely whenever the closed shell nucleus is normal, the neighbouring nuclei superfluid and the energy of the excited state above the energy gained by distorting the nucleus. If the shell is large enough to allow addition or subtraction of many neutrons in such a way that

the pair vibration gets lower than the energy associated with the superfluidity, then this state will loose its collectivity. In a few cases (^{48}Ca etc.) the opposite coexistence, that between a normal ground state and a superfluid excited state, is an open possibility. One would in such cases not expect the pairing force with constant matrix element to be able to describe these higher order effects accurately. In transitional regions a further coexistence between spherical and deformed pairing states can be expected.

The very collective surface multipole vibrations are in several cases close in energy to the pairing excitations and it is likely that they borrow transfer strength by admixture.

We summarize in fig. 39 the systematics of the positions of pair vibrations at major neutron shell closures.

The stimulating influence of Prof. A. Bohr made me write in 1965 the computer program used for the present calculation. At that time it was not clear whether the pair vibrations required a description including anharmonicities but the same source of inspiration caused the initiation of a still increasing number of experiments directed at testing the validity of the assumptions made concerning the structure of pairing states. I am very grateful toward the large number of experimentalists which so readily furnished me with unpublished or preliminary data.

Appendix 1. Parameters and Boson Hamiltonians

Table 1 gives the neutron pairing strengths G and table 2 the single particle states and energies for each closed neutron shell considered. In table 3 we give the calculated boson Hamiltonians, in order that one may understand the type of anharmonicity present and judge the convergence of the fourth order expansion. The parametrization follows eqs. (2.13) or (2.14) and (2.15), except that $B_1' = B_1 + \frac{1}{2}\omega_1$ and $B_2' = B_2 + \frac{1}{2}\omega_2$. The quantities $2B_1'$ and $2B_2'$ give the energies associated with the normal mode bosons (which in the harmonic approximation were ω_1 and ω_2) and the coefficient A_1 measures the amount of RPA type ground state correlation (although RPA could not be used if A_1 is large, the condition being that ρ_2 of eq. (A.11) in appendix 2 stays positive) The remaining coefficients specifies the types of anharmonic correlations between several collective boson quanta.

Table 1

Pairing strengths G

N_0-nucleus	G	N_0-nucleus	G
^{4}He	4.00	^{54}Fe	0.35
^{12}C	1.80	^{56}Ni	0.411
^{16}O	1.125	^{68}Ni	0.293
^{18}Ne	0.95	^{70}Zn	0.36
^{24}Ne	0.60	^{88}Sr	0.22
^{26}Mg	1.0	^{90}Zr	0.234
^{28}Si	0.9	^{114}Cd	0.178
^{32}S	0.719	^{116}Sn	0.178
^{38}Ar	0.55	^{120}Sn	0.163
^{40}Ca	0.575	^{134}Te	0.143
^{40}Ca (HF)	0.55	^{140}Ce	0.143
^{48}Ca	0.38	^{142}Nd	0.143
^{48}Ca (HF)	0.40	^{144}Sm	0.16
^{50}Ti	0.419	^{208}Pb	0.086
^{52}Cr	0.30	^{228}U	0.095

Table 2

Single particle levels and energies

^{4}He	$0s_{1/2}$	$0p_{3/2}$	$0p_{1/2}$				
ε	-10.78	10.78	15.38				
^{12}C	$0s_{1/2}$	$0p_{3/2}$	$0p_{1/2}$	$0d_{5/2}$	$1s_{1/2}$		
ε	-20.5	-6.89	6.89	11.1	12.7		
^{16}O	$0s_{1/2}$	$0p_{3/2}$	$0p_{1/2}$	$0d_{5/2}$	$1s_{1/2}$	$0d_{3/2}$	$0f_{7/2}$
ε	-33.47	-9.7	-5.75	5.75	6.01	10.77	18.21
^{18}Ne							
ε	-33.0	-9.0	-5.5	5.5	6.3	10.9	18.5
^{24}Ne	$0p_{3/2}$	$0p_{1/2}$	$0d_{5/2}$	$1s_{1/2}$	$0d_{3/2}$	$0f_{7/2}$	
ε	-14.0	-10.0	-2.0	2.0	3.0	10.0	
^{26}Mg							
ε	-14.0	-9.0	-2.328	2.328	3.33	10.5	
^{28}Si							
ε	-18.0	-12.0	-4.35	4.35	6.1	8.0	

(continued)

Table 2 Continued

^{32}S	$0d_{5/2}$	$1s_{1/2}$	$0d_{3/2}$	$0f_{7/2}$	$1p_{3/2}$			
ε	-6.0	-3.22	3.22	5.82	6.0			
^{38}Ar	$0d_{5/2}$	$1s_{1/2}$	$0d_{3/2}$	$0f_{7/2}$	$1p_{3/2}$	$1p_{1/2}$	$0f_{5/2}$	
ε	-5.42	-4.3	-2.625	2.625	2.75	3.7	5.7	
^{40}Ca	$0d_{5/2}$	$1s_{1/2}$	$0d_{3/2}$	$0f_{7/2}$	$1p_{3/2}$	$1p_{1/2}$		
ε	-9.27	-6.11	-3.62	3.62	5.5	6.0		
ε(HF)	-7.7	-5.5	-3.62	3.62	4.2	5.0		
^{48}Ca	$0d_{5/2}$	$1s_{1/2}$	$0d_{3/2}$	$0f_{7/2}$	$1p_{3/2}$	$1p_{1/2}$	$0f_{5/2}$	$0g_{9/2}$
ε	-4.5	-4.27	-4.25	-2.4	2.4	4.5	4.8	7.0
ε(HF)	-5.9	-4.2	-4.3	-2.4	2.4	3.76	3.6	6.0
^{50}Ti	$0d_{3/2}$	$1s_{1/2}$	$0f_{7/2}$	$1p_{3/2}$	$1p_{1/2}$	$0f_{5/2}$	$0g_{9/2}$	
ε	-4.05	-3.85	-2.283	2.283	3.65	5.37	5.6	
^{52}Cr								
ε	-5.02	-4.8	-2.045	2.045	2.175	2.665	4.0	
^{54}Fe								
ε	-6.66	-5.11	-2.16	2.16	3.0	2.6	3.2	

(continued)

UCRL-18834

Table 2 Continued

^{56}Ni	$0d_{5/2}$	$1s_{1/2}$	$0d_{3/2}$	$0f_{7/2}$	$1p_{3/2}$	$0f_{5/2}$	$1p_{1/2}$	$0g_{9/2}$		
ε	-5.9	-5.7	-4.9	-2.4	2.4	4.15	4.3	7.35		
^{68}Ni	$0f_{7/2}$	$0f_{5/2}$	$1p_{3/2}$	$1p_{1/2}$	$0g_{9/2}$	$1d_{5/2}$	$2s_{1/2}$	$1d_{3/2}$	$0g_{7/2}$	
ε	-5.5	-4.95	-3.7	-2.0	2.0	3.4	4.95	6.05	6.15	
^{70}Zn	$1p_{3/2}$	$0f_{5/2}$	$1p_{1/2}$	$0g_{9/2}$	$1d_{5/2}$	$2s_{1/2}$				
ε	-2.3	-1.3	-1.2	1.2	1.7	3.2				
^{88}Sr	$0f_{7/2}$	$0f_{5/2}$	$1p_{3/2}$	$1p_{1/2}$	$0g_{9/2}$	$1d_{5/2}$	$2s_{1/2}$	$1d_{3/2}$	$0g_{7/2}$	$0h_{11/2}$
ε	-4.45	-3.2	-2.6	-2.4	-2.35	2.35	4.0	5.5	5.6	7.5
^{90}Zr										
ε	-4.5	-3.95	-2.8	-2.45	-2.4	2.4	3.7	5.0	5.1	7.5
^{114}Cd	$1p_{1/2}$	$0g_{9/2}$	$1d_{5/2}$	$2s_{1/2}$	$0g_{7/2}$	$1d_{3/2}$	$0h_{11/2}$	$1f_{7/2}$	$2p_{3/2}$	$2p_{1/2}$
ε	-8.15	-6.15	-1.65	-0.9	-0.6	0.6	1.55	5.0	5.1	7.0
^{116}Sn										
ε	-8.6	-6.5	-2.0	-0.8	-0.6	0.6	2.0	6.4	6.5	8.6

(continued)

Table 2 Continued

^{120}Sn	$1p_{1/2}$	$0g_{9/2}$	$1d_{5/2}$	$2s_{1/2}$	$0g_{7/2}$	$1d_{3/2}$	$0h_{11/2}$	$1f_{7/2}$	$2p_{3/2}$	$2p_{1/2}$
ε	-9.5	-7.4	-3.0	-0.8	-1.3	-0.6	0.6	3.5	3.6	7.6
^{122}Te	$1d_{5/2}$	$0g_{7/2}$	$2s_{1/2}$	$0h_{11/2}$	$1d_{3/2}$	$1f_{7/2}$	$0i_{13/2}$	$0h_{9/2}$	$2p_{3/2}$	$1f_{5/2}$
ε	-4.56	-3.87	-3.35	-2.12	-1.84	1.84	2.47	3.34	3.62	4.22
^{122}Te	$2p_{1/2}$	$0i_{11/2}$	$1g_{9/2}$							
ε	4.78	7.89	8.79							
^{140}Ce	$1d_{5/2}$	$0g_{7/2}$	$2s_{1/2}$	$0h_{11/2}$	$1d_{3/2}$	$1f_{7/2}$	$0i_{13/2}$	$0h_{9/2}$	$2p_{3/2}$	$1f_{5/2}$
ε	-4.7	-4.0	-3.5	-2.37	-1.79	1.79	2.7	3.5	3.8	4.4
^{142}Ne										
ε	-4.7	-4.0	-3.5	-2.4	-1.85	1.85	3.15	2.11	4.2	4.73
^{144}Sm										
ε	-5.05	-4.3	-2.25	-3.5	-1.85	1.85	3.15	1.95	2.05	-4.8
^{140}Ce	$2p_{1/2}$									
ε	5.0									
^{142}Ne										
ε	4.7									

(continued)

Table 2 Continued

$^{144}_{Sm}$									
ε	-4.7								
$^{208}_{Pb}$	$0h_{9/2}$	$1f_{7/2}$	$0i_{13/2}$	$2p_{3/2}$	$1f_{5/2}$	$2p_{1/2}$	$1g_{9/2}$	$0i_{11/2}$	$0j_{15/2}$
ε	-4.65	-3.55	-3.05	-2.15	-2.0	-1.716	1.716	2.74	3.28
$^{208}_{Pb}$	$2d_{5/2}$	$3s_{1/2}$	$1g_{7/2}$	$2d_{3/2}$					
ε	3.5	4.2	4.8	4.9					
$^{228}_{U}$	$1f_{7/2}$	$0i_{13/2}$	$2p_{3/2}$	$1f_{5/2}$	$2p_{1/2}$	$1g_{9/2}$	$0i_{11/2}$	$0j_{15/2}$	$2d_{5/2}$
ε	-6.31	-5.76	-4.9	-4.76	-3.83	-0.39	0.39	1.03	1.19
$^{228}_{U}$	$3s_{1/2}$	$1g_{7/2}$	$2d_{3/2}$						
ε	1.89	2.49	2.59						

Table 3

Boson Hamiltonians

	ω_1	ω_2	B'_1	B'_2	A_1	A_2	A_3	A_4	A_5	A_6	A_7
^{4}He	11.47	17.56	5.73	8.78	6.69	0	-1.25	-3.35	2.09	2.00	0
^{12}C	9.78	9.96	4.89	4.98	5.10	0	-0.93	-1.19	1.18	0.94	0
^{16}O	5.34	9.98	2.67	4.99	3.91	0	-0.33	-1.39	0.65	0.69	0
^{18}Ne	6.28	9.74	3.14	4.87	3.13	0	-0.29	-1.13	0.56	0.58	0
^{24}Ne	2.77	2.04	1.39	1.02	2.01	0	-0.42	-0.31	0.40	0.32	0
^{26}Mg	1.93	1.19	0.97	0.60	4.07	0	-0.60	-0.58	0.62	0.55	0
^{28}Si,TDA	6.08	5.67	3.04	2.84	3.94	0	-0.51	-0.58	0.60	0.49	0
^{28}Si,RPA	3.99	3.60	3.79	3.84	-3.16	1.51	-3.45	-3.72	1.29	1.36	3.01
^{32}S	3.45	5.37	1.72	2.69	2.56	0	-0.25	-0.81	0.44	0.46	0
^{38}Ar	0.97	3.59	0.48	1.79	3.31	0	-0.20	-0.50	0.29	0.33	0
^{40}Ca	4.20	5.76	2.10	2.88	2.54	0	-0.22	-0.47	0.31	0.34	0
^{40}Ca(HF)	3.93	5.72	1.96	2.86	2.68	0	-0.21	-0.46	0.28	0.33	0
^{48}Ca	3.46	2.42	1.73	1.21	2.53	0	-0.32	-0.18	0.26	0.22	0
^{48}Ca(HF)	2.88	2.43	1.44	1.22	3.05	0	-0.25	-0.23	0.26	0.23	0

(continued)

Table 3 Continued

	ω_1	ω_2	B_1'	B_2'	A_1	A_2	A_3	A_4	A_5	A_6	A_7
^{50}Ti	2.87	2.40	1.44	1.20	2.63	0	-0.28	-0.24	0.29	0.23	0
^{52}Cr	2.19	2.72	1.10	1.36	2.04	0	-0.13	-0.22	0.17	0.16	0
^{54}Fe	1.63	2.74	0.81	1.37	2.52	0	-0.13	-0.27	0.18	0.19	0
^{56}Ni	3.17	2.48	1.59	1.24	2.75	0	-0.30	-0.23	0.28	0.24	0
^{68}Ni	1.66	3.48	0.83	1.74	1.65	0	-0.09	-0.43	0.17	0.23	0
^{70}Zn	-0.34	0.77	-0.17	0.39	2.46	0	-0.15	-0.24	0.19	0.19	0
^{88}Sr	3.69	2.32	1.85	1.16	2.05	0	-0.21	-0.08	0.15	0.12	0
^{90}Zr	3.63	2.41	1.81	1.20	2.29	0	-0.21	-0.10	0.16	0.13	0
^{114}Cd	0.45	0.10	0.22	0.05	1.34	0	-0.13	-0.10	0.13	0.10	0
^{116}Sn	0.60	0.12	0.30	0.06	1.12	0	-0.15	-0.09	0.13	0.10	0
^{120}Sn	0.05	0.41	0.02	0.20	1.29	0	-0.09	-0.11	0.09	0.11	0
^{134}Te	1.76	2.60	0.88	1.30	2.30	0	-0.06	-0.12	0.09	0.08	0
^{140}Ce	2.17	2.77	1.09	1.39	1.81	0	-0.07	-0.12	0.09	0.10	0
^{142}Nd	1.97	2.87	0.98	1.43	1.91	0	-0.06	-0.12	0.08	0.10	0
^{144}Sm	1.33	3.02	0.66	1.51	1.88	0	-0.05	-0.19	0.09	0.12	0
^{208}Pb,RPA	2.11	2.63	1.11	1.38	-0.07	0.05	-0.16	-0.19	0.09	0.10	0.11
^{228}U	-0.44	0.22	-0.22	0.11	1.08	0	-0.03	-0.09	0.06	0.06	0

Appendix 2. Potential Energy Surfaces for the Collective Pairing Degree of Freedom

We define the pairing distortion operator by

$$\Delta = -\frac{1}{2} G \sum_j \hat{j} A_j^+ \tag{A.1}$$

so that its expectation value Δ coincides with the distortion (gap) parameter employed in the definition of the pairing distorted (quasi-particle) average field. Performing the boson expansion on the right hand side of (A.1) and retaining only the collective bosons and only first order terms, we get

$$\Delta = -\alpha_1 c_1^+ + \alpha_2 c_2 \tag{A.2}$$

where

$$\alpha_1 = \frac{G}{\sqrt{2}} \sum_{j>} \hat{j} r_1(j) , \quad \alpha_2 = \frac{G}{\sqrt{2}} \sum_{j\leqslant} \hat{j} r_2(j) . \tag{A.3}$$

It is tempting to look at the consequences of assuming that Δ is the variable which describes the collective pairing states in the same sense as the surface parameters $\alpha_{\lambda\mu}$ describes the collective multipole particle-hole excitations. Following the analogy we shall assume that (A.2) rather than (A.1) defines Δ, thereby removing non-collective boson terms from it. If the pairing average potential is distorted ($\Delta \neq 0$), the system will be characterized by a single phase angle ϕ (Bo 69), so that we can define an intrinsic coordinate system with a real deformation parameter

$$\Delta' = e^{-2i\phi} \Delta \quad . \tag{A.4}$$

Quite generally the transformation of any operator to the intrinsic system is given by the gauge angle ϕ and the particle addition number n carried by the operator

$$F'_n = e^{-ni\phi} F_n \quad . \tag{A.5}$$

Introducing the pairing momentum operator $\overline{\Pi}$ satisfying

$$[\Delta, \overline{\Pi}^+] = i \quad , \tag{A.6}$$

we can express the boson operators by

$$\begin{aligned} c_1^+ &= \frac{-\alpha_1}{\alpha_1^2 + \alpha_2^2} \left(\Delta - 2i\alpha_2^2 \overline{\Pi}\right), \\ c_2^+ &= \frac{\alpha_2}{\alpha_1^2 + \alpha_2^2} \left(\Delta^+ - 2i\alpha_1^2 \overline{\Pi}^+\right). \end{aligned} \tag{A.7}$$

Using (A.7), (A.4) and the corresponding

$$\overline{\Pi} = e^{2i\phi} \Pi' \tag{A.8}$$

we can now express the collective boson Hamiltonian (2.15) and collective part of (2.14) in the intrinsic coordinate system,

$$H_{intr.} = T(\Delta', \Pi') + V(\Delta') \quad . \tag{A.9}$$

Assuming for simplicity the TDA normal mode representation we may write the potential energy

$$V(\Delta) = \rho_0 + \rho_2\Delta^2 + \rho_4\Delta^4 + \ldots \quad , \tag{A.10}$$

where

$$\rho_2 = \frac{2}{(\alpha_1^2 + \alpha_2^2)^2} \left\{ \left(\frac{\omega_1}{2} + B_1 \right) \alpha_1^2 + \left(\frac{\omega_2}{2} + B_2 \right) \alpha_2^2 - A_1 \alpha_1 \alpha_2 \right\} \quad ,$$

$$\rho_4 = \frac{2}{(\alpha_1^2 + \alpha_2^2)^4} \left\{ -A_3 \alpha_1^3 \alpha_2 - A_4 \alpha_1 \alpha_2^3 + A_5 \alpha_1^4 + A_6 \alpha_2^4 \right\} . \tag{A.11}$$

The sign of ρ_2 tells whether $\Delta=0$ is a minimum or a maximum. In order to have a possible coexistence of separate potential valleys, higher than fourth order terms will have to be included in $V(\Delta)$, which similarly would require a more refined boson calculation than the one presented above.

Typical examples of the potential energy surfaces (A.10) corresponding to cases considered in sect. 4 are given in figs. 40 to 43. Besides clearly exhibiting the concepts of superfluidity and non-superfluidity we observe in fig. 43 the second possibility of coexistence mentioned in sect. 5, namely where the depth of the superfluid minimum is so that the ground state will be mainly confined here but the pair vibration is at a sufficiently high energy to be less affected by the potential raise at $\Delta=0$. This is the reason why the pair vibration can at all be expected to exist for non-magic isotopes. As soon as one goes away from a non-superfluid closed shell nucleus, a BCS gap will appear and hence the ground state be superfluid. However, near to the closed shell the

depth of the superfluid $V(\Delta)$ minimum is so small that it is not felt above some excitation energy.

An investigation of the intrinsic Hamiltonian (A.9) in the adiabatic approximation is being made by Broglia and Kumar (Br 69).

References

Aj 68, F. Ajzenberg-Selove and T. Lauritsen, Nucl. Phys. A114 (1968) 1 and T. L. and F. A.-S., Nucl. Phys. 78 (1966) 1

Aj 69, F. Ajzenberg-Selove and T. Lauritsen, to be published

As 68, R. Ascuitto and N. Glendenning, Annual Report, Lawrence Radiation Laboratory Report No. UCRL-18667 (1968) and to be published

Ba 63, J. Ball et al., Phys. Rev. 130 (1963) 2342

Ba 64, G. Bassani et al., Int. Congr. Nucl. Phys., Paris 1964, pp. 494-495 and Ann. Progr. Rep., U. of Minnesota 1964

Ba 64a, G. Bassani et al., Phys. Rev. 136 (1964) B1006

Ba 65, D. Bachelier et al., Phys. Letters 16 (1965) 304

Ba 65a, G. Bassani et al., Phys. Rev. 139 (1965) B830

Ba 68, B. Bayman and N. Hintz, Phys. Rev. 172 (1968) 1113

Ba 69, J. Bar-Touv and A. Goswami, Phys. Letters 28B (1969) 391

Ba 69a, J. Ball et al., Phys. Rev. 177 (1969) 1699

Ba 69b, J. Ball et al., Phys. Letters, to be published , and private communication

Be 36, H. Bethe and R. Backer, Rev. Mod. Phys. 8 (1936) 82

Be 66, D. Bès and R. Broglia, Nucl. Phys. 80 (1966) 289

Be 66a, T. Belote et al., Phys. Rev. 142 (1966) 624

Be 67, W. Benenson et al., Nucl. Phys. A97 (1967) 510

Be 68, J. Beery, Thesis, Los Alamos Scientific Laboratory 1968 and to be published

Be 68a, D. Bès and G. Dussel, Nucl. Phys. to be published

Bj 66, J. Bjerregaard et al., Nucl. Phys. 86 (1966) 145

Bj 66a, J. Bjerregaard et al., Nucl. Phys. 89 (1966) 337

Bj 67, J. Bjerregaard et al., Nucl. Phys. A103 (1967) 33

Bj 67a, J. Bjerregaard et al., Nucl. Phys. A94 (1967) 457

Bj 68, J. Bjerregaard et al., Nucl. Phys. A113 (1968) 484

Bj 68a, J. Bjerregaard et al., Nucl. Phys. A110 (1968) 1

Bl 69, A. Blair et al., Phys. Letters, to be published

Bo 64, A. Bohr, Int. Congr. Nucl. Phys., Paris 1964, Vol. I

Bo 68, A. Bohr, Proc. of Int. Symp. on Nucl. Structure, Dubna, 1968

Bo 69, A. Bohr and B. Mottelson, Nuclear Structure, Benjamin, to be published

Br 67, D. Bromley, Proc. of Int. Conf. on Nucl. Structure, Tokyo 1967, p. 255

Br 67a, R. Broglia and C. Riedel, Nucl. Phys. A92 (1967) 145

Br 67b, R. Broglia and C. Riedel, Nucl. Phys. A93 (1967) 241

Br 68, R. Broglia and B. Sørensen, Nucl. Phys. A110 (1968) 241

Br 68a, H. Brunnader et al., Phys. Rev. 174 (1968) 1247

Br 68b, R. Broglia et al., Nucl. Phys. A106 (1968) 421

Br 68c, R. Broglia et al., Nucl. Phys. A115 (1968) 273

Br 69, R. Broglia and K. Kumar, private communication

Ca 67, P. Cavanagh and C. Coleman, PLA Progress Report 1967, Rutherford H.E. Laboratory

Ce 64, J. Cerny and R. Pehl, Phys. Rev. Letters 12 (1964) 619

Ce 64a, J. Cerny et al., Phys. Letters 12 (1964) 234

Ce 65, J. Cerny et al., Phys. Rev. Letters 15 (1965) 300

Ce 68, J. Cerny, Ann. Rev. of Nucl. Sci. 18 (1968) 27

Ce 69, J. Cerny et al., private communication

Ch 65, P. Christensen and F.-C. Yang, Nucl. Phys. 72 (1965) 657

Ch 67, P. Chevallier et al., Phys. Rev. 160 (1967) 827

Ch 68, R. Chapman et al., Nucl. Phys. A119 (1968) 305

Co 66, T. Conlon et al., Phys. Rev. 144 (1966) 941

Co 66a, B. Cohen and R. Middleton, Phys. Rev. 146 (1966) 748

Co 67, S. Cosper et al., Phys. Letters 25B (1967) 324

Co 67a, B. Cohen et al., Phys. Rev. 157 (1967) 1033

Da 67, W. Davies et al., PLA Progress Report 1967, Rutherford H.E. Laboratory

Da 68, W. Davies et al., Phys. Letters 27B (1968) 363

Da 68a, W. Davies et al., PLA Progress Report 1968, Rutherford H.E. Laboratory

Da 69, Darcey, Chapman and Hinds, private communication

Dr 69, R. Drisko et al., to be published

Dö 67, F. Dönau et al., Nucl. Phys. A101 (1967) 495

Ec 68, J. L'Ecuyer et al., PLA Progress Report 1968, Rutherford H.E. Laboratory

En 67, P. Endt and C. v. d. Leun, Nucl. Phys. A105 (1967) 1

Fe 62, J. Ferguson et al., Jour. Inorg. Nucl. Chem. 24 (1962) 1

Fl 67, E. Flynn et al., Phys. Rev. Letters 19 (1967) 798

Fl 69, E. Flynn, private communication

Fr 61, J. French and M. MacFarlane, Nucl. Phys. 26 (1961) 168 and R. Bansal and J. French, Phys. Letters 11 (1964) 145

Ga 64, G. Garvey et al., Phys. Rev. Letters 12 (1964) 726

Ga 67, N. Ganguly et al., PLA Progress Report 1967, Rutherford H.E. Laboratory

Ga 68, N. Ganguly et al., Z. f. Phys. 208 (1968) 73

Ga 69, G. Garvey and J. Cerny, to be published

Ga 69a, G. Garvey, private communication

Ge 67, W. Gerace and A. Green, Nucl. Phys. 93 (1967) 110

Ge 69, W. Gerace and A. Green, Nucl. Phys. A123 (1969) 241

Gl 65, N. Glendenning, Phys. Rev. 137 (1965) B102

Gl 67, R. Glover and A. Douglas, Phys. Letters 25B (1967) 333

Gl 67a, N. Glendenning, Phys. Rev. 156 (1967) 1344

Gl 68, N. Glendenning, Preprint 1968 (UCRL-18225)

Gl 69, R. Glover, private communication

Go 63, C. Goodman et al., Direct Int. and Nucl. React. Mechanism, p. 435, Gordon & Breach 1963

Gr 66, R. Griffiths et al., PLA Progress Report, 1966, Rutherford H.E. Laboratory

Gr 67, R. Griffiths et al., PLA Progress Report 1967, Rutherford H.E. Laboratory

Gr 68, R. Griffiths et al., PLA Progress Report 1968, Rutherford H.E. Laboratory

Ha 66, J. Hardy et al., Phys. Letters 23 (1966) 487

Ha 67, J. Hardy et al., PLA Progress Report 1967, Rutherford H.E. Laboratory

Ha 67a, J. Hardy and I. Towner, Phys. Letters 25B (1967) 577

Ha 69, J. Hardy et al., private communication

Hi 61, S. Hinds et al., Phys. Rev. Letters 6 (1961) 113

Hi 61a, S. Hinds et al., Proc. Phys. Soc. 78 (1961) 473

Hi 62, S. Hinds et al., Nucl. Phys. 38 (1962) 81

Hi 65, S. Hinds et al., Nucl. Phys. 67 (1965) 257

Hi 65a, S. Hinds et al., Phys. Letters 14 (1965) 48

Hi 65b, S. Hinds and R. Middleton, private communication

Hi 66, S. Hinds et al., Phys. Letters 21 (1966) 328

Hi 67, S. Hinds and R. Middleton, Nucl. Phys. A92 (1967) 422

Hi 67a, S. Hinds et al., Phys. Letters 24B (1967) 89

Ho 65, C. Hoot et al., Nucl. Phys. 71 (1965) 449

Ho 67, G. Holland et al., Proc. of Int. Conf. on Nucl. Structure, Tokyo 1967, Abstract No. 8.81

Ho 67a, G. Holland et al., Proc. of Int. Conf. on Nucl. Structure, Tokyo 1967, Abstract No. 8.86

Hu 68, F. Hudson et al., Phys. Letters 27B (1968) 84

Ig 68, G. Igo, P. Barnes and E. Flynn, private communication

Is 67, Y. Ishizaki et al., Proc. of Int. Conf. on Nucl. Structure, Tokyo 1967, Abstract No. 4.88

Ja 59, N. Jarmie and M. Silbert, Phys. Rev. Letters 3 (1959) 50

Ja 60, A. Jaffe et al., Proc. Roy. Soc. 76 (1960) 914

Ja 60a, N. Jarmie and M. Silbert, Phys. Rev. 120 (1960) 914

Ja 66, K. Jantsch, Kernenergie 9 (1966) 127

Ko 64, M. Kondo et al., Bull. Am. Phys. Soc. 9 (1964) 544

Ko 67, A. Kobzev et al., J. Nucl. Phys. (U.S.S.R.) 5 (1967) 510

Ko 69, K. Kolltveit, Nucl. Phys. A126 (1969) 115

Ku 62, B. Kuhn et al., J. Exp. i Theor. Phys. 43 (1962) 1660

Kü 63, B. Kühn and B. Schlenk, Phys. Letters 5 (1963) 91

Ku 68, K. Kumar and M. Baranger, Nucl. Phys. A110 (1968) 529

Le 63, J. Legg, Phys. Rev. 129 (1963) 272

Le 67, C. Lederer et al., Table of Isotopes, Wiley, New York 1967

Ma 65, J. Mattanch et al., Nucl. Phys. 67 (1965) 1

Ma 66, N. Mangelson et al., Nucl. Phys. 88 (1966) 137

Ma 66a, J. Maxwell et al., Phys. Rev. 151 (1966) 1000

Mc 66, L. McIntyre, Phys. Rev. 152 (1966) 1013

Mc 67, R. McGrath et al., Phys. Rev. Letters 18 (1967) 243

Mc 68, R. McGrath et al., Phys. Letters 27B (1968) 443

Mc 68a, J. McGrory and B. Wildenthal, Phys. Letters 28B (1968) 237

Mi 63, R. Middleton and H. Marchant, Nuclidic Masses (2nd Int. Conf., Vienna 1963) p. 329, Springer, Wien 1964

Mi 64, R. Middleton and D. Pullen, Nucl. Phys. 51 (1964) 63

Mi 64a, R. Middleton and D. Pullen, Nucl. Phys. 51 (1964) 77

Mo 65, R. Moreh, Nucl. Phys. 70 (1965) 293

Mo 67, M. Mori et al., Int. Jour. Appl. Rad. Isotopes 18 (1967) 579

Ne 67, J. Nelson et al., PLA Progress Report 1967, Rutherford H.E. Laboratory

Ne 68, J. Nelson et al., PLA Progress Report 1968, Rutherford H.E. Laboratory

Oo 66, K. van Oostrum et al., Phys. Rev. Letters 16 (1966) 528

Pa 68, J. Parikh and J. Svenne, Phys. Rev. 174 (1968) 1343

Pe 63, F. Perey, Phys. Rev. 131 (1963) 745

Pe 67, R. Peterson, U. of Princeton, Progr. Rep. 1967, PUC 937-260

Pe 68, R. Peterson, Phys. Rev. 170 (1968) 1003

Po 63, L. Pomorski et al., Proc. on 3rd Conf. on React. between Complex Nuclei, Asilomar 1963, p. 135; U. C. Press 1963

Pu 62, D. Pullen et al., Nucl. Phys. 36 (1962) 1

Re 67, G. Reynolds et al., Phys. Rev. 153 (1967) 1282

Re 69, M. Redlich, private communication

Ri 64, M. Rickey et al., Phys. Rev. Letters 13 (1964) 444

Ri 64a, M. Rickey et al., Proc. on Conf. on Nucl. Spectroscopy with direct React., Argonne 1964, Vol. 2, ANL Report 6878

Ri 68, C. Riedel et al., Nucl. Phys. A113 (1968) 503

Sa 67, G. Satchler, Nucl. Phys. A92 (1967) 273

Sc 69, J. Schiffer, Proc. of 2nd Conf. on Nucl. Isospin, Pacific Grove 1969

Sh 64, Y. Shida et al., Phys. Letters 13 (1964) 59

Sm 67, S. Smith et al., Phys. Rev. 169 (1967) 951

Sm 69, S. Smith et al., Nucl. Phys. A125 (1969) 339

Sø 67, B. Sørensen, Nucl. Phys. A97 (1967) 1

Sø 68, B. Sørensen, Nucl. Phys. A119 (1968) 65

Sø 69, B. Sørensen, Proc. of 2nd Conf. on Nuclear Isospin, Asilomar, Pacific Grove, California 1969

Sø 69a, B. Sørensen, to be published

Ta 67, H. Taketani et al., Contr. No. 8.42 to Int. Conf. on Nucl. Structure, Tokyo 1967

Ta 69, H. Taketani et al., J. Phys. Soc. Japan 26 (1969) 204

Va 67, G. Vallois et al., Phys. Letters 24B (1967) 512

Wh 66, C. Whitten, Thesis, Princeton U. 1966 and Bull. Am. Phys. Soc. 10 (1965) 121

Wh 67, C. Whitten, Phys. Rev. 156 (1967) 1228

Wi 66, D. Williams et al., Phys. Letters 22 (1966) 162

Wi 67, D. Williams et al., Phys. Rev. 164 (1967) 1421

Wo 68, S. Wong and W. Davies, Phys. Lett. 28B (1968) 77

Ya 67, K. Yagi et al., Proc. of Int. Conf. on Nucl. Structure, Tokyo 1967 Abstract No. 4.77

Ya 68, K. Yagi et al., Nucl. Phys. A111 (1968) 129

Figure Captions

Fig. 1. Schematic display of the hieraki of neutron pairing states. An energy term linear in $N-N_0$ has been added in order to make the ground state energies of N_0-2 and N_0+2 equal.

Fig. 2. Schematic display of some distortions of the pure neutron pairing states. a: Isospin structure. b: Coupling to "two-phonon" multipole states. c: Coexistence of spherical (S) and deformed (D) states with indication of strong two-nucleon transfer possibilities.

Fig. 3. Sharing of t,p (figures to the left) and p,t (figures to the right) strengths between pairing and multipole states in a fictitious closed shell nucleus. (a) Pure pairing picture, (b) the multipole states does not produce ground state correlations (TDA) and (c) ground state correlations present (RPA). The same picture holds in a non-closed-shell nucleus, except that the role of the pair vibration $|pv\rangle$ is played by a set of non-collective pairing states.

Fig. 4. He-isotopes. The symbols used in this and the following figures are explained in sect. 4.

Fig. 5. C-isotopes. Experimental ^{18}O cross sections are from Ja 60.

Fig. 6. DWBA differential cross sections for the reaction $^{12}C(t,p)$ at E_t = 11.0 MeV leading to the ground state and the 6.58 MeV level of ^{14}C. The experimental points are from Mi 64 and the calculated ones used G-coefficients for eq. (2.25) extracted from the boson wave functions, $(G_0, G_1, G_2) = (-0.0387, -0.4501, 0.2528)$ for the ground state and (0.0340, 0.2663, 0.3765) for the transition leading to the non-collective pairing excitation predicted at 8.07 MeV. The proton optical model parameters are from Pe 63.

Fig. 7. O-isotopes. The labelled experiments are a (Ja 60), b (Ja 60a), c (Mi 64) and d (Mo 65).

Fig. 8. Ne-isotopes. Calculation based on ^{18}Ne.

Fig. 9. Ne-isotopes. Calculation based on ^{24}Ne.

Fig. 10. Mg-isotopes. The labelled experiments are a (Ce 69), b (Co 67 at E_p = 20 MeV), c (Co 67 at E_p = 54 MeV) and d (Gr 67). In the middle column quadrupole 0+ states are denoted Q, otherwise the notation follows fig. 1.

Fig. 11. Si-isotopes. The experimental labels are a (Ha 67), b (Ha 69) and c (Ha 67a).

Fig. 12. Comparison between calculated spectra and transfer cross sections in Si-isotopes, obtained either from the TDA representation (employed in fig. 11) or from the RPA representation.

Fig. 13. S-isotopes.

Fig. 14. Ar-isotopes.

Fig. 15. Ca-isotopes. Calculation based on ^{40}Ca. Key to experimental labels: a (Ce 68), b (Ba 64), c (Mi 64a), d (Wi 67), e (Bj 67), f (Pe 68) and g (Da 67) and (Sm 69). The relative ground state intensities labelled e are based on the full angular range 0° - 180°, most of the others are ratios at a fixed angle or averages of short angular ranges.

Fig. 16. Comparison of experimental Ca ground state energies minus either constant or $A^{-1/3}$ varying Coulomb energy with various calculated energies. A term linear in N has been added to the calculated energies, so that either the energies of N=18 and N=22 become equal (cases labelled I) or so that the energies of N=24 and N=26 coincide with the experimental ones with constant Coulomb energy (cases labelled II).

Fig. 17. Ca-isotopes. Two calculations based on ^{40}Ca, using different single particle energies, cf. table 2 of appendix 1.

Fig. 18. Ca-isotopes. Calculation based on ^{48}Ca. For explanation of labels on experimental cross sections see caption to fig. 15. The ^{40}Ca(p,t) experimental absolute intensity (0.31) is normalized to ^{48}Ca(p,t), whereas the ^{42,44}Ca(p,t) intensities labelled g are not normalized to any other.

Fig. 19. Ca-isotopes. Two calculations based on ^{48}Ca, using different single particle energies, cf. table 2 of appendix 1.

Fig. 20. Ti-isotopes. Labelling: a (Ba 64) and b (Ri 64a). States listed in middle columns are built of certain basic quanta of which the one denoted 2_+ creates the lowest 2+ state in ^{52}Ti from the ^{50}Ti ground state, 2_- similarly and ^{48}Ti 2+ state, whereas $2'_-$ creates the ^{46}Ti 2+ state from the ^{48}Ti ground state. Finally $(2+)^2_N$ is two quadrupole-phonon 0+ states in the N-isotope.

Fig. 21. Cr-isotopes. Label a refers to Wh 67. The two-phonon quadrupole states are denoted Q_-(N=26), Q (28) and Q_+(30), the corresponding 2+ quanta 2_-(N=26) and 2_+(30).

Fig. 22. Fe-isotopes. Labelling: a (Ga 64), b (Ce 66), c (Ce 67), d (Ba 64a) and e (Ri 64a).

Fig. 23. Ni-isotopes. Calculation based on ^{56}Ni. Labels: a (Ho 65), b (Da 68a), c (Ri 64a), d (Ga 69a), e (Da 69) and f (Ba 64a). The ground state ratios quoted by a and c are ratios of the second maxima. At this particular angle they agree with the references from which ratios of integrated cross sections are quoted (b and f, the latter integrated over the interval $5° \leqslant \theta_{CM} \leqslant 40°$). The dashed lines in middle columns are ground state energies from the same calculation which gives the left columns, but with a different term proportional to N subtracted.

Fig. 24. Ni-isotopes. Calculation based on ^{68}Ni. Labelling follows fig. 23.

Fig. 25. Zn-isotopes. Labels: a (Ba 64a), b (Mc 66), and c (Ya 67). The ground state cross sections labelled b are ratios of second maxima and presumably not reliable.

Fig. 26. Sr-isotopes. The spin assignment of the excited ^{86}Sr state is by us. The state is not resolved from a nearby known 2+ state, but the triton angular distribution is characteristic of mixed L = 0 and 2 transfer.

Fig. 27. Zr-isotopes. Labels: a (Ba 69a), b (Ba 69b), c (Be 68), d (Ba 64) and e (Bl 69). Regarding the disagreements between the ground state transitions of the experiments b and c, which are rather close to each other in proton and triton energies, a detailed discussion is given in fig. 28, and in the text. The ground state cross sections labelled c contain some corrections quoted by Fl 69. The 1.51 MeV level in ^{38}Zr is also observed by Ta 69, with 14% of the ground state intensity.

Fig. 28. Angular distributions for Zr (p,t) experiments at E_p = 38 MeV (Ba 69b), at 31 MeV (Ba 69a) and Zr (t,p) experiments at E_t = 20 MeV (Be 68 and Bl 69). The calculated curves are results of a DWBA calculation, using modified form factors whose radial parts are harmonic oscillator wave functions (with $\nu = A^{-1/3}$ fm) matched with Hankel functions. The optical model parameters were the same in all cases, for protons V = 51.4 MeV, W = 2.59 MeV, W_D = 7.5 MeV, r = 1.17 fm, r' = 1.31 fm, r_c = 1.2 fm, a = 0.73 fm, a' = 0.65 fm (Sa 67) and for tritons V = 170.1 MeV, W = 19 MeV, r = 1.15 fm, r' = 1.52 fm, r_c = 1.4 fm, a = 0.74 fm, a' = 0.76 fm (Dr 69). All calculated cross sections are in the absolute units, they are not

normalized to the experimental ones and the stripping interaction was the same in all cases. The structure factors were calculated with the pairing wave functions corresponding to fig. 27.

Fig. 29. Cd-isotopes.

Fig. 30. Sn-isotopes. The closed shell is ^{116}Sn. Labels: a (Ya 68), b (Br 68c), c (Ho 67), d (Be 68, the spin assignments in ^{124}Sn is from other sources, the dashed lines indicate the first strong states involving higher shells, not necessarily 0+ levels) and e (Ba 65a).

Fig. 31. Sn-isotopes. The closed shell is ^{120}Sn. The ground state transition ratios for the ^{116,118}Sn(t,p) and for the ^{122,124}Sn(t,p) experiments are normalized independently. For further explanation see the caption to fig. 30.

Fig. 32. Occupation numbers N_j for the ^{120}Sn ground state calculated with the parameters of the boson calculation (bars), cf. fig. 30, compared to the filling parameters v_j^2 of the BCS ground state (curve).

Fig. 33. Te-isotopes.

Fig. 34. Ce-isotopes.

Fig. 35. Nd-isotopes. Since the resolution in the (p,t) experiments was poor, most of the angular distribution were not pure L = 0. For this leason the cross sections are very inaccurate.

Fig. 36. Sm-isotopes. Labels: a (Ma 66a), b (Is 67) and c (Ga 67). The uncertainty in the ^{142}Sm mass (Ga 67) is indicated by vertical lines.

Fig. 37. Pb-isotopes. Labels: a (Bj 67a, Bj 66a), b (Re 67), c and d (Ho 67a and Br 67 at E_p = 20 and 22 MeV, respectively), e (Fl 67) and f (Ig 68). The ratio of ^{208}Pb(t,p) to ^{206}Pb(t,p) at E_t = 20 MeV and $\theta_{CM} = 30°$ is 0.25 (Ig 68). The angular distribution of the latter reaction is

not yet available, but the $^{208}Pb(t,p)$ cross section shows a 3rd maximum around $\theta_{CM} = 50°$, which has as large an intensity as the 30° maximum. Since this is not so in the earlier $^{206}Pb(t,p)$ experiment (at $E_t = 12$ MeV), we think that a change in the ^{210}Pb angular distribution has been caused by the decrease in Q-value, and tentatively increase the ratio from 0.25 to 0.40, estimated by assuming that the $^{206}Pb(t,p)$ angular distribution is the same at $E_t = 12$ and 20 MeV. DWBA calculations show that the ratio of total cross sections can be expected to be twice the ratio taken at $\theta = 30°$ (2. max.).

Fig. 38. U-isotopes.

Fig. 39. Excitation energies of pair vibrations at the most stable neutron closed shell nuclei. The open triangles correspond to T = 0, 1, and 2 experimental 0+ levels which may be interpreted as split pair vibrations.

Fig. 40. Potential energy surface for ^{208}Pb.

Fig. 41. Potential energy surface for ^{120}Sn.

Fig. 42. Potential energy surface for ^{48}Ca.

Fig. 43. Potential energy surface for ^{136}Ce. The parameters are the same as for the ^{140}Ce calculation.

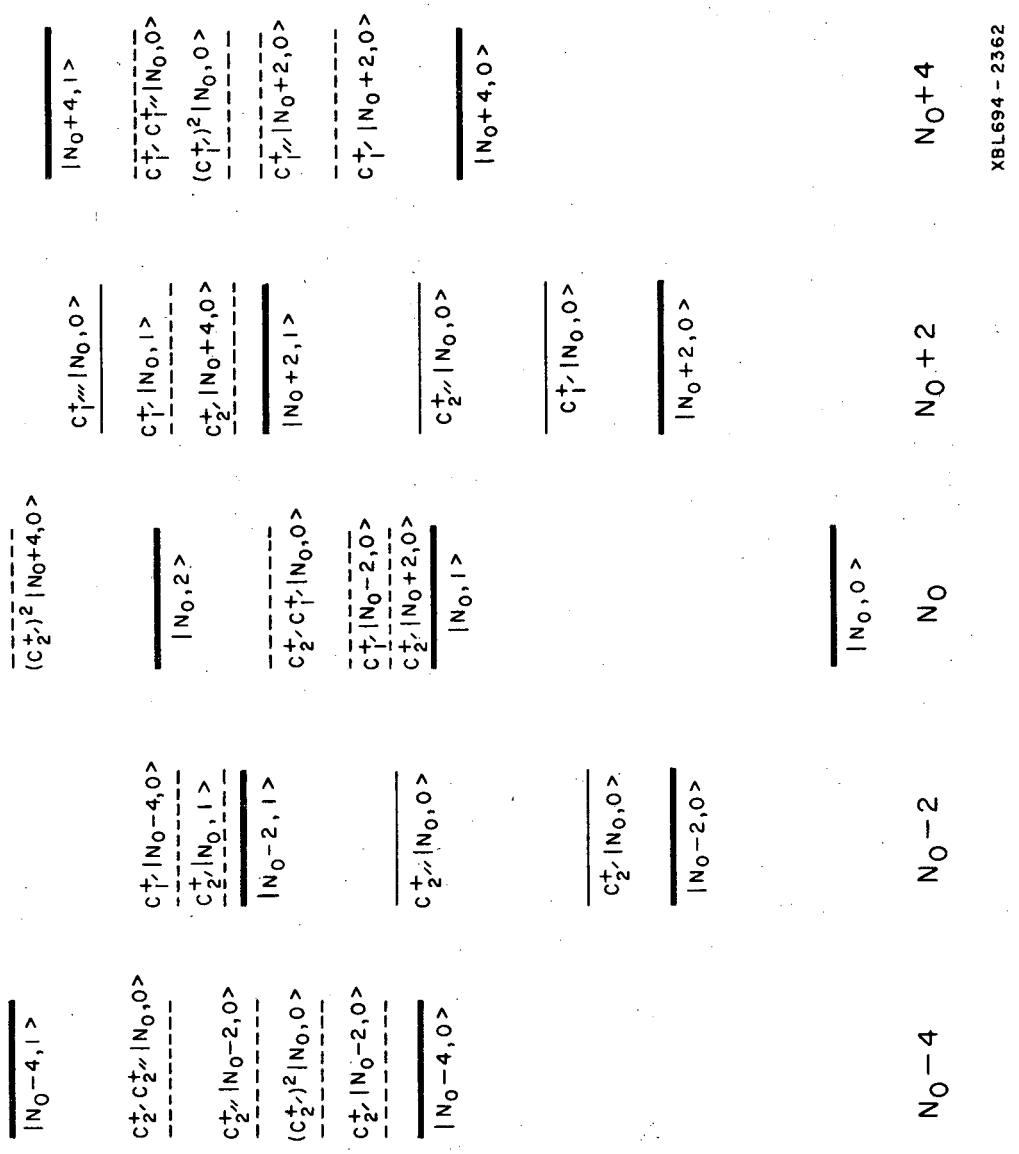
$|N_0-4,1\rangle$
$c_2^{+\prime} c_2^{+\prime\prime} |N_0,0\rangle$
$c_2^{+\prime\prime} |N_0-2,0\rangle$
$(c_2^{+\prime})^2 |N_0,0\rangle$
$c_2^{+\prime} |N_0-2,0\rangle$
$|N_0-4,0\rangle$
$(c_2^{+\prime})^2 |N_0+4,0\rangle$
$|N_0,2\rangle$
$c_2^{+\prime} c_1^{+} |N_0,0\rangle$
$c_1^{+} |N_0-2,0\rangle$
$c_2^{+\prime} |N_0+2,0\rangle$
$|N_0,1\rangle$
$c_1^{+\prime\prime} |N_0,0\rangle$
$c_1^{+\prime} |N_0,1\rangle$
$c_2^{+\prime} |N_0,1\rangle$
$|N_0-2,1\rangle$
$c_1^{+\prime} |N_0-4,0\rangle$
$c_2^{+\prime} |N_0,1\rangle$
$|N_0-4,0\rangle$
$|N_0,0\rangle$
$c_2^{+\prime} |N_0,0\rangle$
$|N_0-2,0\rangle$
$c_1^{+\prime\prime} |N_0,0\rangle$
$c_1^{+\prime} |N_0,1\rangle$
$c_2^{+\prime} |N_0+4,0\rangle$
$|N_0+2,1\rangle$
$c_2^{+\prime\prime} |N_0+2,0\rangle$
$|N_0+4,1\rangle$
$c_1^{+\prime} c_1^{+\prime\prime} |N_0,0\rangle$
$(c_1^{+\prime})^2 |N_0,0\rangle$
$c_1^{+\prime\prime} |N_0+2,0\rangle$
$c_1^{+\prime} |N_0+2,0\rangle$
N_0-4
N_0-2
N_0
N_0+2
N_0+4
XBL694-2362

Fig. 1.

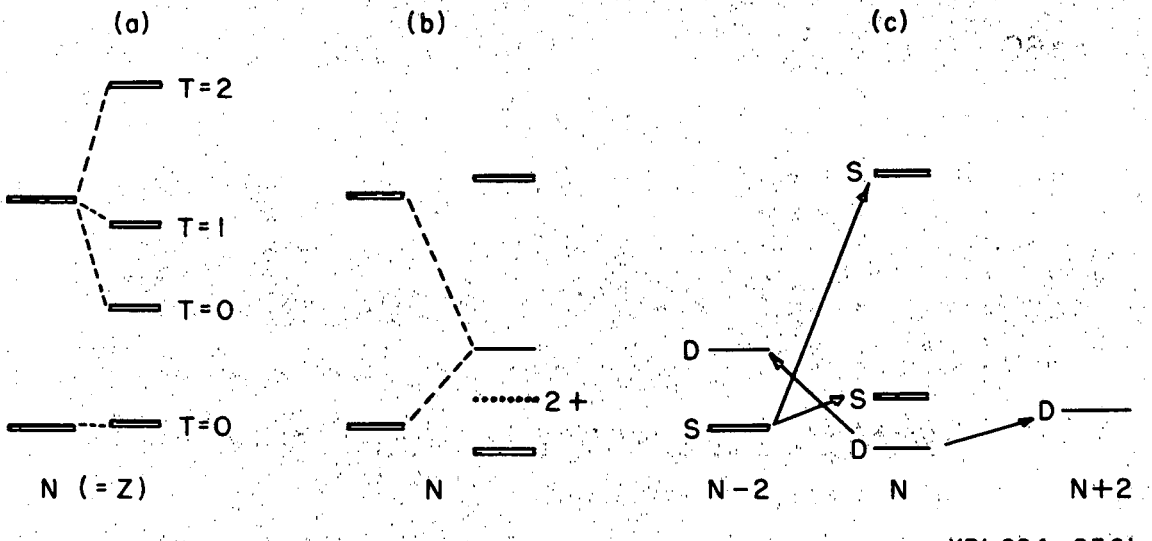

Fig. 2.

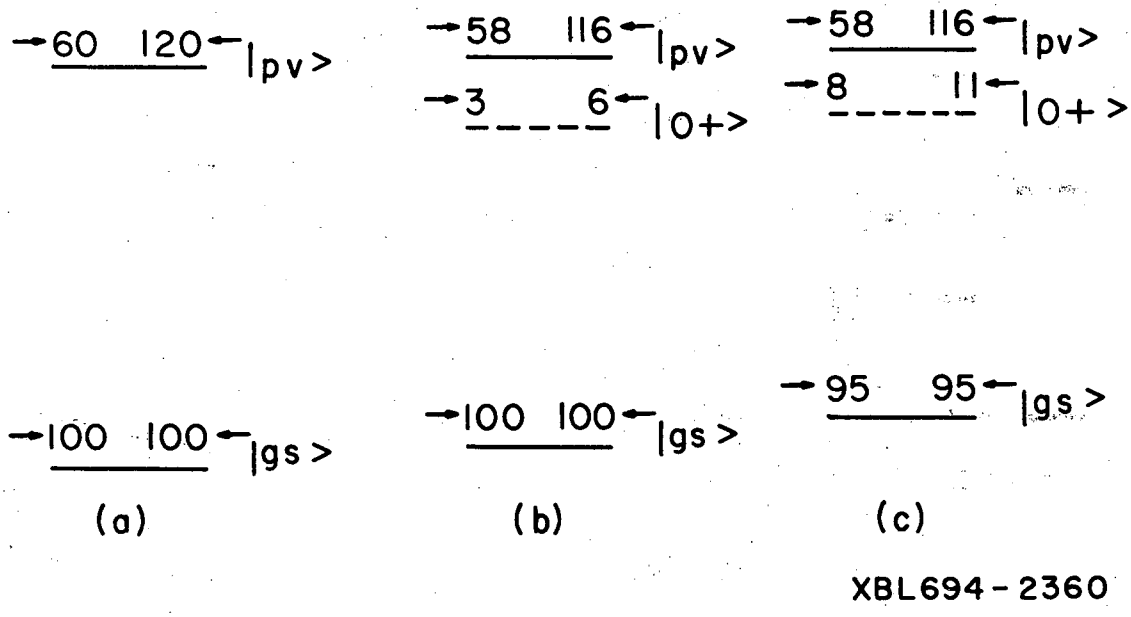
→60 120← |pv>
→58 116← |pv>
→3 6← |0+>
→58 116← |pv>
→8 11← |0+>
→100 100← |gs>
→100 100← |gs>
→95 95← |gs>
(a)
(b)
(c)
XBL694-2360

Fig. 3.

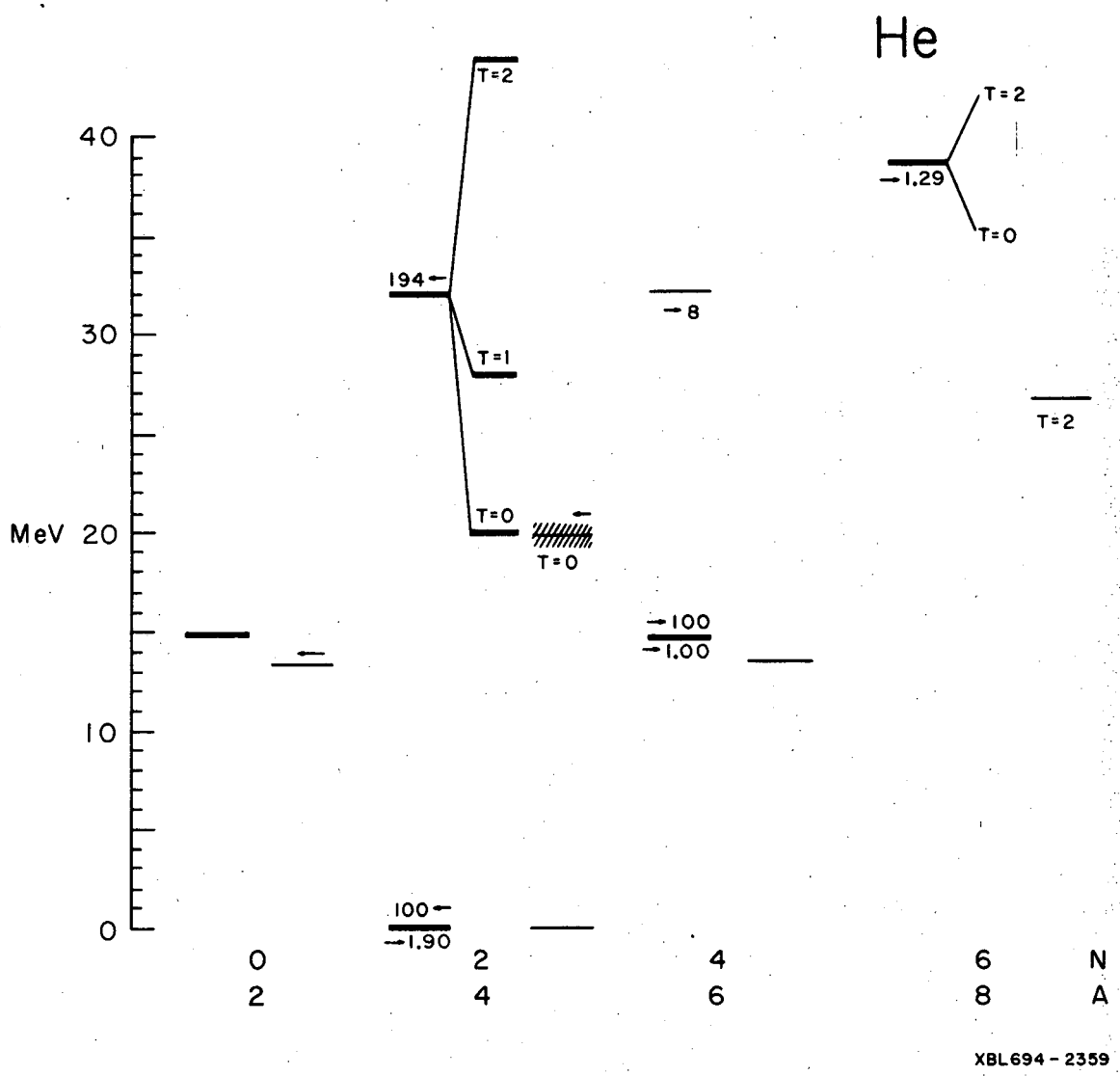
He
T=2
1.29
T=0
40
30
MeV 20
10
0
T=2
194
T=1
T=0
T=0
8
100
1.00
100
1.90
0
2
2
4
4
6
6
8
N
A
XBL694-2359

Fig. 4.

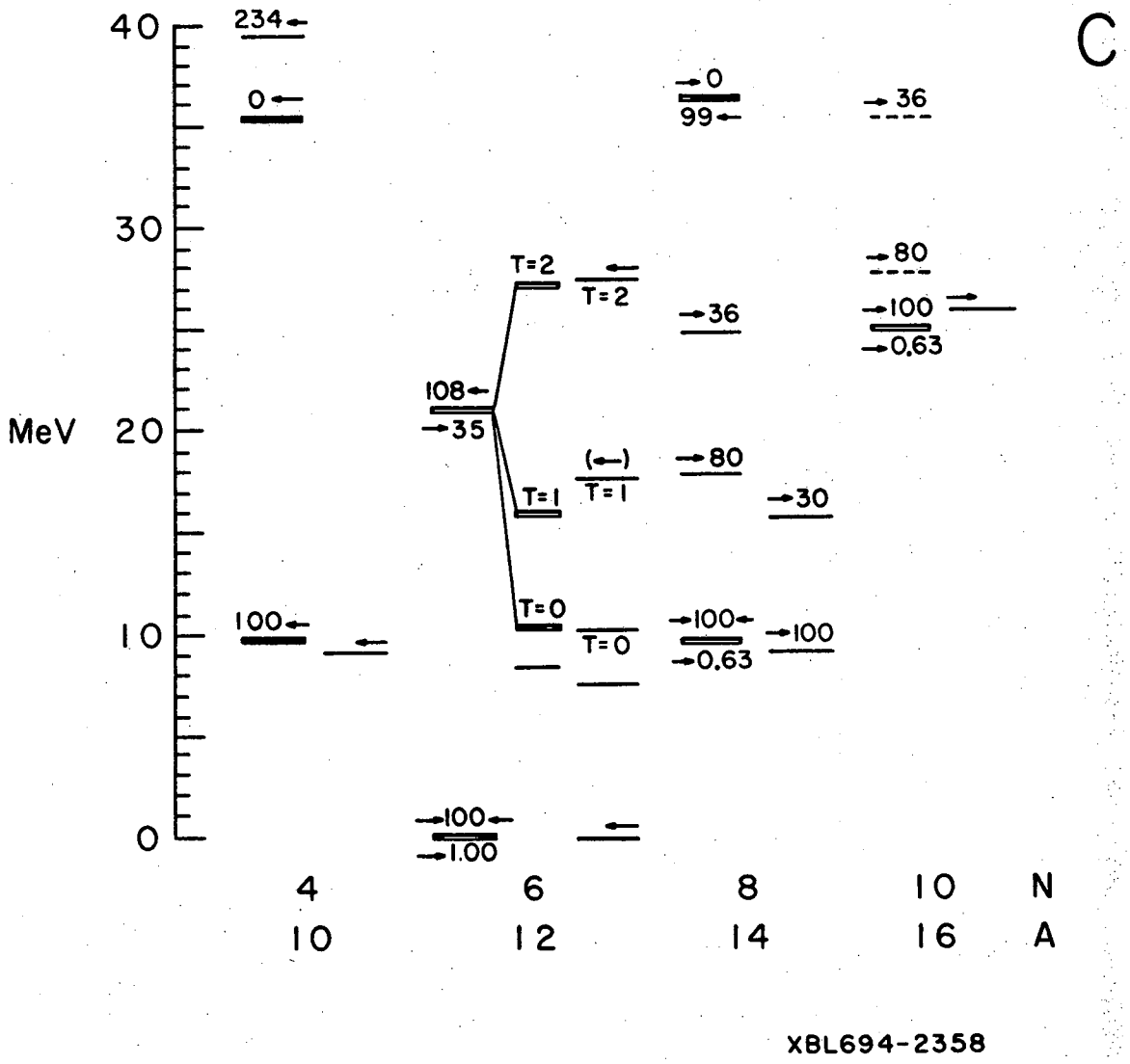
C
MeV
40
30
20
10
0
234
0
100
T=2
T=2
108
35
T=1
(←)
T=1
T=0
T=0
100
1.00
0
99
36
36
80
80
100
0.63
100
0.63
30
100
4
10
6
12
8
14
10
16
N
A
XBL694-2358

Fig. 5.

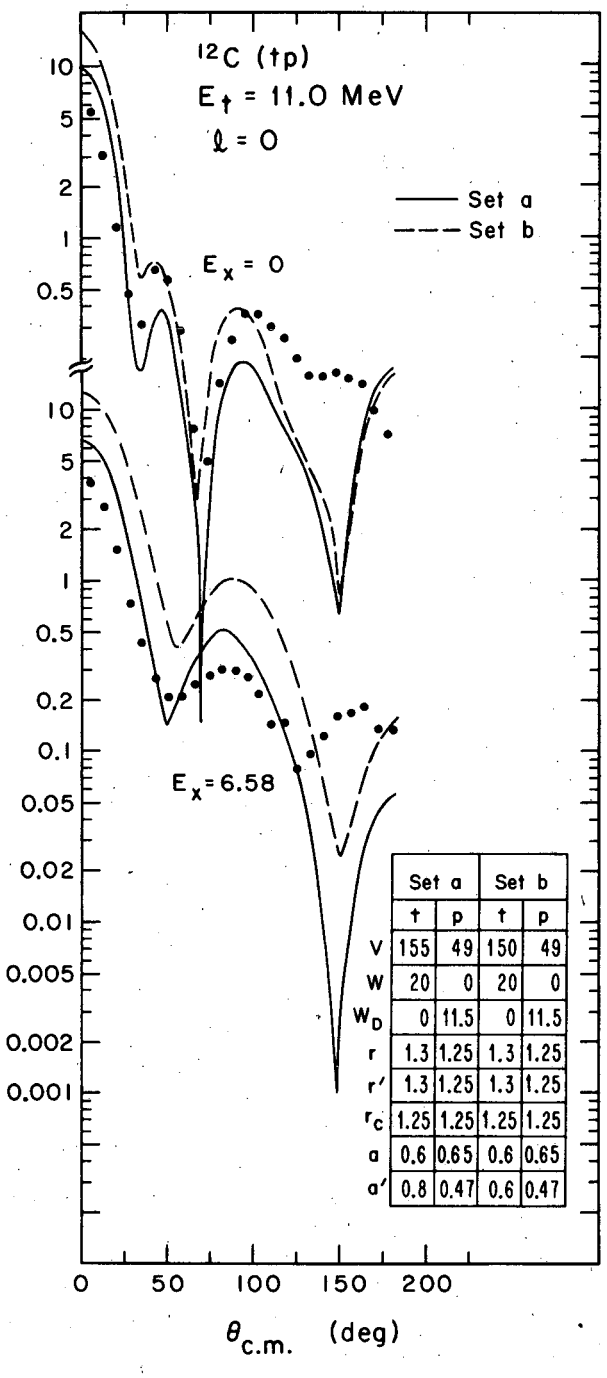

	Set a		Set b	
	t	p	t	p
V	155	49	150	49
W	20	0	20	0
W_D	0	11.5	0	11.5
r	1.3	1.25	1.3	1.25
r′	1.3	1.25	1.3	1.25
r_c	1.25	1.25	1.25	1.25
a	0.6	0.65	0.6	0.65
a′	0.8	0.47	0.6	0.47

Fig. 6.

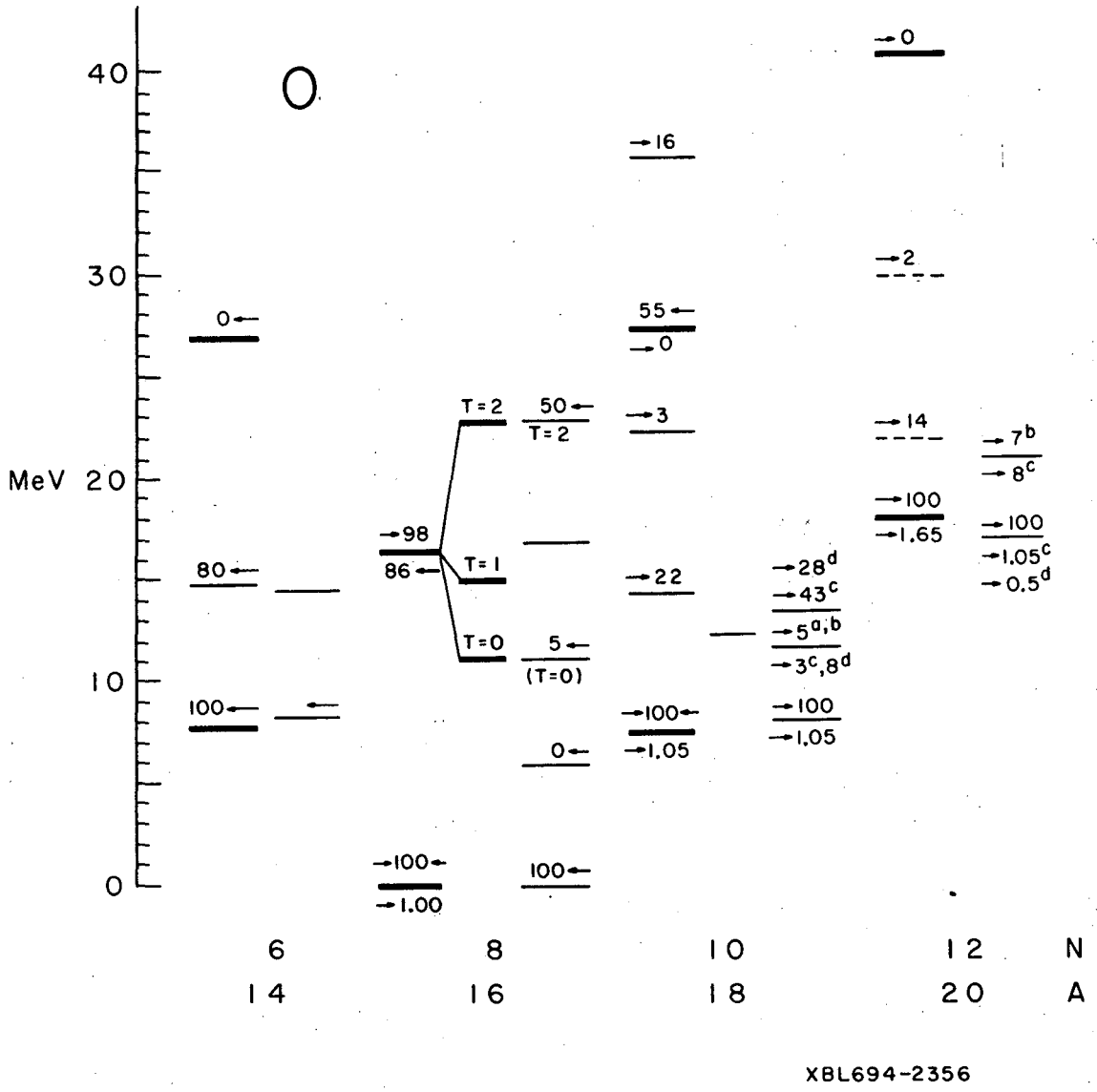
O
MeV
40
30
20
10
0
0
80
100
98
86
T=2
T=1
T=0
50
T=2
5
(T=0)
0
100
1.00
100
16
55
0
3
22
100
1.05
28d
43c
5a,b
3c,8d
100
1.05
0
2
14
100
1.65
7b
8c
100
1.05c
0.5d
6
8
10
12
N
14
16
18
20
A
XBL694-2356

Fig. 7.

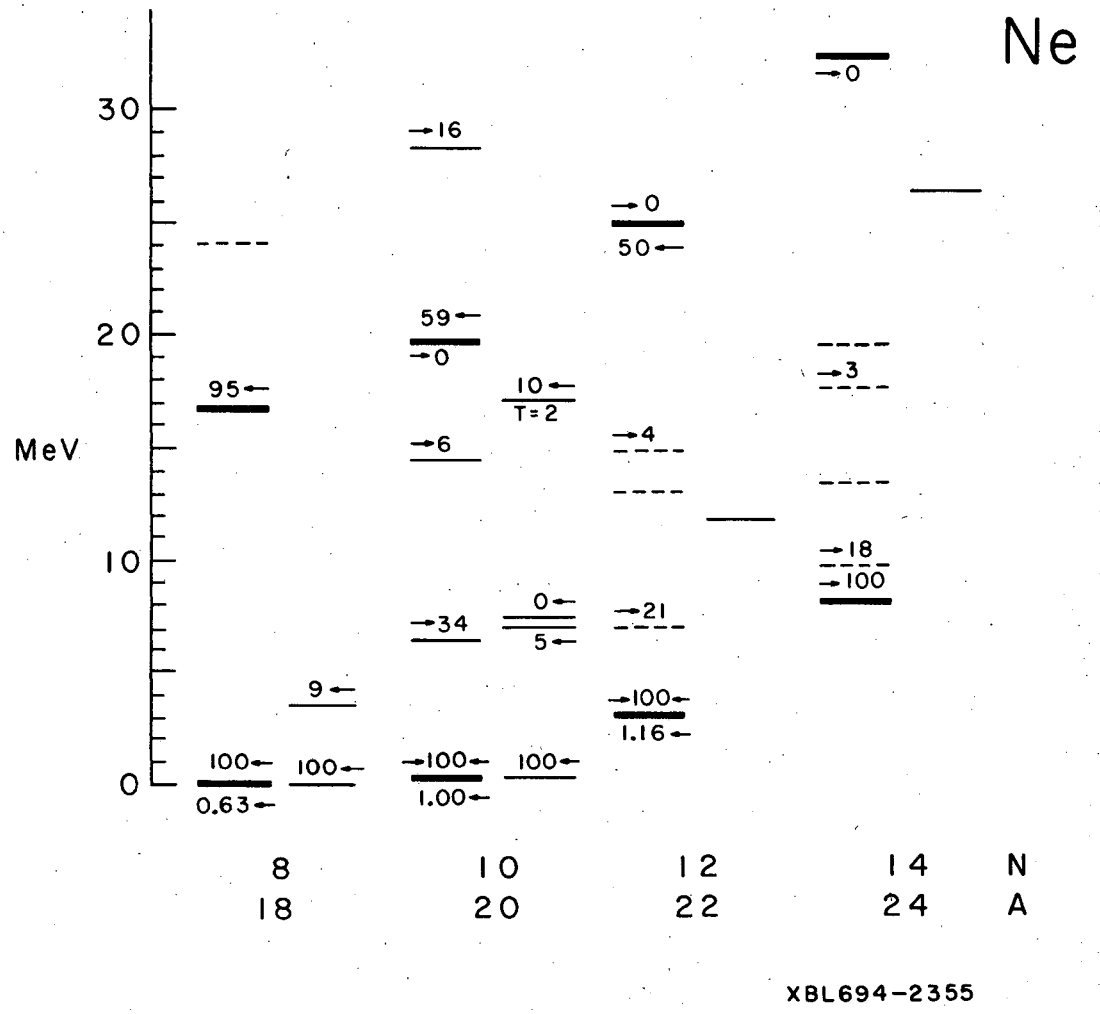
Ne
MeV
30
20
10
0
16
0
50
59
0
95
10
T=2
3
6
4
18
100
34
0
5
21
9
100
1.16
100
100
100
0.63
1.00
8
10
12
14
N
18
20
22
24
A
XBL694-2355

Fig. 8.

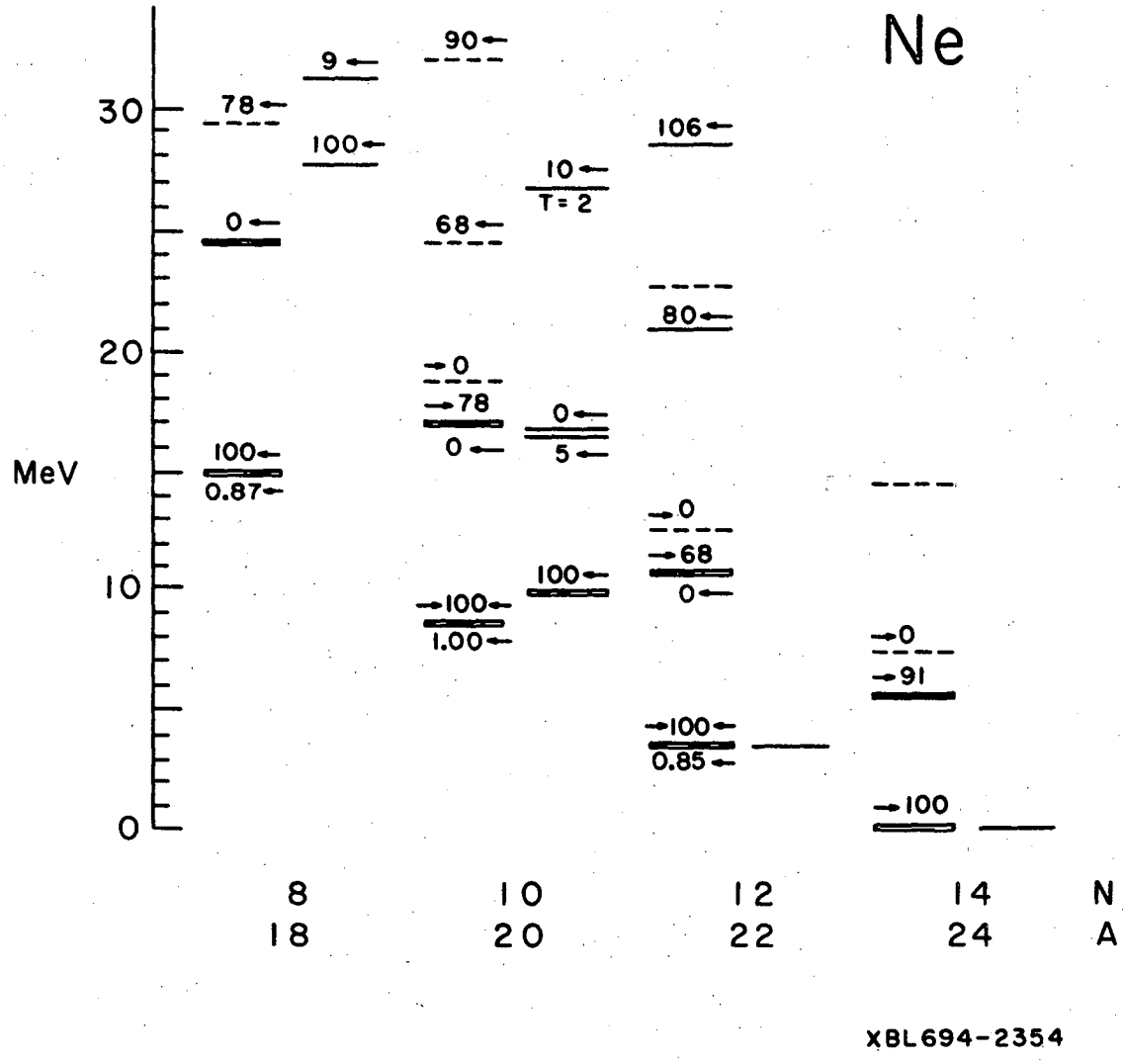
Ne
MeV
30
20
10
0
78
0
100
0.87
9
100
90
68
0
78
0
100
1.00
10
T=2
0
5
100
106
80
0
68
0
100
0.85
0
91
100
8
18
10
20
12
22
14
24
N
A
XBL694-2354

Fig. 9.

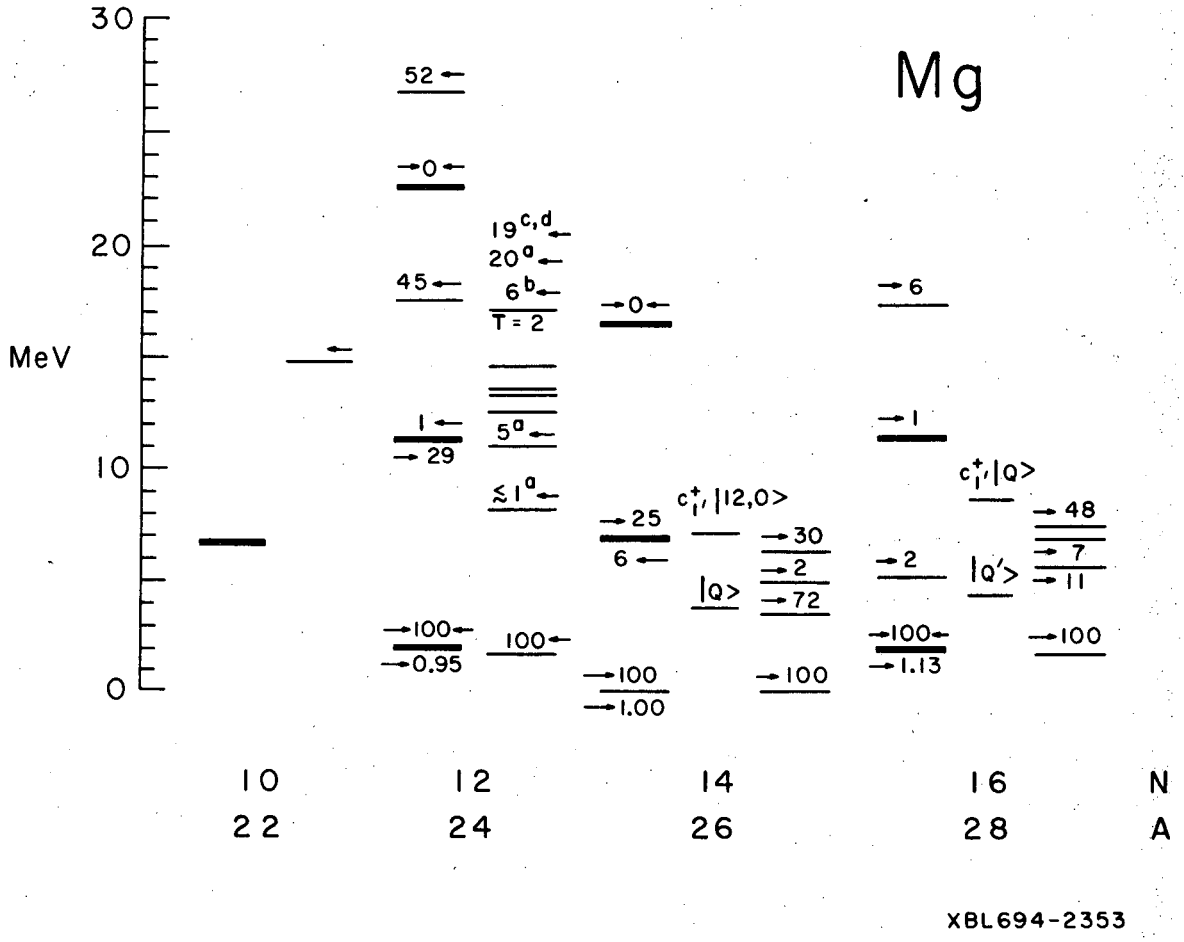
Mg
MeV
30
20
10
0
52
0
45
1
29
100
0.95
19c,d
20a
6b
T = 2
5a
≲1a
100
0
25
6
100
1.00
c1+|12,0>
|0>
30
2
72
100
6
1
2
100
1.13
c1+|0>
|0'>
48
7
11
100
10
12
14
16
N
22
24
26
28
A
XBL694-2353

Fig. 10.

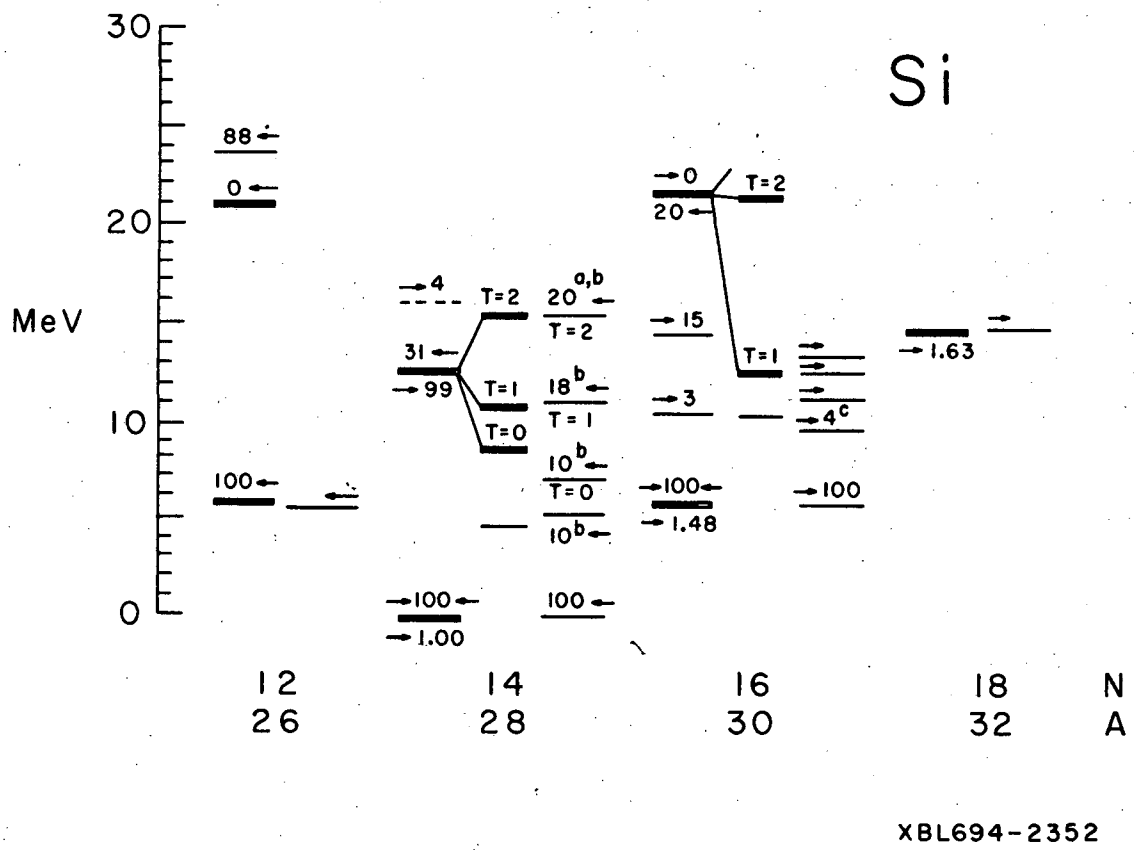
Si
MeV
30
20
10
0
88
0
100
4
31
99
T=2
T=1
T=0
100
1.00
20 a,b
T=2
18 b
T=1
10 b
T=0
10 b
100
0
20
T=2
15
3
100
1.48
T=1
4 c
100
1.63
12
26
14
28
16
30
18
32
N
A
XBL694-2352

Fig. 11.

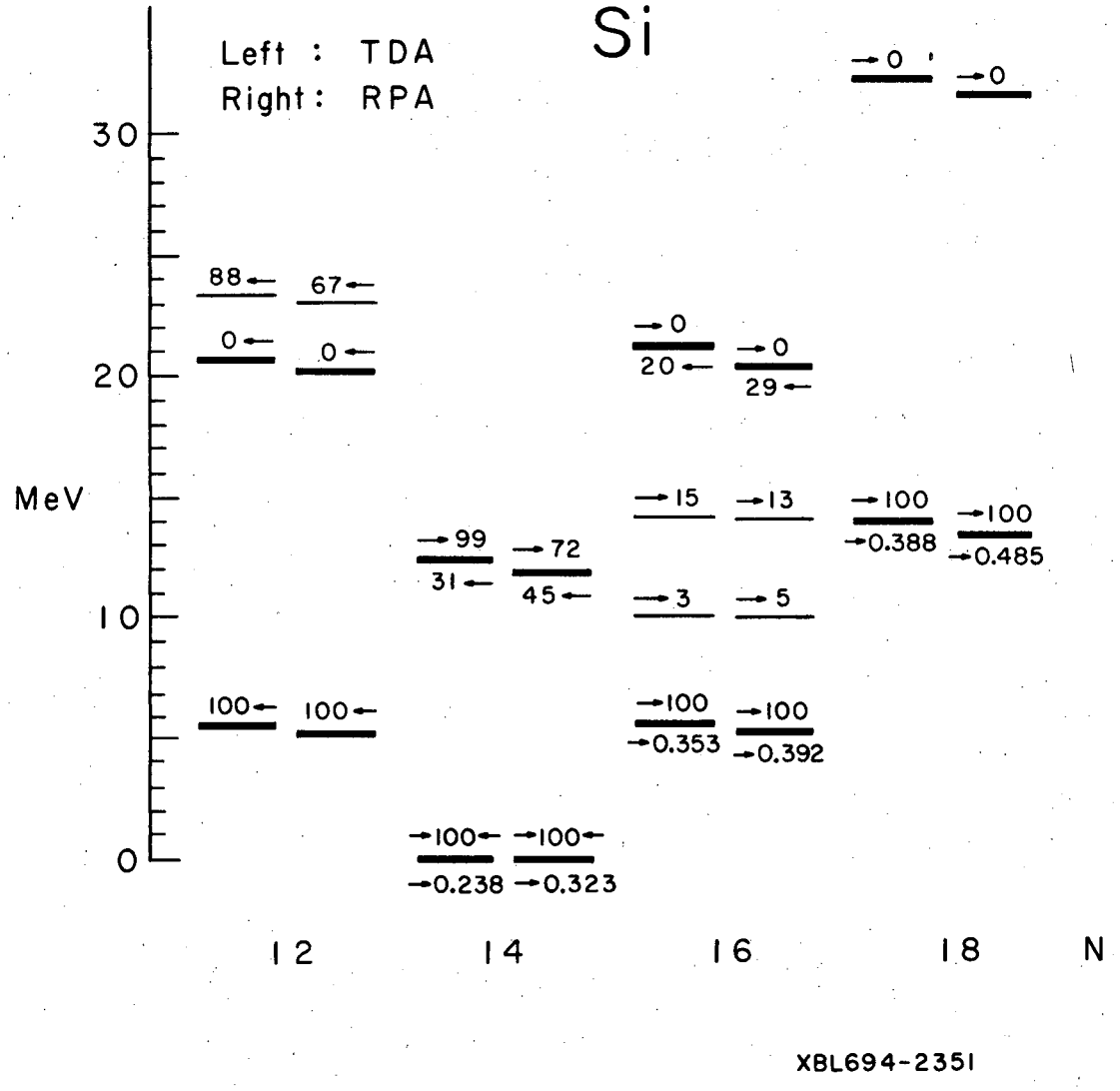
Si
Left : TDA
Right : RPA
MeV
30
20
10
0
88
67
0
0
100
100
99
31
72
45
100
100
0.238
0.323
0
0
20
29
15
13
3
5
100
100
0.353
0.392
0
0
100
100
0.388
0.485
12
14
16
18
N
XBL694-2351

Fig. 12.

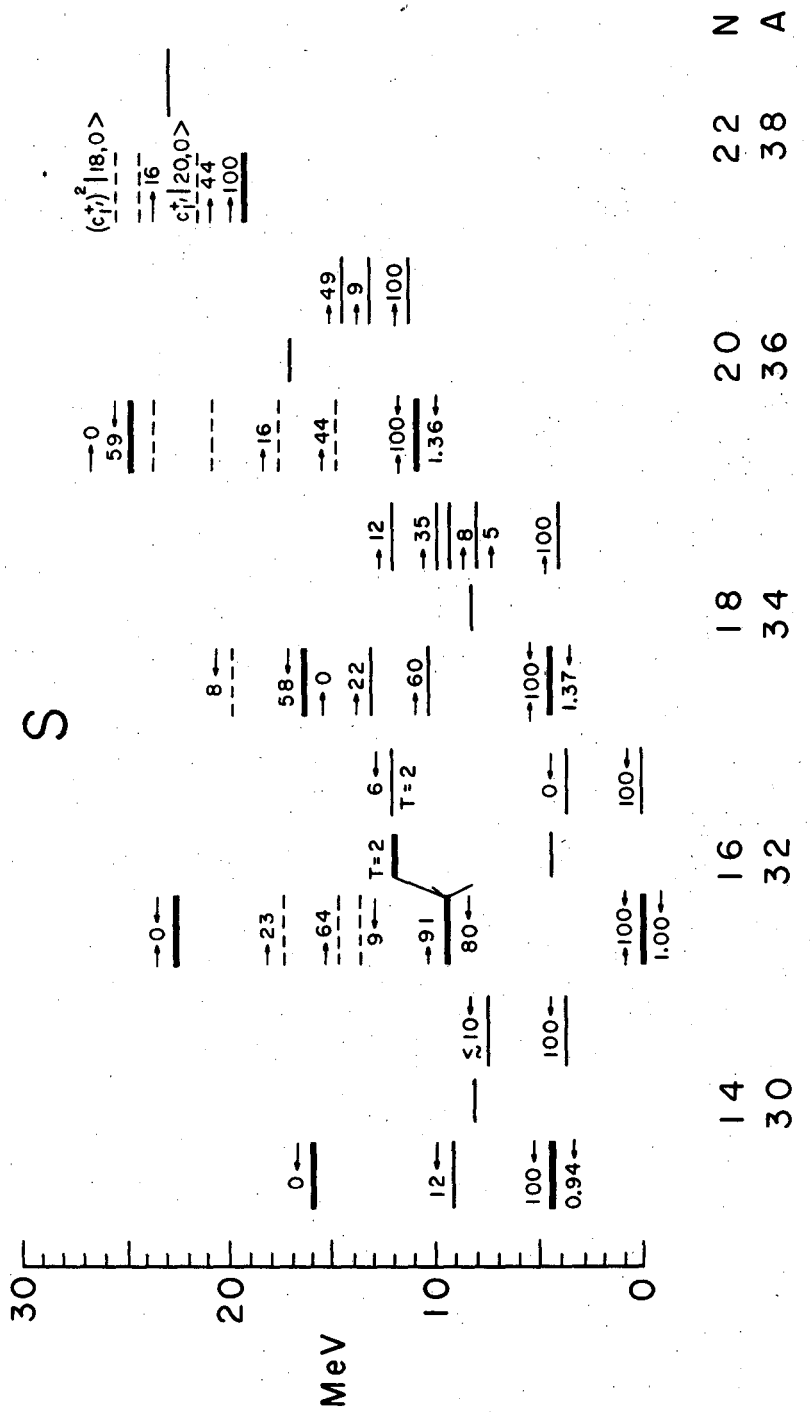

Fig. 13.

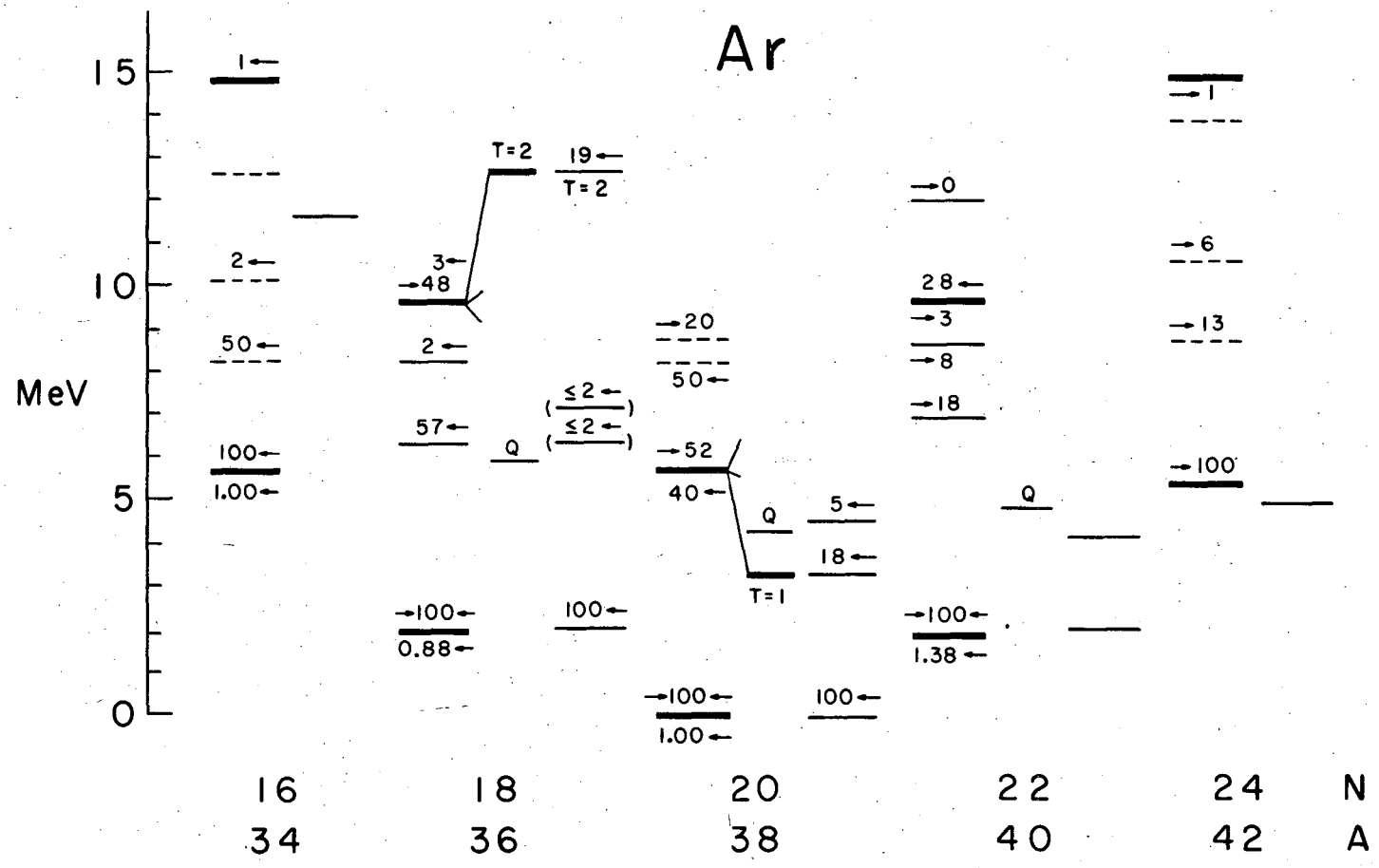

XBL694-2349

Fig. 14.

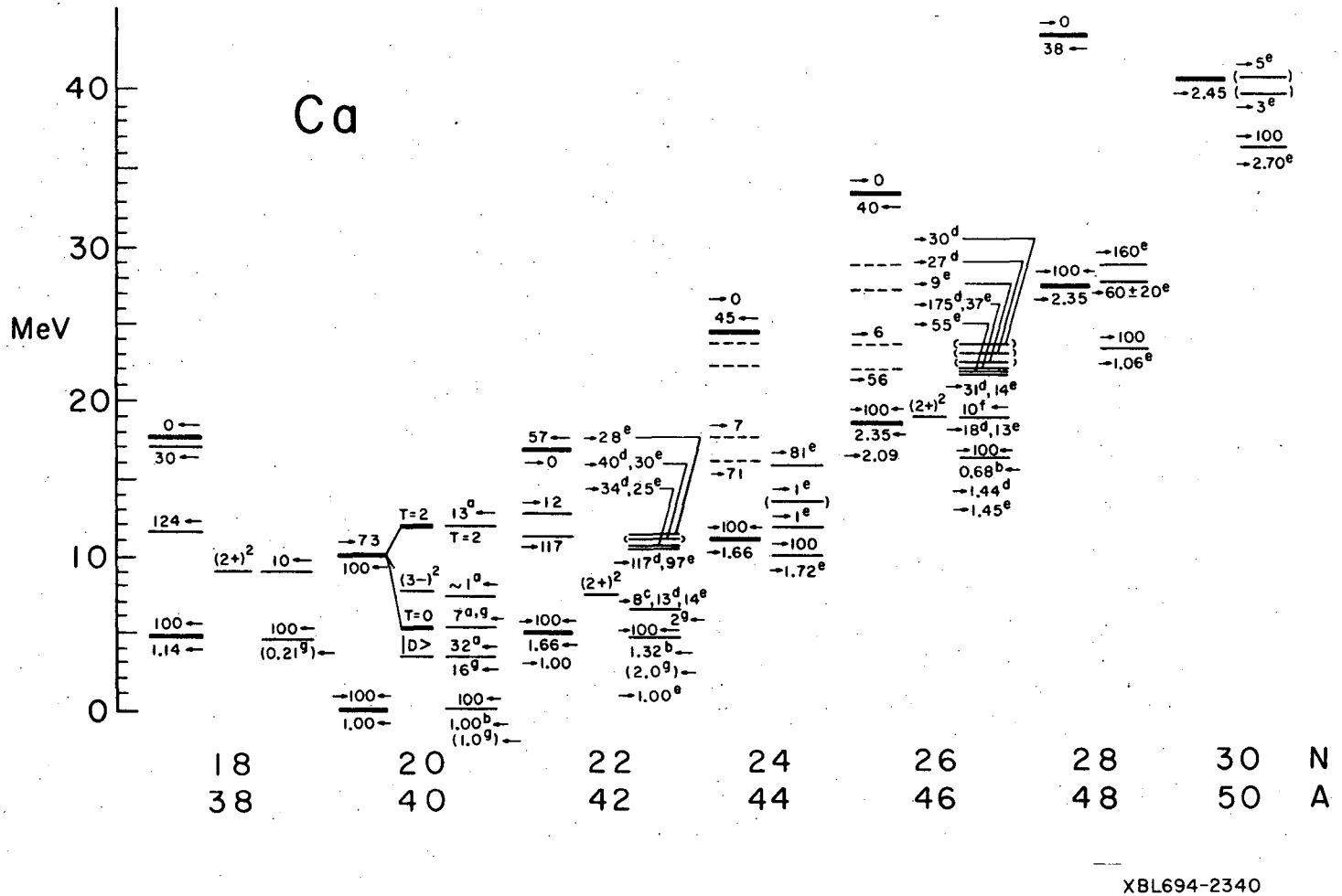
Ca
MeV
40
30
20
10
0
18
20
22
24
26
28
30
N
38
40
42
44
46
48
50
A
XBL694-2340

Fig. 15.

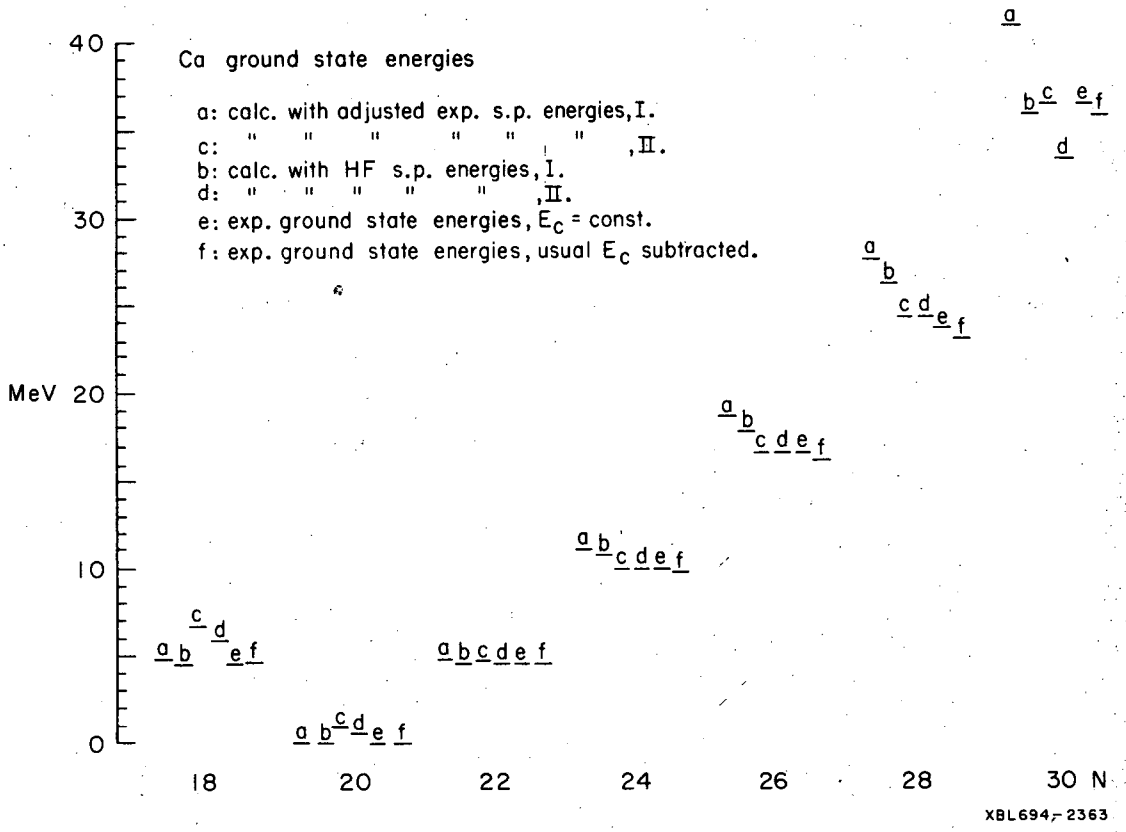
Ca ground state energies
a: calc. with adjusted exp. s.p. energies, I.
c: " " " " " " ,II.
b: calc. with HF s.p. energies, I.
d: " " " " " ,II.
e: exp. ground state energies, E_c = const.
f: exp. ground state energies, usual E_c subtracted.
MeV
40
30
20
10
0
18
20
22
24
26
28
30 N
XBL694-2363

Fig. 16.

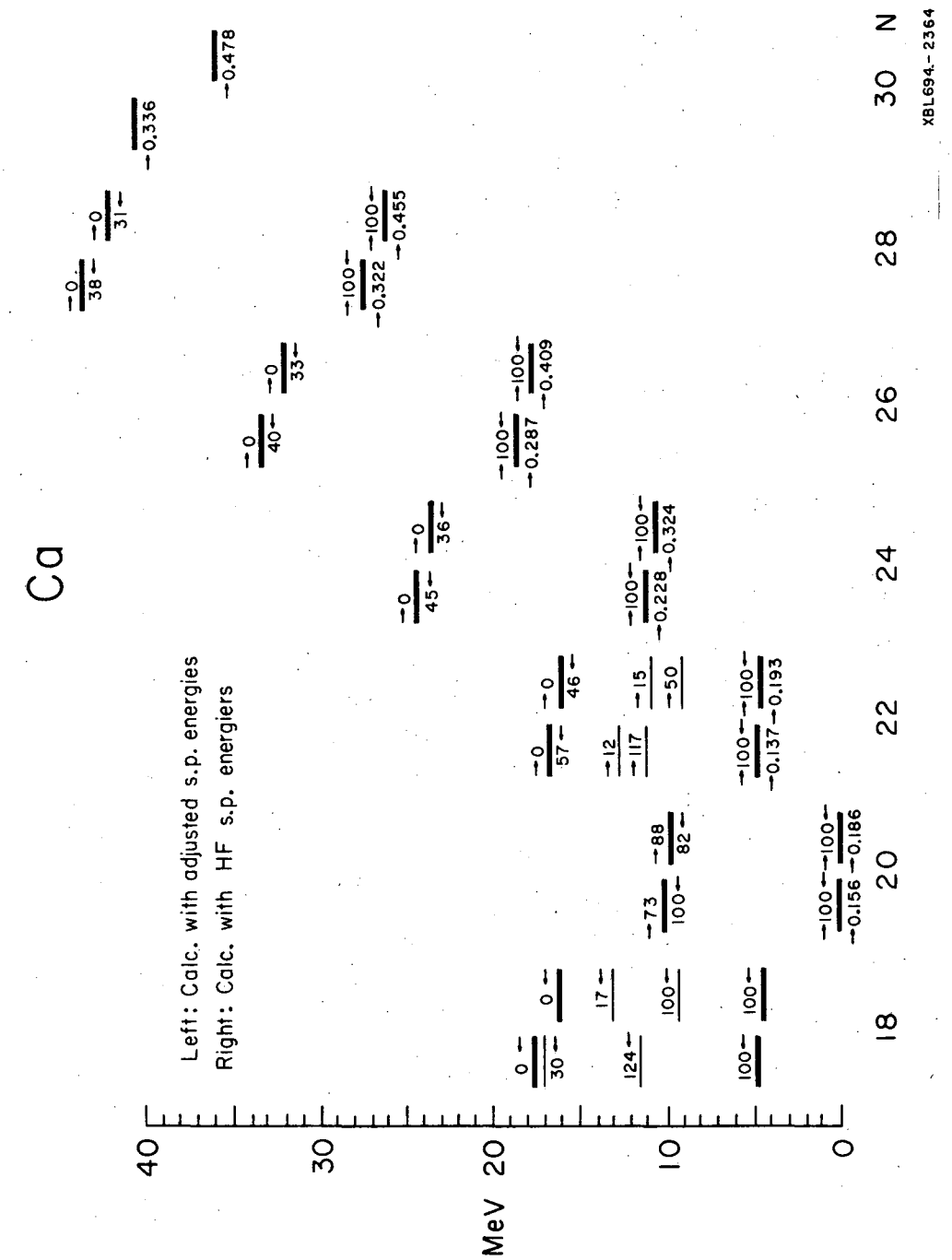
Ca
Left: Calc. with adjusted s.p. energies
Right: Calc. with HF s.p. energiers
MeV
40
30
20
10
0
18
20
22
24
26
28
30 N
XBL694-2364

Fig. 17.

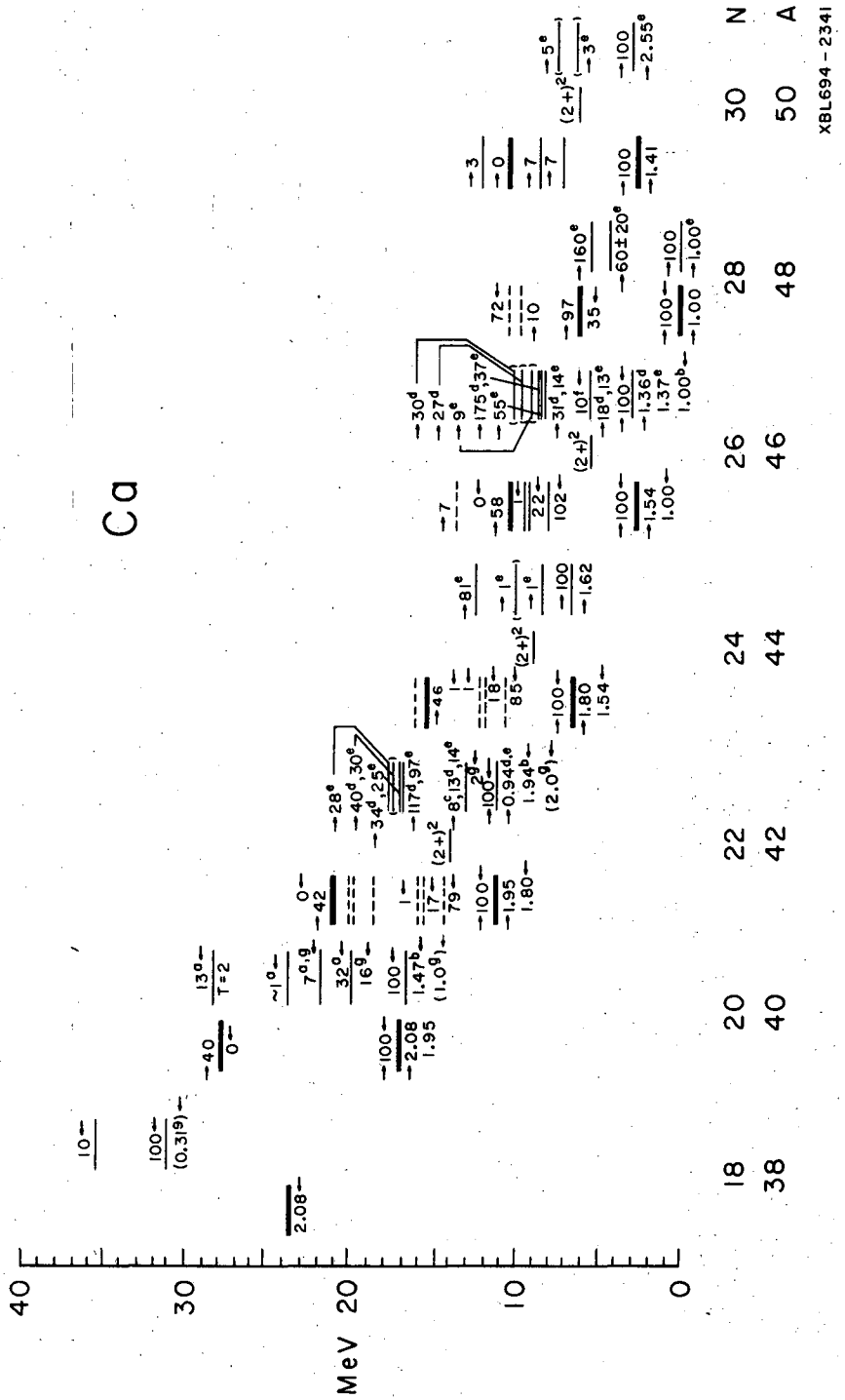
Ca
MeV
40
30
20
10
0
18
20
22
24
26
28
30
N
38
40
42
44
46
48
50
A
XBL694-2341

Fig. 18.

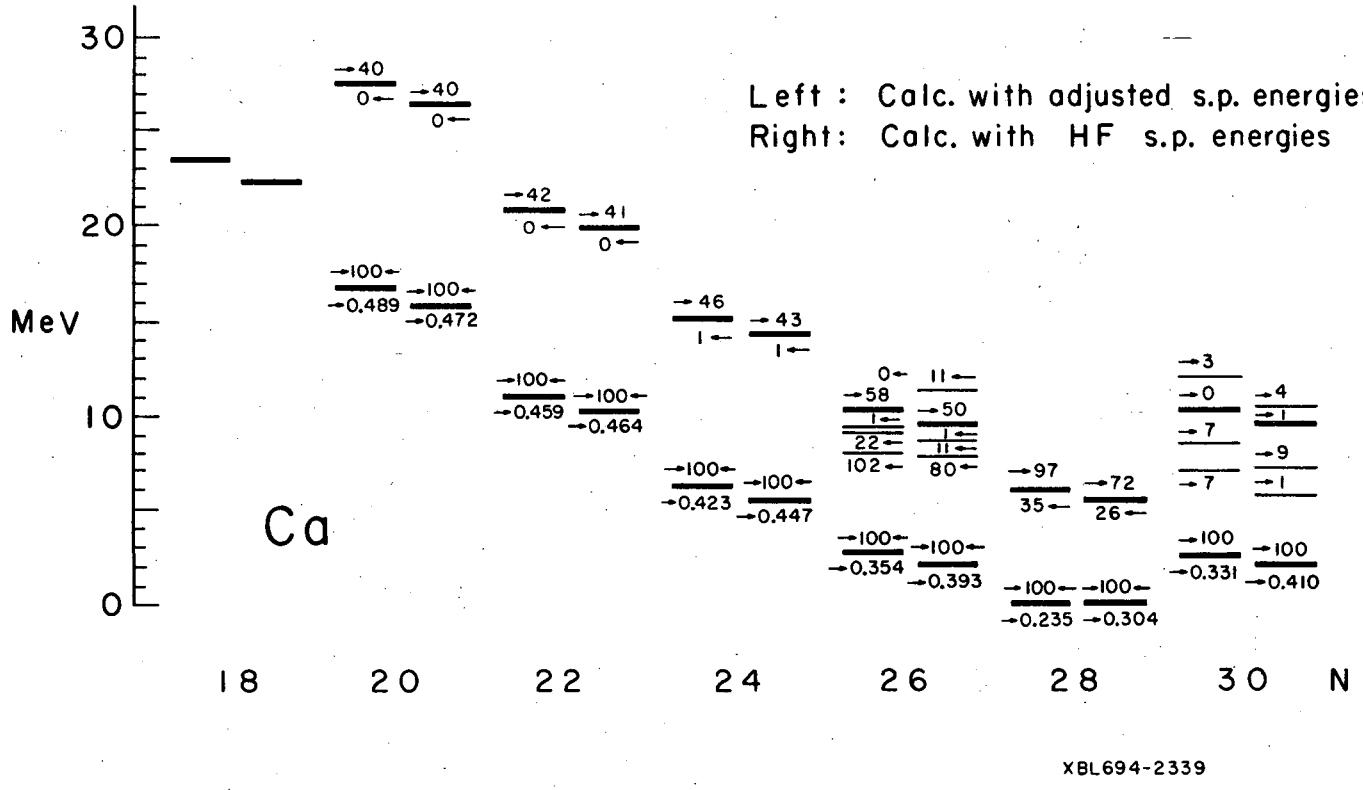
Left : Calc. with adjusted s.p. energies
Right: Calc. with HF s.p. energies
MeV
30
20
10
0
Ca
18
20
22
24
26
28
30
N
XBL694-2339

Fig. 19.

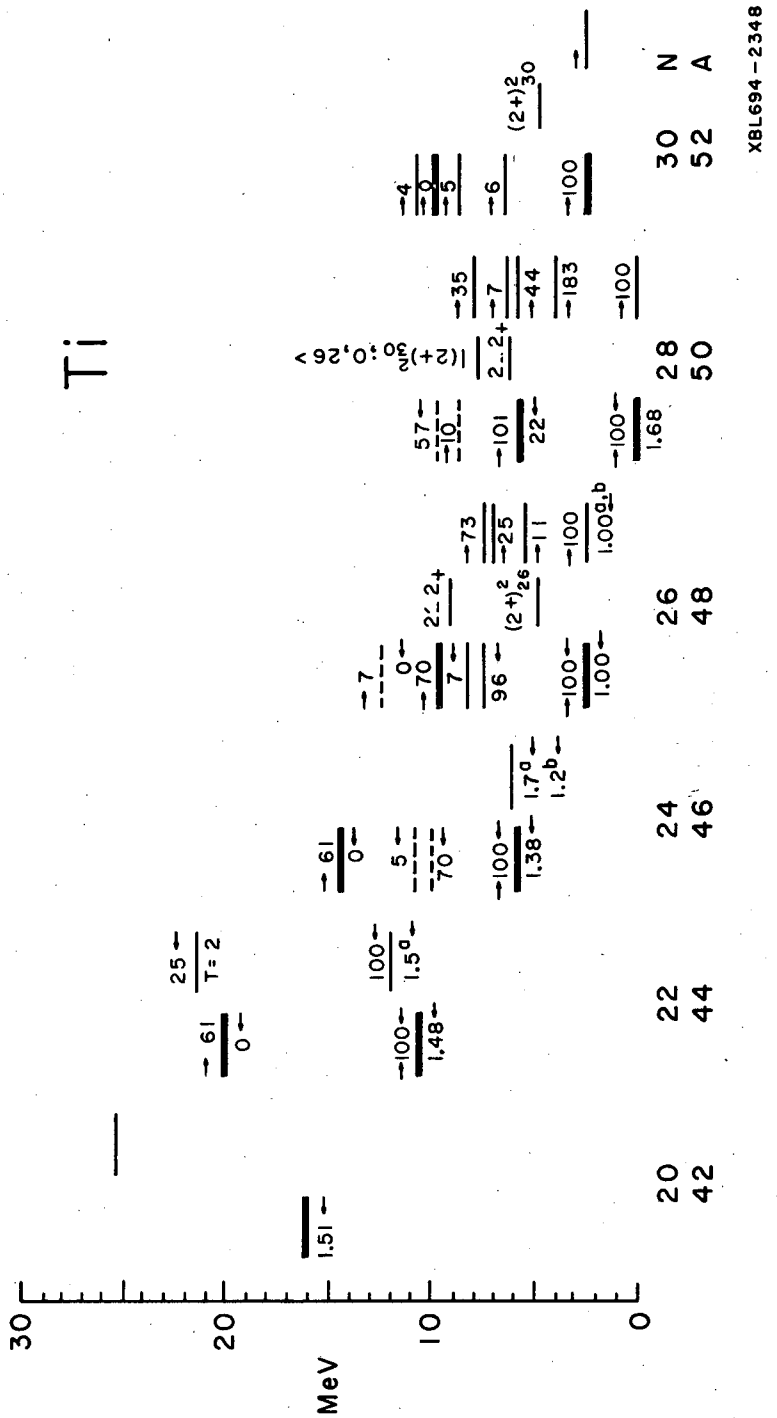

Fig. 20.

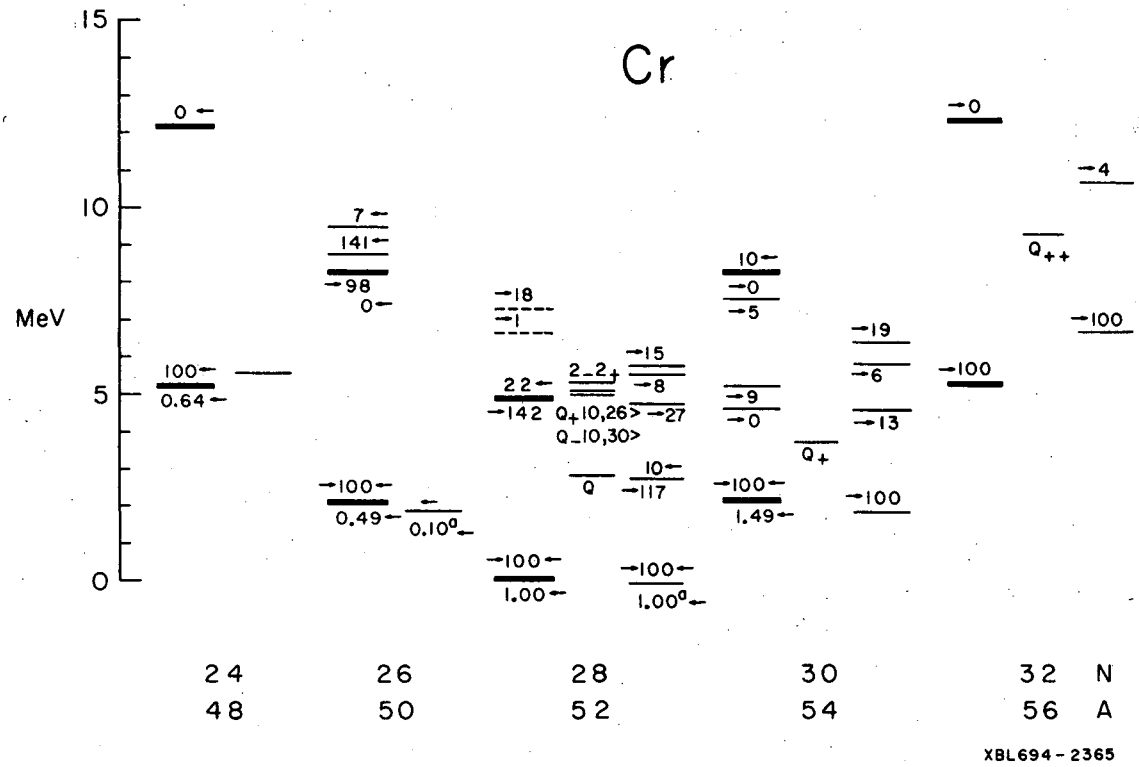
Cr
MeV
15
10
5
0
0
100
0.64
7
141
98
0
100
0.49
0.10
18
1
22
142
2-2+
Q+10,26>
Q-10,30>
27
15
8
Q
10
117
100
1.00
100
1.00
10
0
5
9
0
100
1.49
Q+
19
6
13
100
0
100
Q++
4
100
24 26 28 30 32 N
48 50 52 54 56 A
XBL694-2365

Fig. 21.

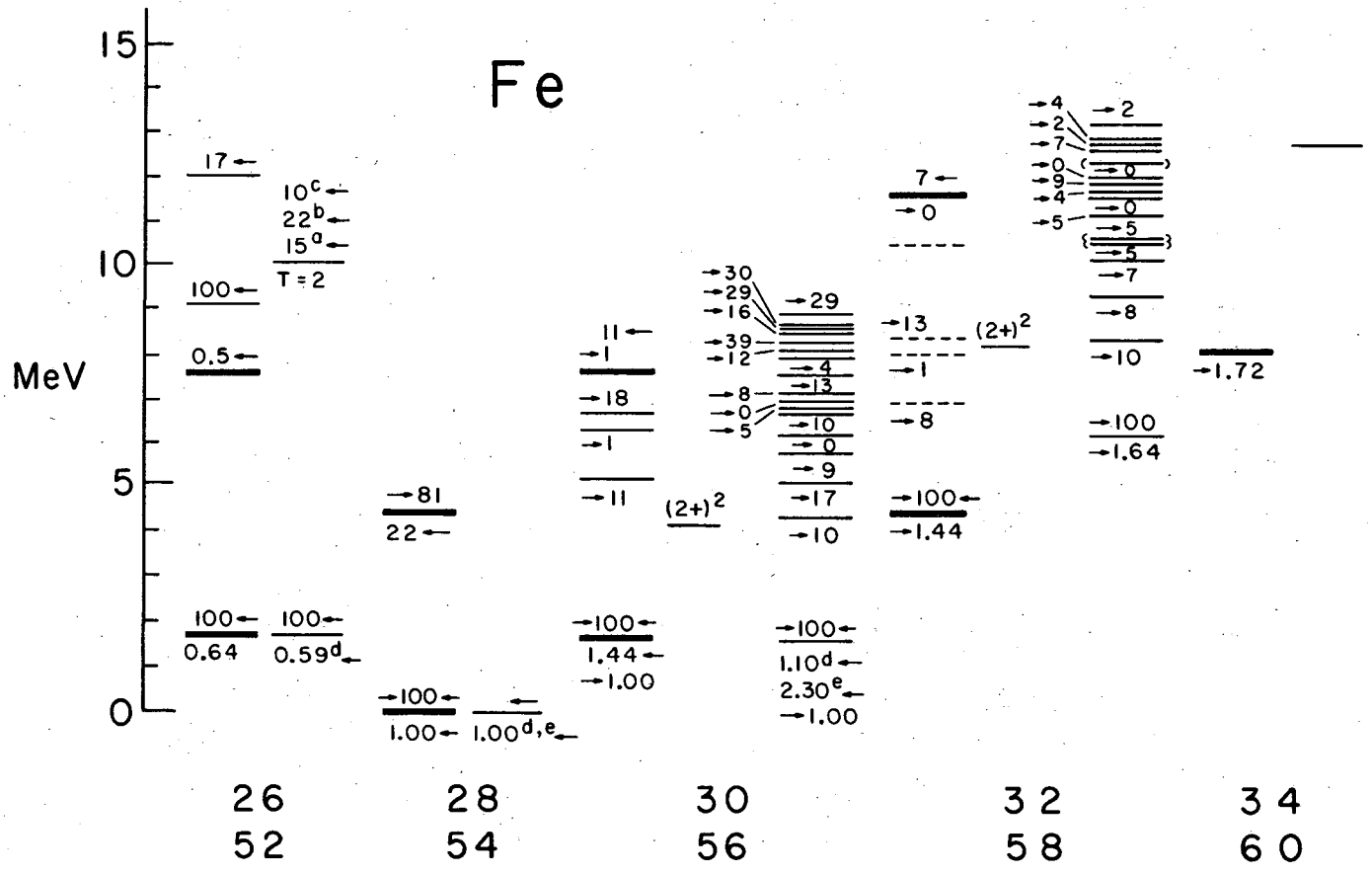

Fig. 22.

UCRL-18834

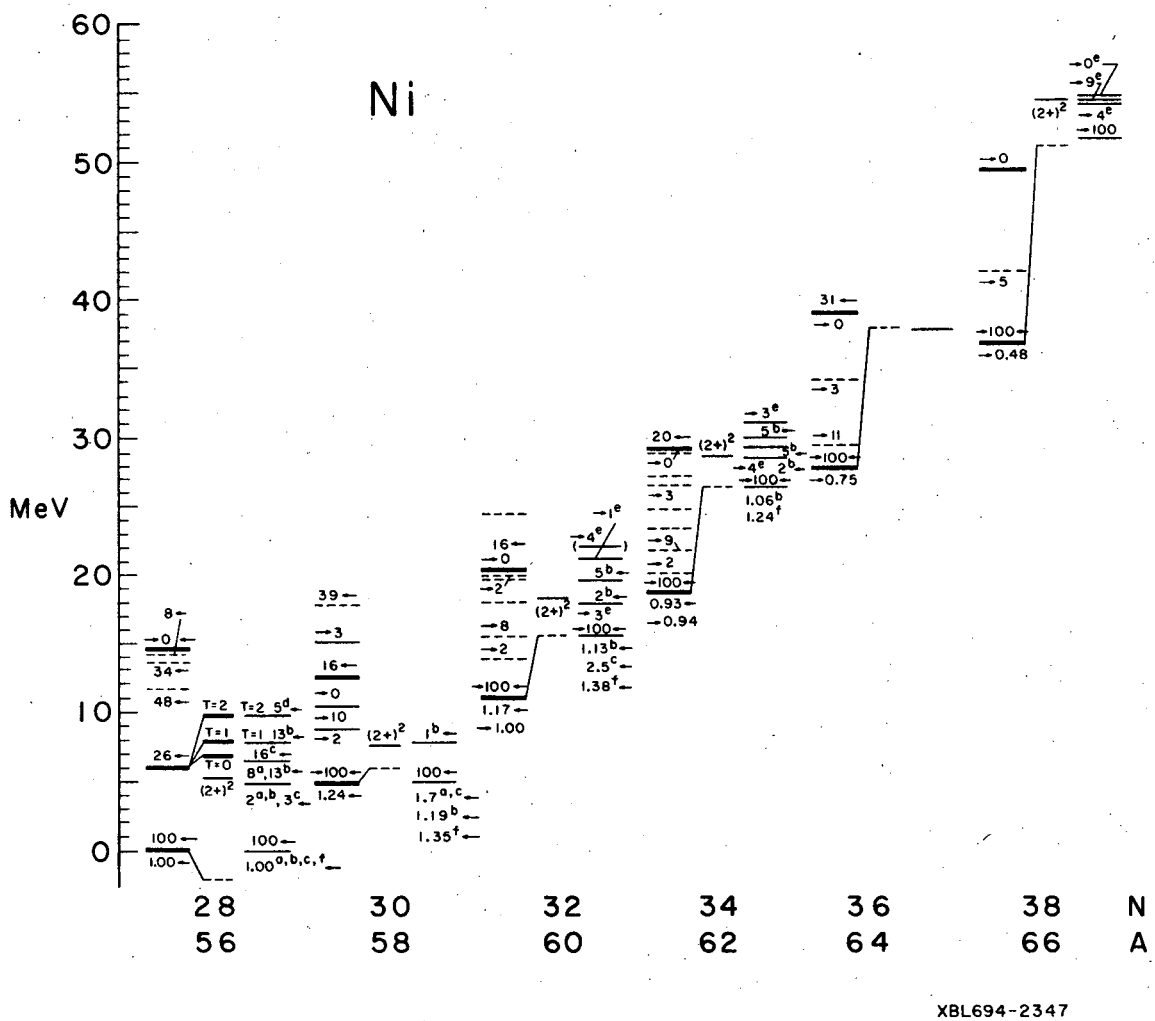
Ni
MeV
60
50
40
30
20
10
0
28
30
32
34
36
38
N
56
58
60
62
64
66
A
XBL694-2347

Fig. 23.

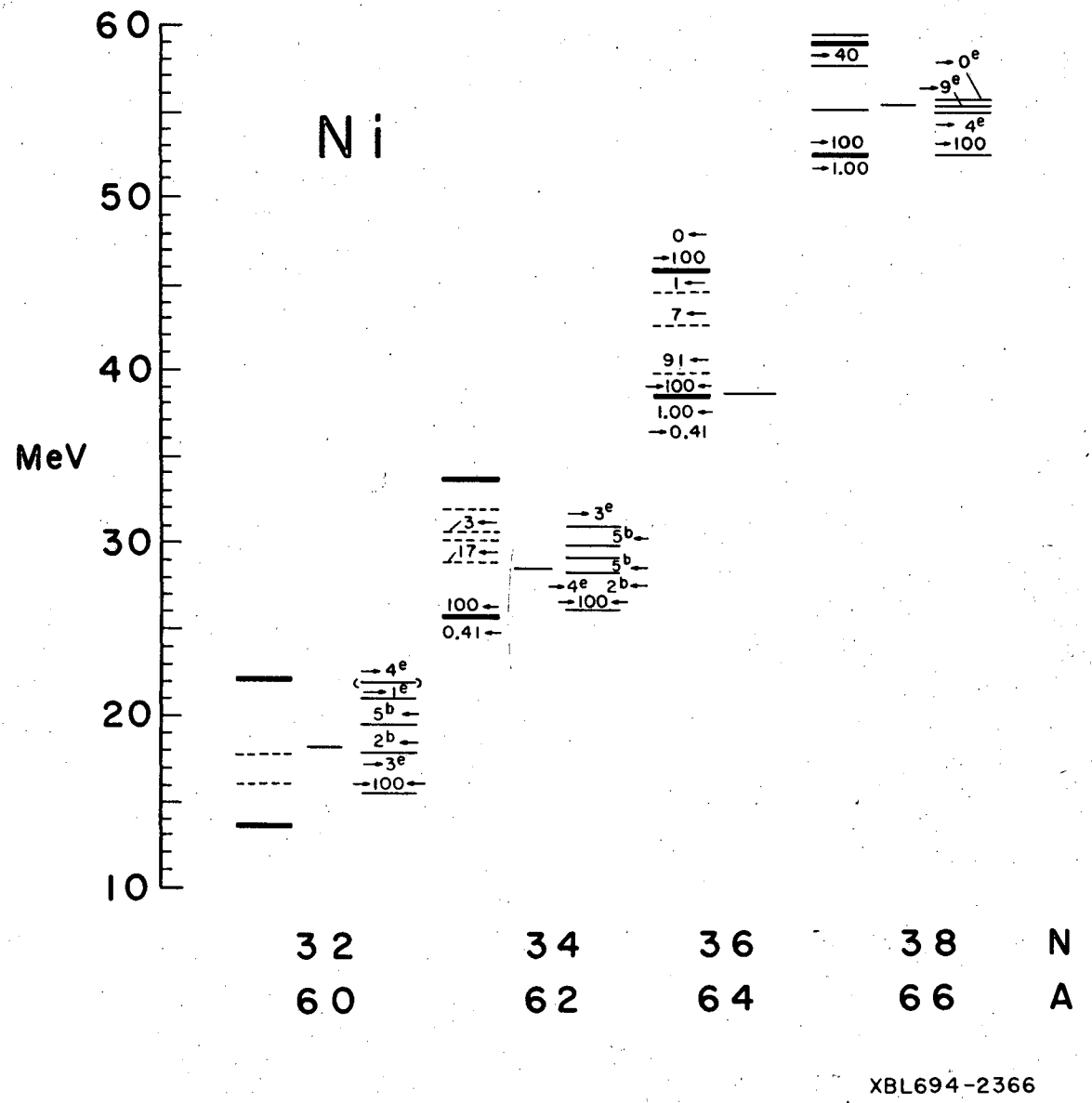

Fig. 24.

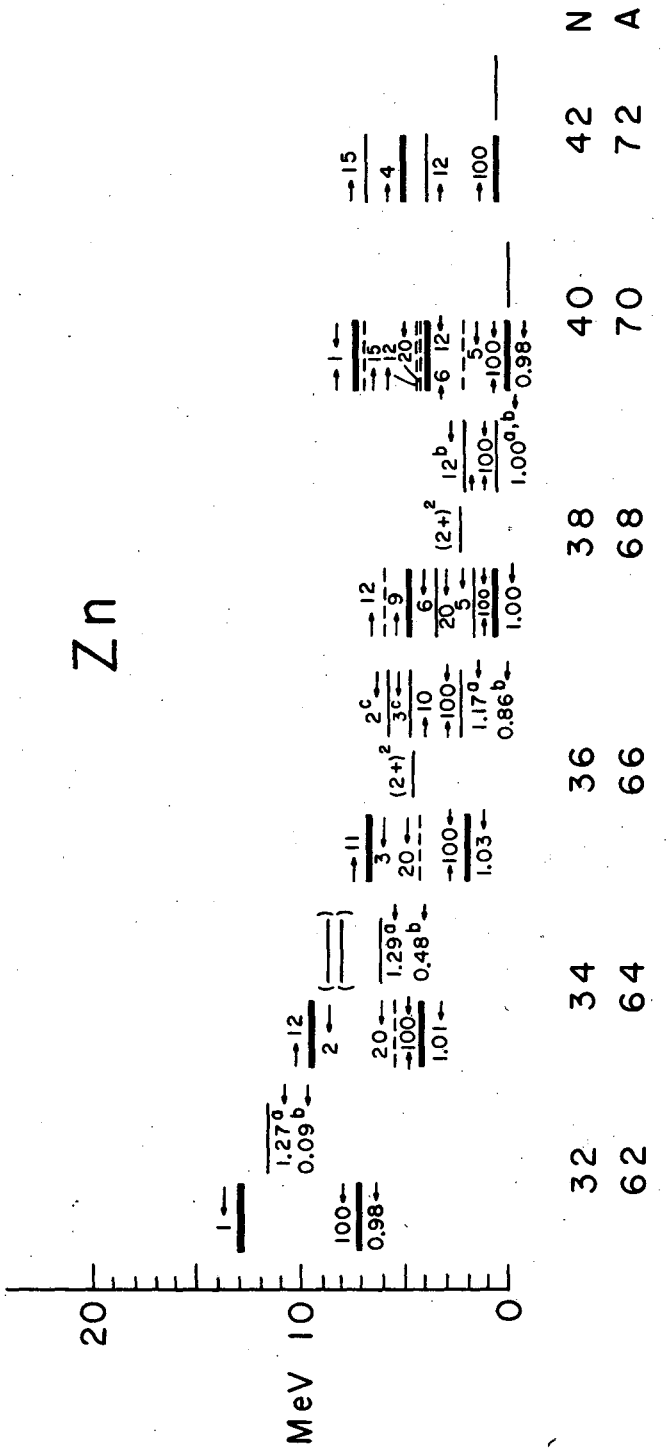

Fig. 25.

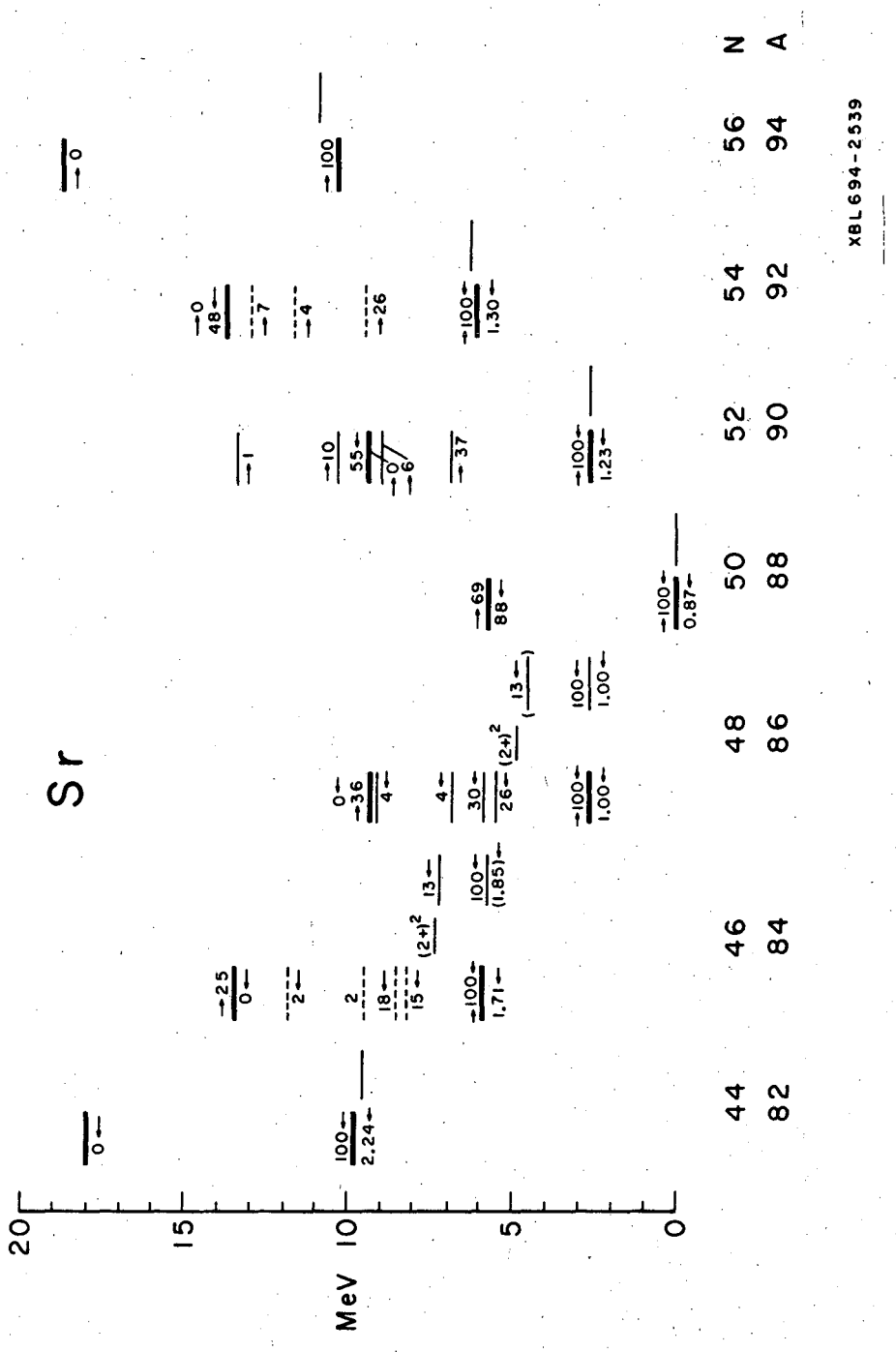
Sr
MeV
20
15
10
5
0
44
46
48
50
52
54
56
N
82
84
86
88
90
92
94
A
XBL694-2539

Fig. 26.

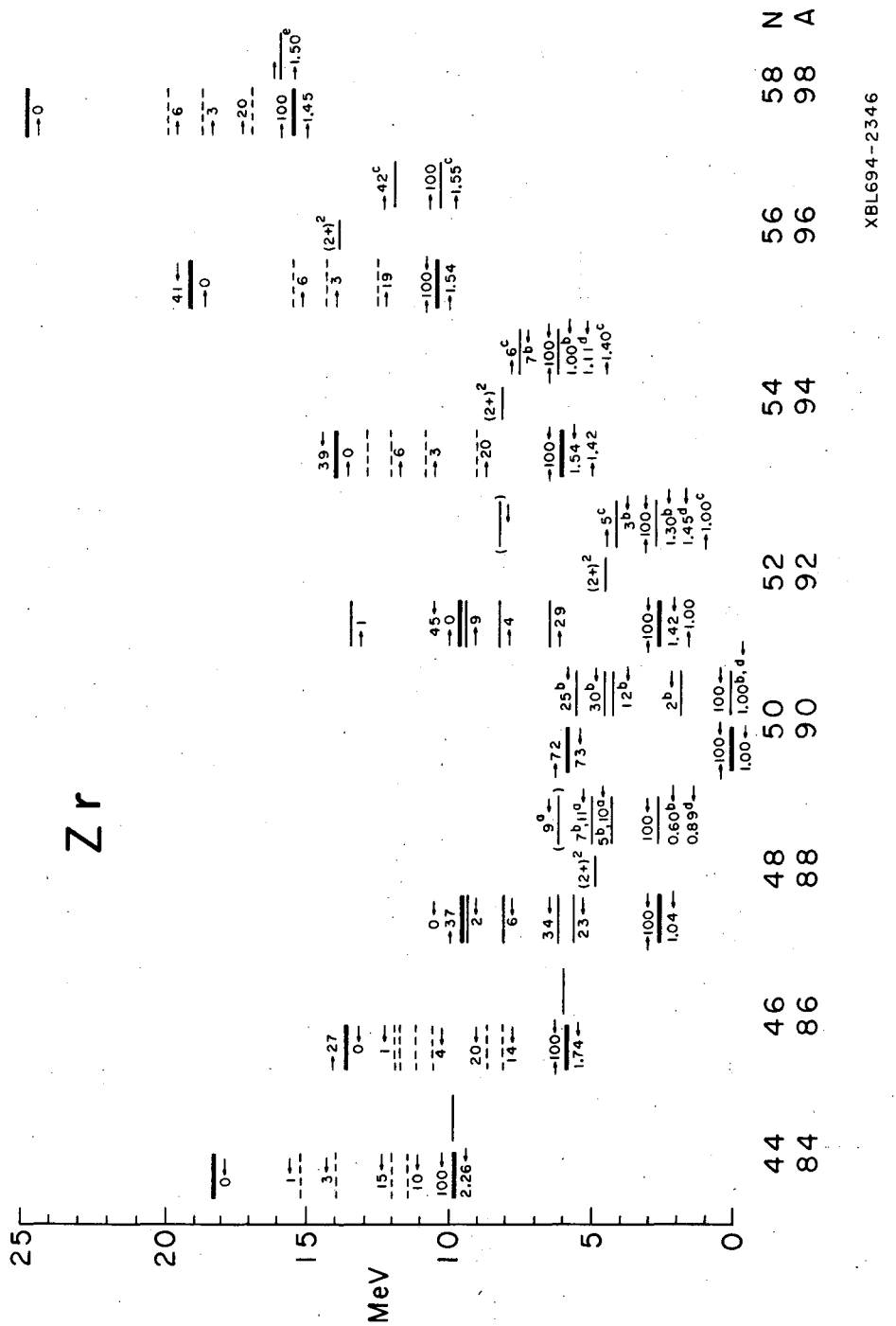
Zr
MeV
25
20
15
10
5
0
44 46 48 50 52 54 56 58 N
84 86 88 90 92 94 96 98 A
XBL694-2346

Fig. 27.

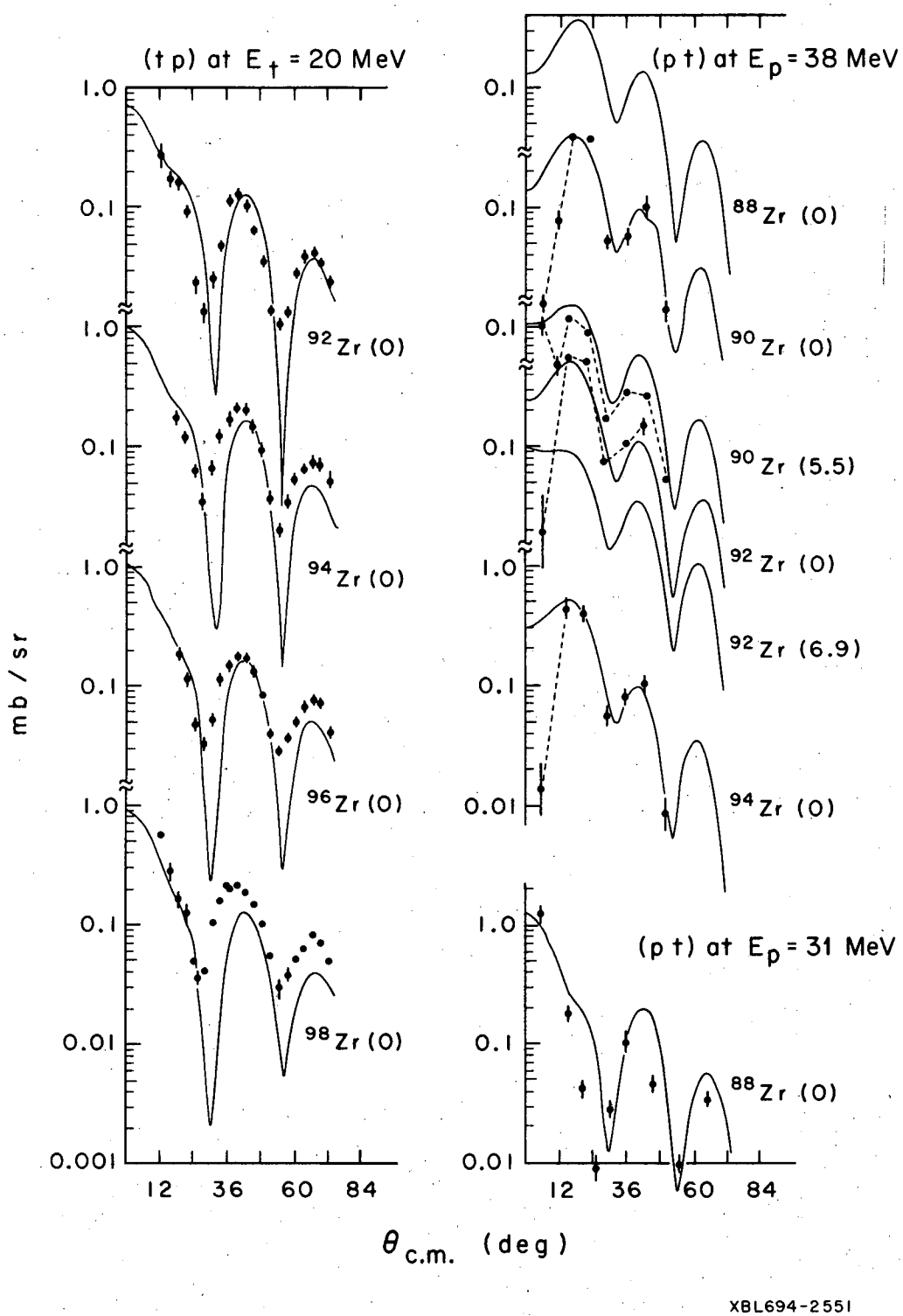
(t p) at E_t = 20 MeV
(p t) at E_p = 38 MeV
(p t) at E_p = 31 MeV
mb / sr
^{92}Zr (0)
^{94}Zr (0)
^{96}Zr (0)
^{98}Zr (0)
^{88}Zr (0)
^{90}Zr (0)
^{90}Zr (5.5)
^{92}Zr (0)
^{92}Zr (6.9)
^{94}Zr (0)
^{88}Zr (0)
1.0
0.1
0.01
0.001
12
36
60
84
$\theta_{c.m.}$ (deg)
XBL694-2551

Fig. 28.

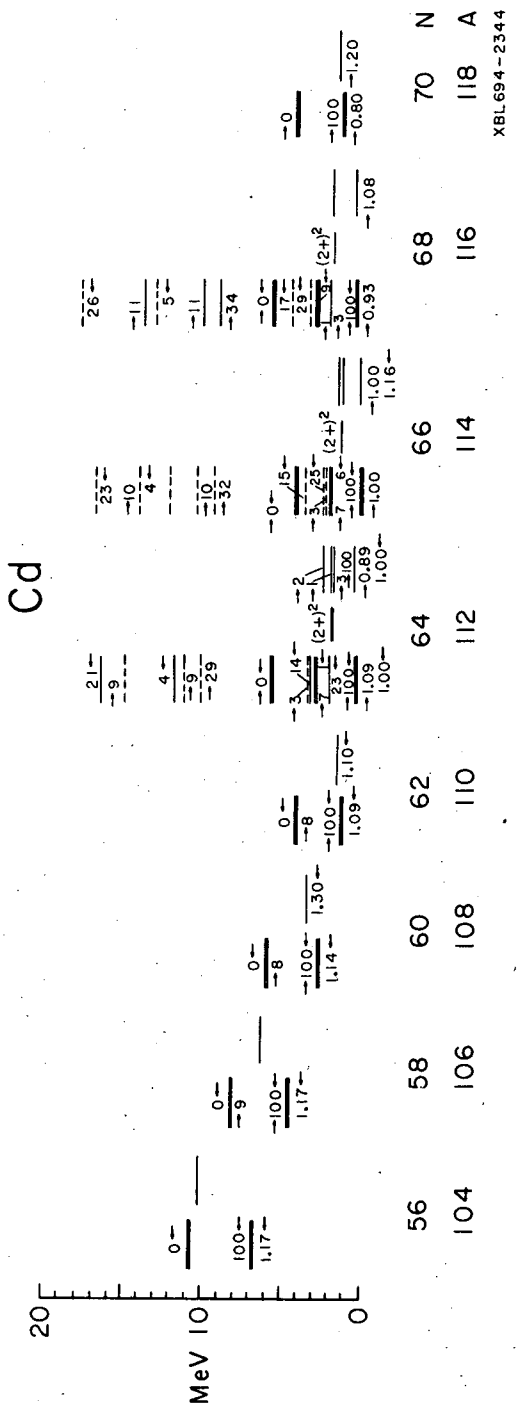
Cd
MeV
20
10
0
56
58
60
62
64
66
68
70
N
104
106
108
110
112
114
116
118
A
XBL694-2344

Fig. 29.

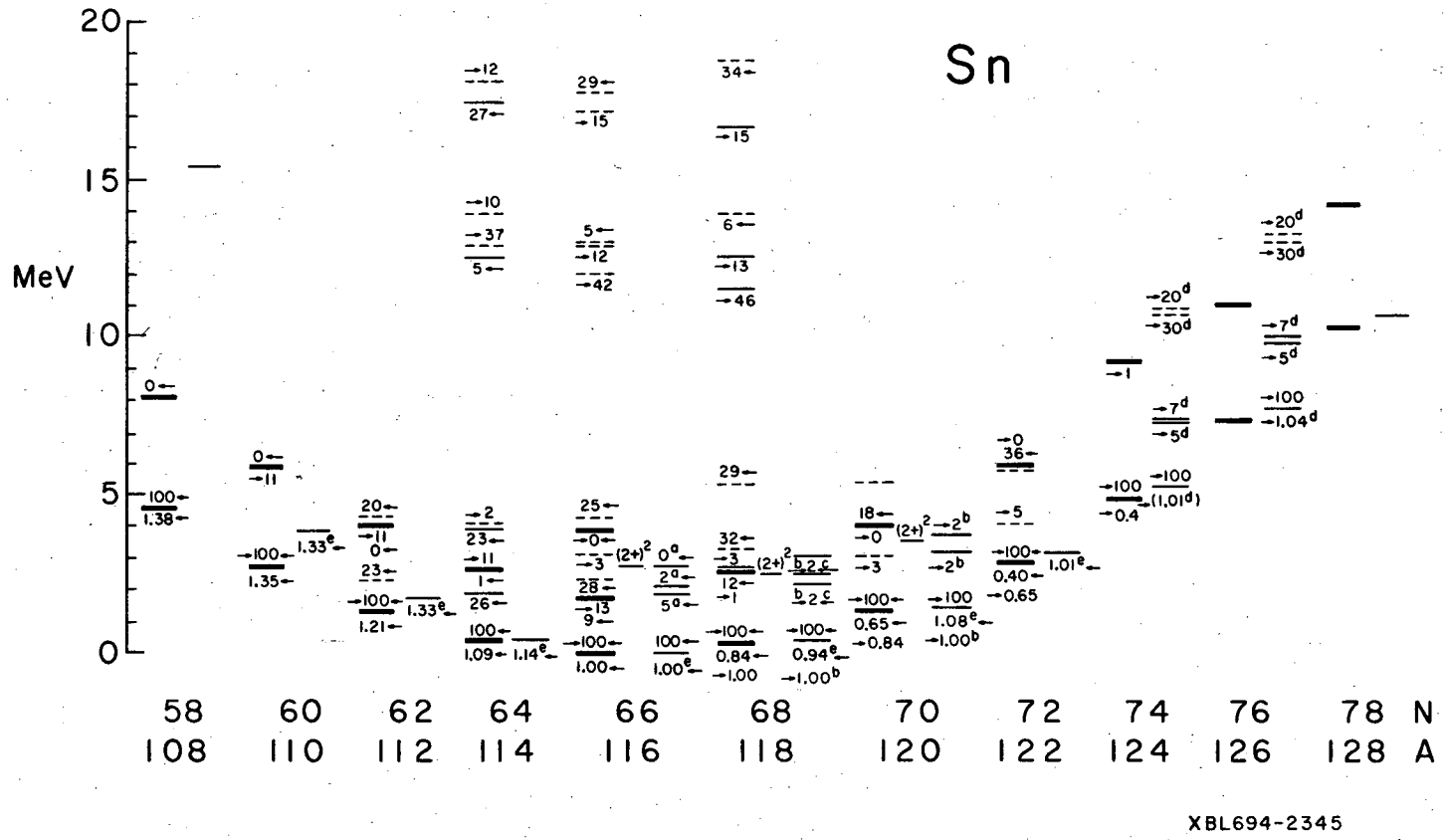

Fig. 30.

UCRL-18834

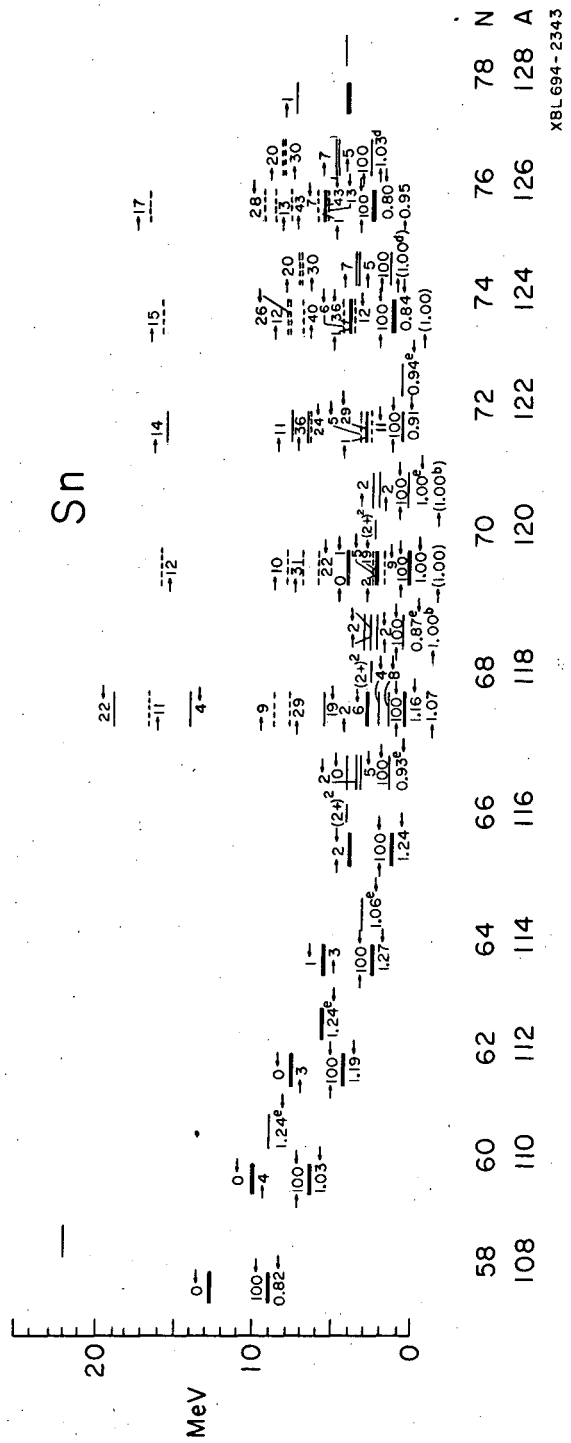
Sn
MeV
20
10
0
58
60
62
64
66
68
70
72
74
76
78 N
108
110
112
114
116
118
120
122
124
126
128 A
XBL694-2343

Fig. 31.

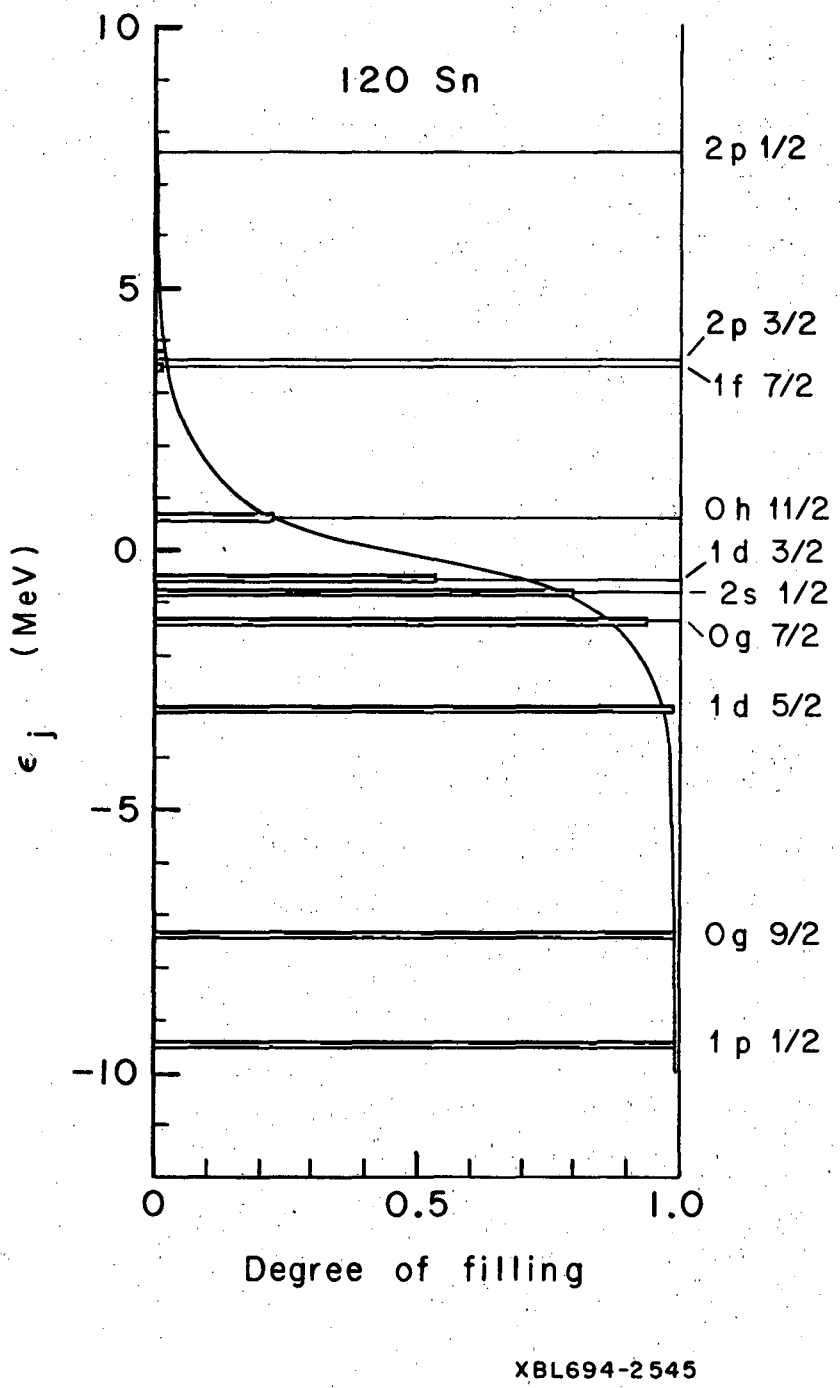
120 Sn
10
5
0
-5
-10
ϵ_j (MeV)
2p 1/2
2p 3/2
1f 7/2
0h 11/2
1d 3/2
2s 1/2
0g 7/2
1d 5/2
0g 9/2
1p 1/2
0
0.5
1.0
Degree of filling
XBL694-2545

Fig. 32.

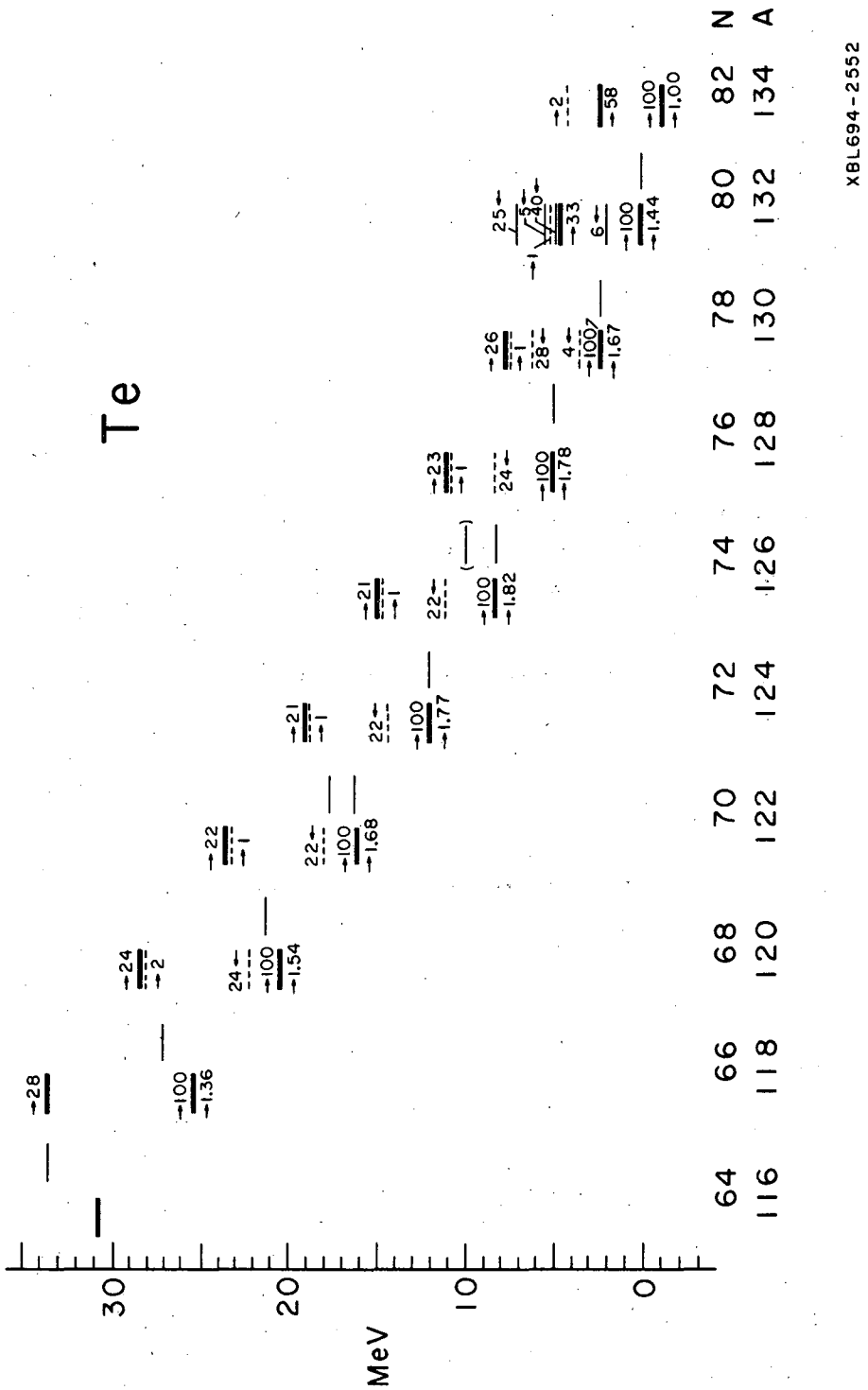
Te
MeV
30
20
10
0
64 66 68 70 72 74 76 78 80 82 N
116 118 120 122 124 126 128 130 132 134 A
XBL694-2552

Fig. 33.

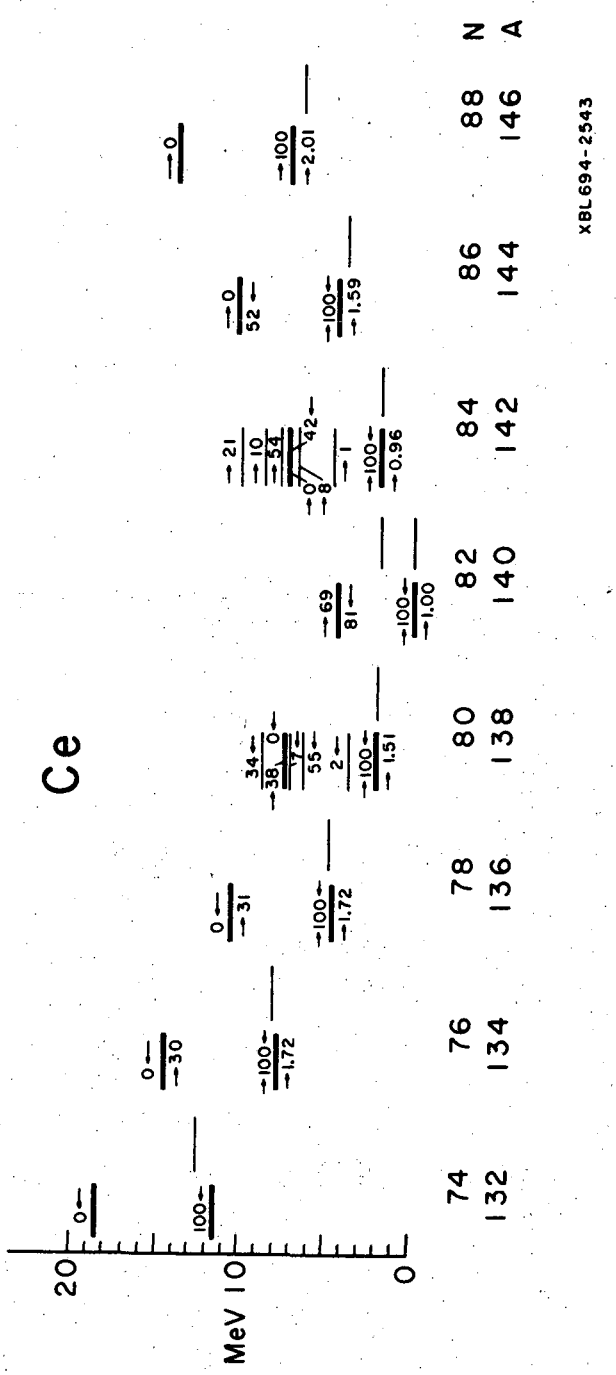
Ce
N
A
74
132
76
134
78
136
80
138
82
140
84
142
86
144
88
146
MeV
20
10
0
XBL694-2543

Fig. 34.

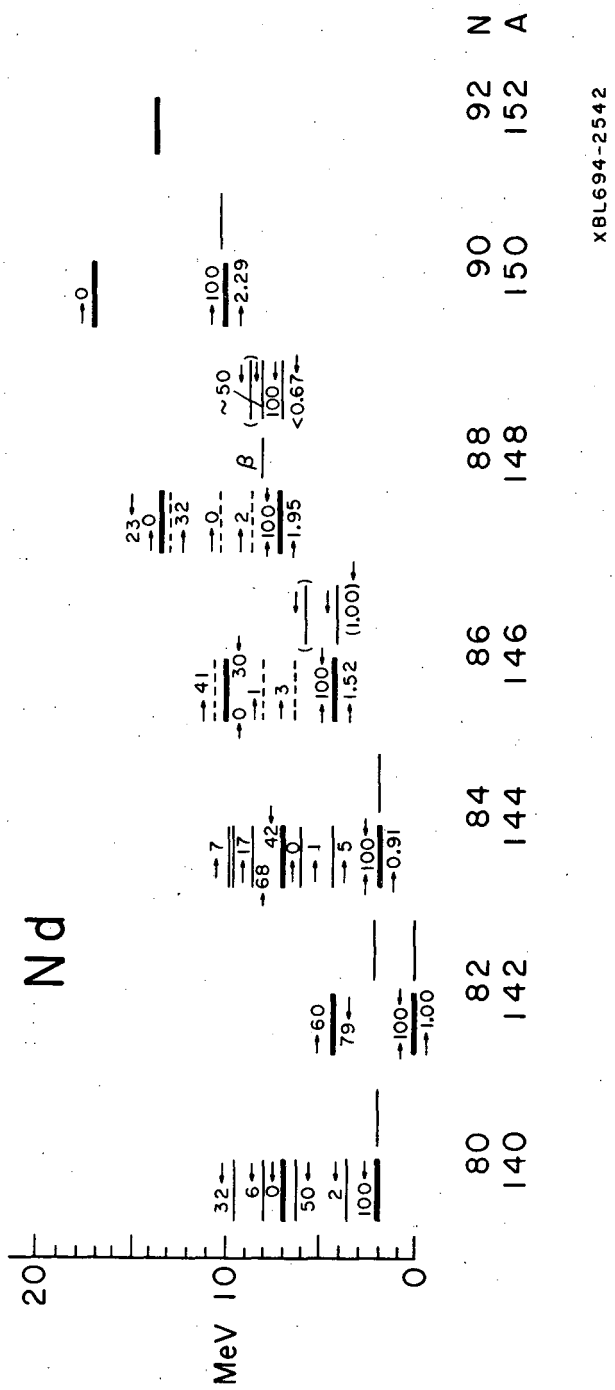
Nd
MeV
20
10
0
80
140
82
142
84
144
86
146
88
148
90
150
92
152
N
A
XBL694-2542

Fig. 35.

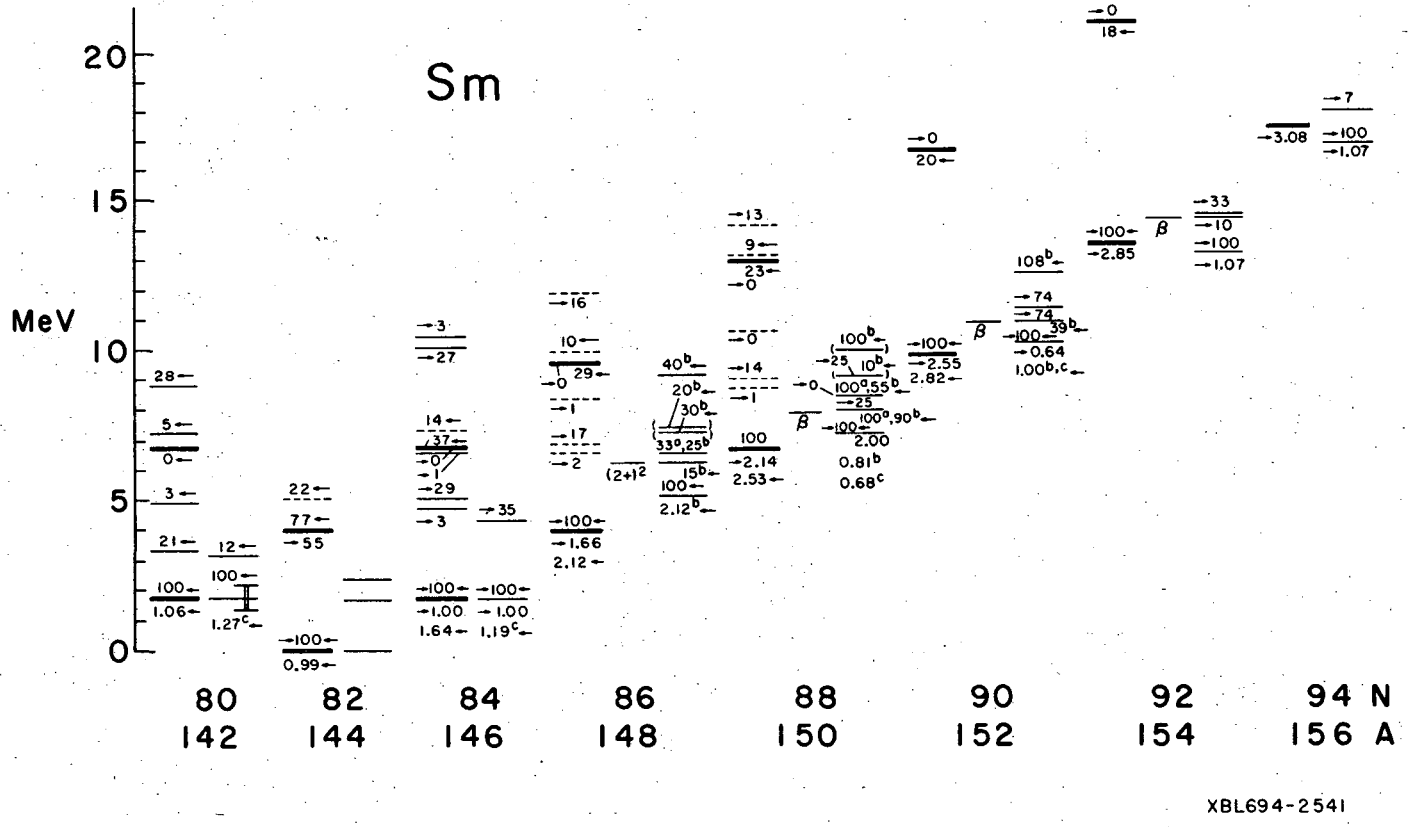
Sm
MeV
20
15
10
5
0
80
142
82
144
84
146
86
148
88
150
90
152
92
154
94 N
156 A
XBL694-2541

Fig. 36.

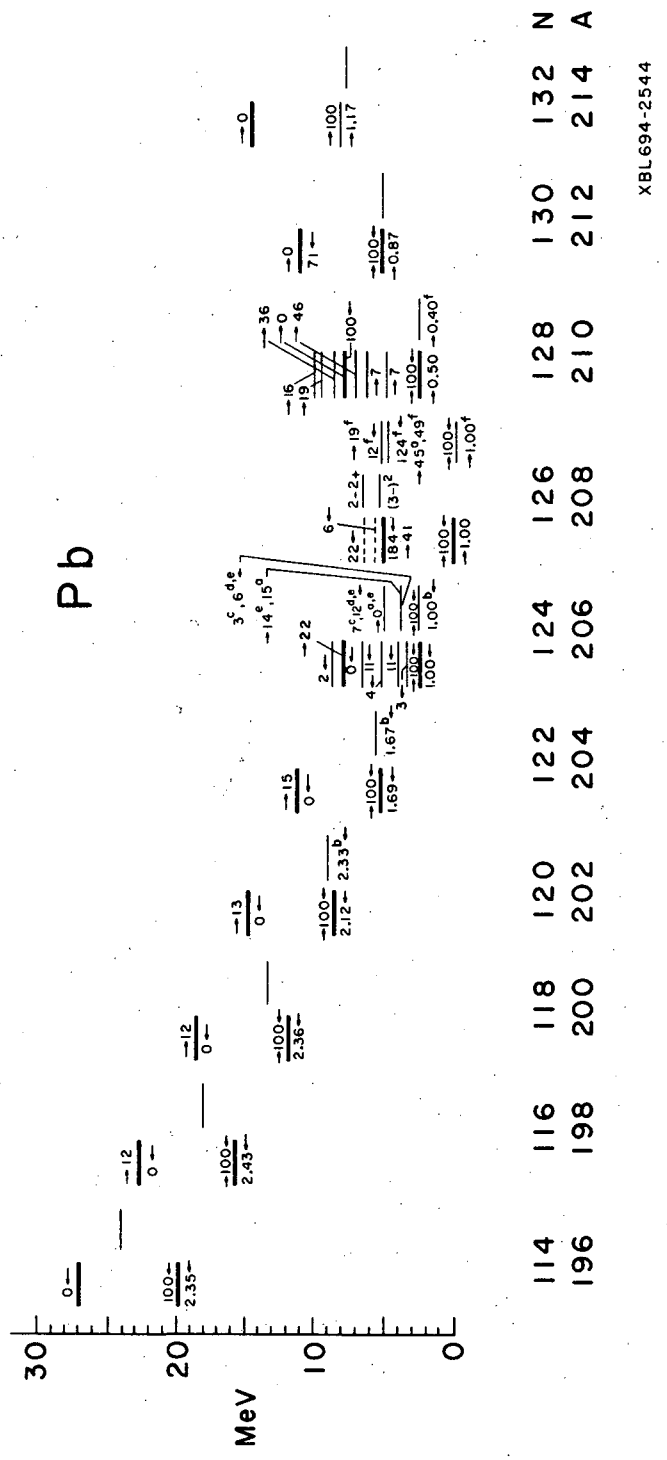
Pb
MeV
30
20
10
0
114 116 118 120 122 124 126 128 130 132 N
196 198 200 202 204 206 208 210 212 214 A
XBL694-2544

Fig. 37.

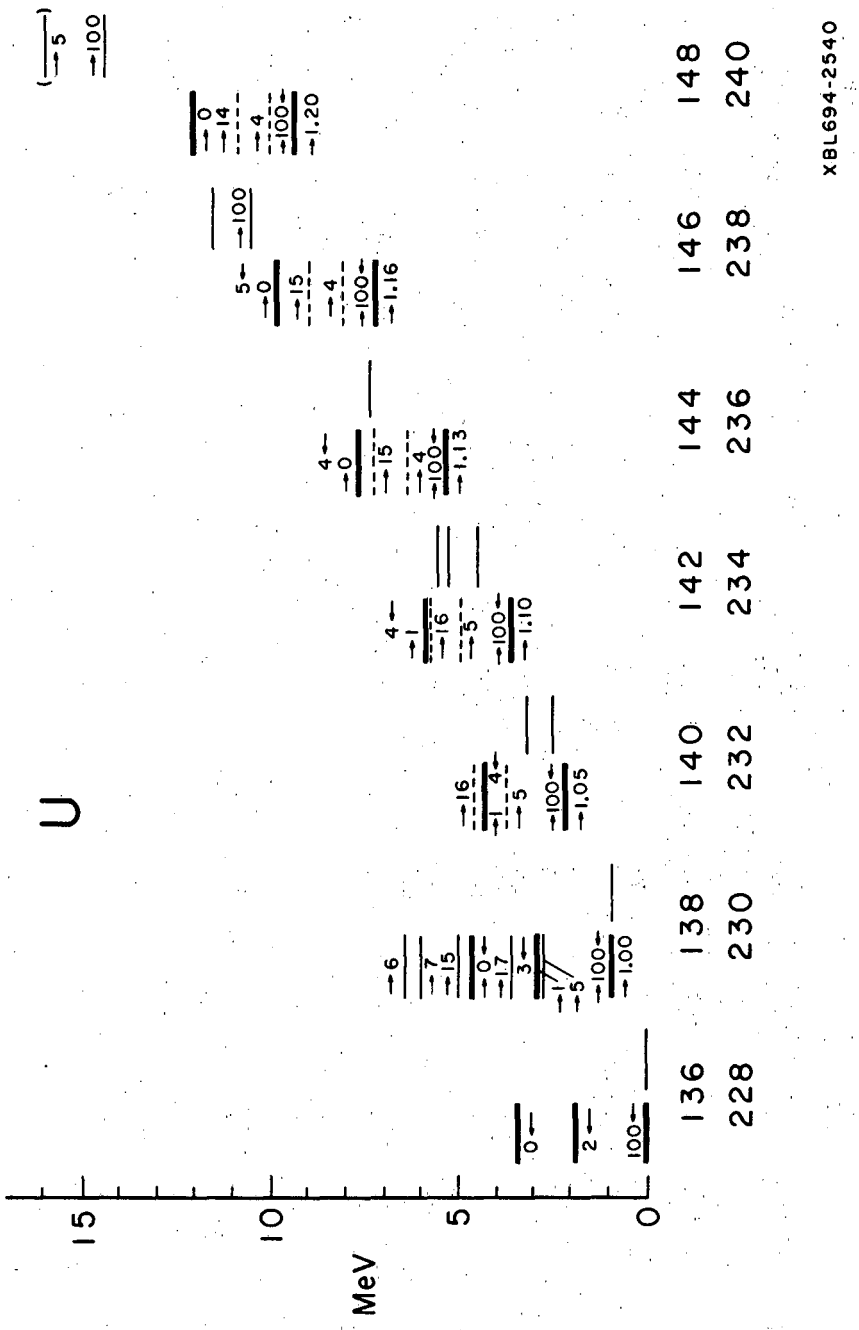
U
MeV
15
10
5
0
136 138 140 142 144 146 148 N
228 230 232 234 236 238 240 A
XBL694-2540

Fig. 38.

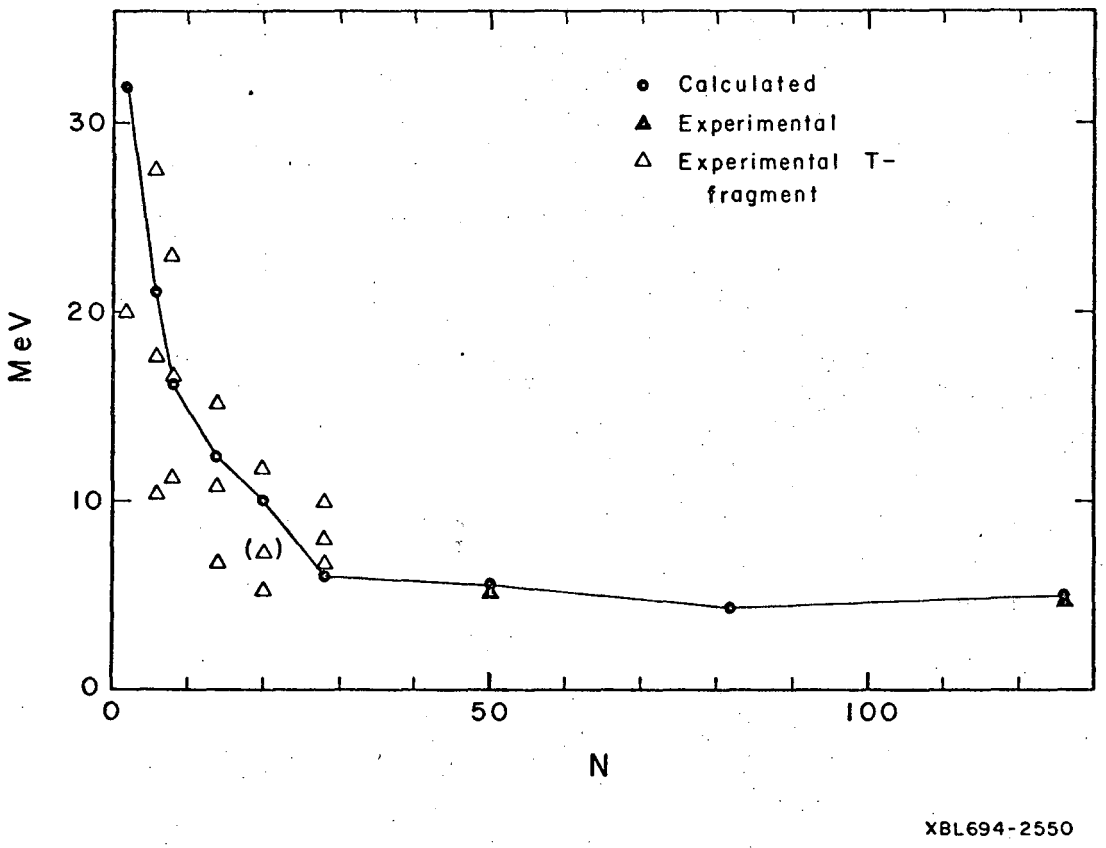
Calculated
Experimental
Experimental T-fragment
MeV
30
20
10
0
0
50
100
N
(△)
XBL694-2550

Fig. 39.

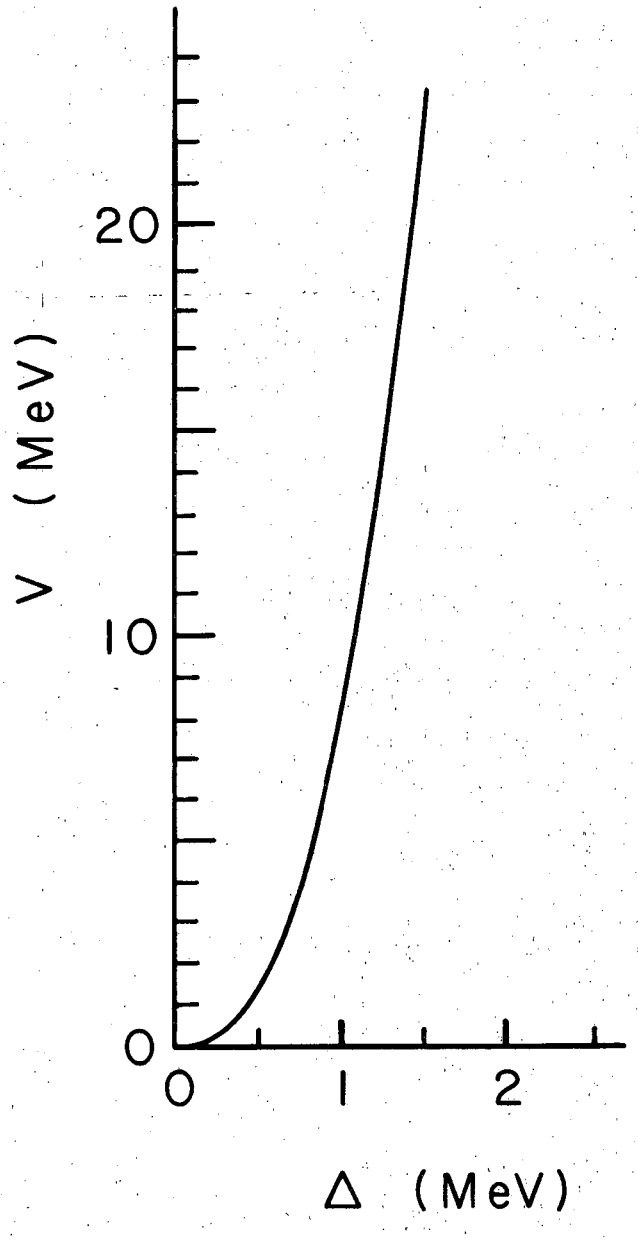

XBL694-2548

Fig. 40.

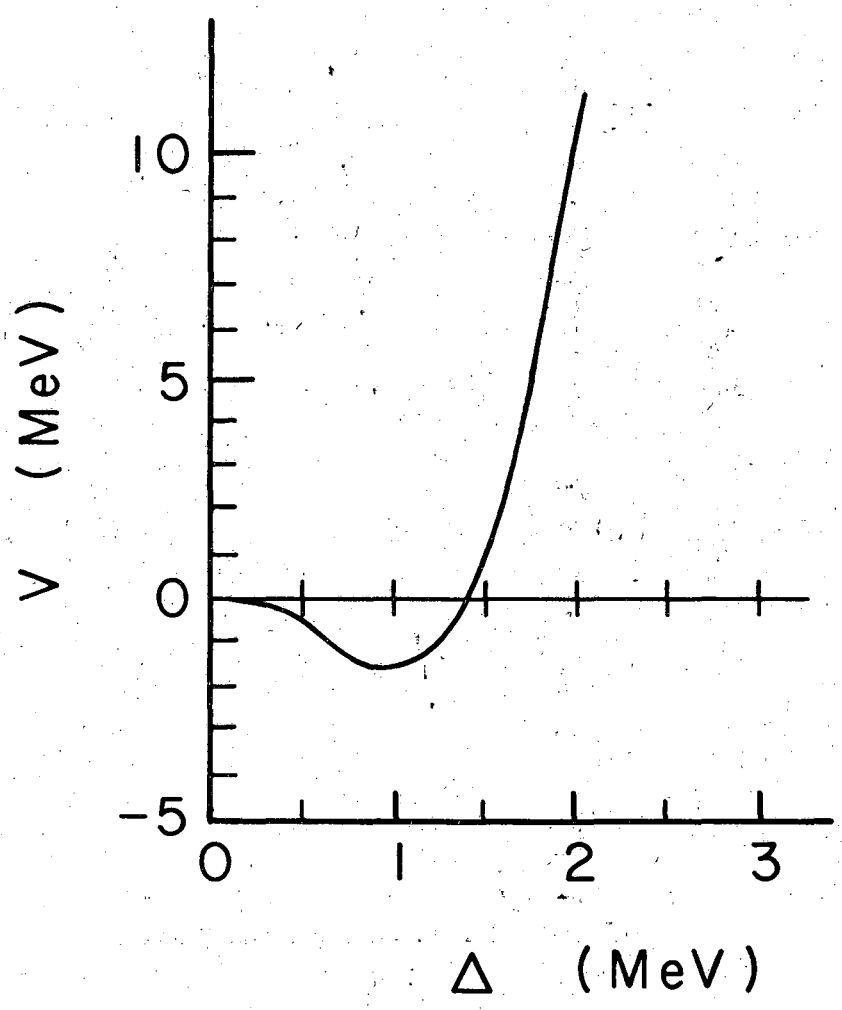

XBL694-2546

Fig. 41.

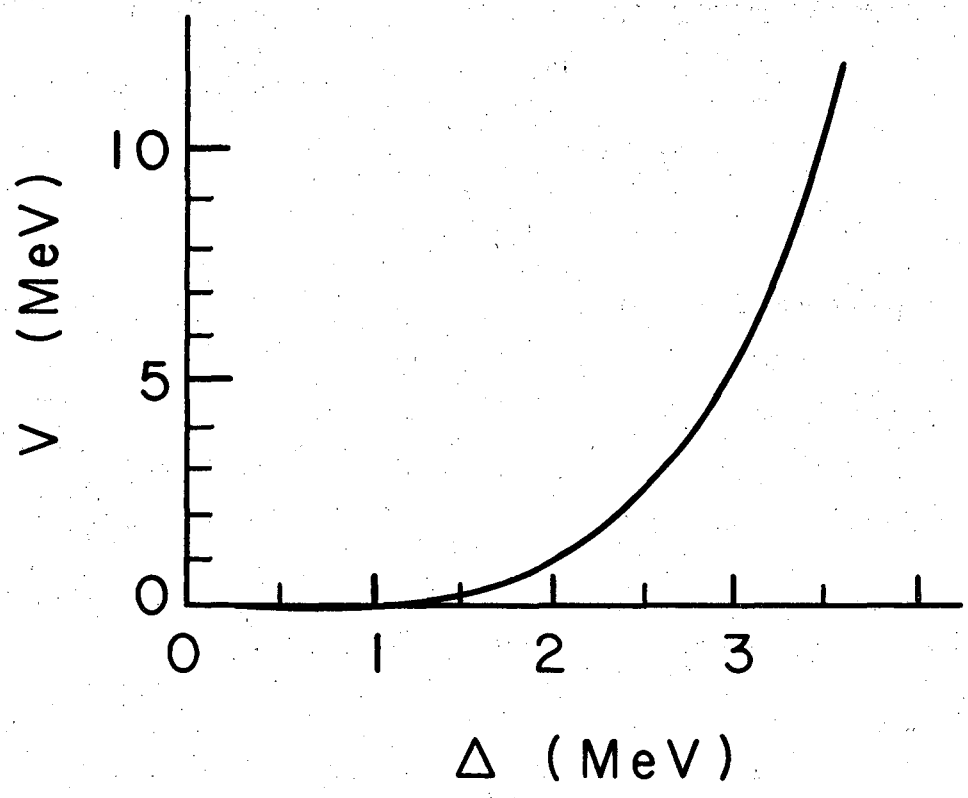

XBL694-2549

Fig. 42.

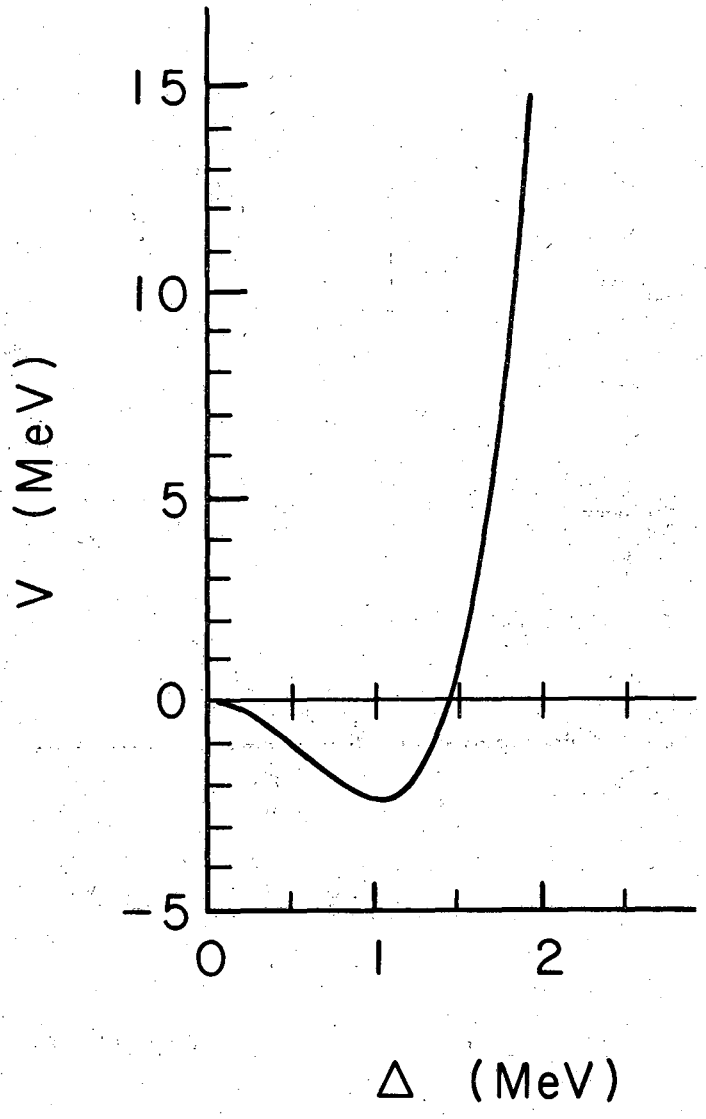

XBL694-2547

Fig. 43.

TECHNICAL INFORMATION DIVISION
LAWRENCE RADIATION LABORATORY
UNIVERSITY OF CALIFORNIA
BERKELEY, CALIFORNIA 94720